EXPERIMENTAL AND THEORETICAL STUDIES ON

DESIGN CALCULATIONS FOR LATENT HEAT STORAGE

A Thesis

Submitted to the Faculty

of

Purdue University

by

Dieter Lindemann

In Partial Fulfillment of the

Requirements for the Degree

of

Masters of Science in Mechanical Engineering

August 1987

PURDUE UNIVERSITY

Graduate School

This is to certify that the thesis prepared

By _____ Dieter Lindemann _____

Entitled

Experimental and Theoretical Studies on

Design Calculations for Latent Heat Storage

Complies with University regulations and meets the standards of the Graduate School for originality and quality

For the degree of   Master of Science in Mechanical Engineering

Signed by the final examining committee:

_____ , chair

_____

_____

_____

Approved by the head of school or department:

July 30, 19 87   School of Mechanical Engineering

This thesis ☐ is ☒ is not to be regarded as confidential

Major professor

This thesis is dedicated

to all who missed me

ACKNOWLEDGEMENTS

The author is thankful to Professor W. Leidenfrost for his encouragement and valuable advice throughout the course of this research.

In addition, thanks are due to Professor R. Viskanta and Professor J. Pearson for serving on my advisory committee. My endeavors would not have been possible without the assistance of all the people working in the School of Mechanical Engineering. I appreciated everyone's help.

The author's research was part of a foreign studies program arranged and supported by the "Deutscher Akademischer Austauschdienst".

TABLE OF CONTENTS

LIST OF TABLES

LIST OF FIGURES

LIST OF FIGURES

LIST OF SYMBOLS

Symbol	Description
a	constant Eq. (3.3.4)
A	constant Eq. (3.3.5)
B	constant Eq. (3.3.6)
Bi	Biot number
c	time ratio Eq. (3.2.2)
c or c_p	specific heat
C	integration constant
D	diameter of capillary
D	tube diameter
F	correction factor Eq. (3.3.1)
F	frozen fraction of PCM
F_0	fraction of PCM that is frozen in a radial plane element at the inlet to the tube-in-shell storage
$\overline{F}$	average frozen fraction averaged over axial length of storage
$\overline{F}_{meet}$	frozen fraction present when solid-liquid inter-phase from neighboring tubes meet and make contact
G	constant in Eq. (3.5.6)
h	convection coefficient
h_f	latent heat of fusion of water

H	geometry constant in Eq. (3.5.6)
J	geometry constant in Eq. (5.2.1.4)
k	conductivity
k_{eff}	effective conductivity including influence of conduction AND convection
k_{lm}	true conductivity (eliminated convection influence)
k_{ser}	conductivity obtained from series model Eq. (3.5.1)
k_{par}	conductivity obtained from parallel model Eq. (3.5.2)
k_{geo}	conductivity obtained from Lichteneker geometrical model Eq. (3.5.3)
k_{emp}	conductivity obtained from empirical model Eq. (3.5.4)
k_{Vein}	conductivity obtained from Veinberg model Eq. (3.5.5)
l	traveled distance of air bubble in capillary
l	axial length of test cell or tube of tube-in shell storage
L	distance of tubes in tube-in-shell storage tank
NTU	number of transfer units
pf	performance factor Eq. (3.4.5)
P	power
q	heat rate
Q_t	energy transfer necessary for total phase change of a certain volume
Q'''	energy density Eq. (3.4.6)
r	radius of solid-liquid interface. See Fig. 3.2.1 and Fig. 5.2.2
r_v	radius of virtual interface. See Fig. 5.2.2

$r_{v,i}$ initial virtual radius of interface when fusion fronts meet

R radius of test cell or radius of tube. See Fig. 3.2.1 and Fig. 5.2.2

R_v radius of virtual cylinder. See Fig. 5.2.2

Ra Rayleigh number

R_t thermal resistance

$R_{t,cond}$ thermal resistance due to conduction

$R_{t,conv}$ thermal resistance due to convection

s storage factor $s = pf \cdot Q'''$

t time for freezing or melting of a certain amount of PCM

t_t time for total freezing of melting of the test cell volume

$t_{t,h}$ time for total melting of test cell volume with test cell in horizontal position

$t_{t,v}$ time for melting of test cell volume with test cell in vertical position

t_0 dimensionless time

T temperature

T_b temperature of constant temperature bath

T_f fusion temperature

T_i initial temperature

T_m mean temperature $T_m = \frac{1}{2}(T_w + T_f)$

T_n nucleation temperature

T_{sur} temperature of surroundings

T_w wall temperature

$T_{w,a}$ average wall temperature

(UA) loss coefficient area

va	ratio of volume to surface area of the shavings $va = \dfrac{V}{A}$
V	volume
V(t)	frozen volume at time t
V_{all}	See Fig. App.B
V_{Δ}	See Fig. App.B
V_{tube}	volume of tubes
x	dimensionless radius x=r/R
z	depth of storage tank in the soil. See Fig. 6.1

Greek Symbols

α	diffusivity
ε	effectiveness
λ	constant in Eq. (3.5.6)
λ	similarity parameter Eq. (5.1.1.4)
ρ	density
$\rho_{i,0}$	density of ice at 0 C
Φ	porosity $\Phi = \dfrac{\text{void space}}{\text{total space}}$
Ψ	auxiliary function from Fig. 5.2.1.2
Ω	auxiliary function from Fig. 5.2.1.2

Subscripts

c	coolant
H_2O	property of pure water

ice	property of pure ice
i,0	property of pure ice at 0 C
lm	overall property of metal and liquid phase of PCM
m	metal property
sm	overall property of metal and solid phase of PCM
table	property obtained from table

Abbreviations

CTB	constant temperature bath
LHTES	latent heat-of-fusion thermal energy storage
PCM	phase change medium
PM	porous medium

ABSTRACT

Lindemann, Dieter. M.S.M.E., Purdue University. August
1987. Experimental and theoretical studies on design cal-
culations for latent heat storage. Major Professor: Prof.
W. Leidenfrost, School of Mechanical Engineering.

Research was conducted to obtain design data of latent
heat-of-fusion thermal energy storage (LHTES) devices. The
devices studied utilize a porous medium (PM) to increase
the effective conductivity of the storage system. Therefore
the melting and freezing process is accelerated. Metal
shavings and metal spheres were used as porous media and
water as the phase change medium (PCM).

A simple experimental method to measure the conduc-
tivity of a water-metal mixture or ice-metal mixture was
applied to obtain conductivity data. These measurements
can be considered fairly accurate because measured conduc-
tivity of pure water and of pure ice agreed very well with
those of accepted tables. The comparison of the measured
conductivity for porous media with values obtained from
several formulas from the literature showed that no formula
predicts the conductivity with an acceptable accuracy.

Evaluation of defined quality values for LHTES showed that metal shavings can enhance significantly the storage performance.

As a practical application, calculation methods for LHTES systems were introduced and applied in a simulation program for residential space heating with energy storage. The simulation showed that metal shavings can help to save about 25% of the annual heating costs when compared with a LHTES system with pure water.

CHAPTER 1 - INTRODUCTION

In the long run, due to the limited amount of fossil
fuels, we must depend on inexhaustible energy sources which
require energy storage. Thermal energy storage is one pos-
sibility which can be achieved in form of sensible heat
storage or latent heat storage. Solid-liquid phase change
is a form of latent heat storage. However its disadvantage
is slow energy flow into and out of the storage system.
This thesis investigates latent heat storage and how water
saturated with metal shavings can be used as the porous
medium to enhance the energy flow. This is because the high
conductivity of the metal can also increase the conduc-
tivity of the water-metal mixture.

1.1   Exhaustible and Inexhaustible Energy Sources

Exhaustible sources are coal, oil, and gas which are
in limited supply. The inexhaustible sources are, on the
other hand, continuously renewable. The earth's biosphere
receives energy naturally from three main sources:

   - intercepted solar radiation

- thermal energy from the earth´s interior (produced largely by the decay of radioactive matter in the earth´s crust)

- tidal energy

Intercepted radiation can be found in application as:

- solar energy

- wind energy

- hydropower

- ocean thermal energy

- biogas

- wood

Fig. 1.1 shows how these sources can be used for space heating.

In early history men used almost exclusively inexhaustible energy. In this way, ships were propelled by wind, wagons by animals, and the houses were heated by wood, turf, or manure. Later, wind and water energy were applied for driving machines. In the beginning of the industrial revolution exhaustible energy usage began with the invention of the steam-engine powered by coal.

Today we can already estimate the time when all exhaustible energy will be depleted. This is

illustrated in [2] and shows that there will be no more U.S. production of petroleum liquids in about the year 2060; therefore, we must now return to the use of inexhaustible energy sources applying modern standards of engineering knowledge.

Exhaustible energy needs no special consideration for its storage because we find this energy already in a stored form. On the other hand, inexhaustible energy does need special considerations for its storage due to the fact that inexhaustible energy sources do not have a steady energy output. A time dependent energy resource can only be collected during a specific time frame. Our energy needs are widly varied and also time dependent but this dependance need not correspond directly to the collection time and therefore energy storage is required.

1.2 Possibilities of Energy Storage

Often energy has to be converted several times until it is finally used, and hence, there are many possibilities for energy storage. Let us consider the example of popcorn production from hydropower (Fig 1.2). In this example the energy can be stored in a reservoir, a battery, or in thermal storage, or the product (here: popcorn) can also be stored. It is our work to determine what the most economical storage possibility is. In this case,

for someone who likes fresh popcorn, as opposed to someone
who prefers stored popcorn, the choice is obvious when
storage losses are considered. In situations where it is
not so obvious what the most economical storage possi-
bility is, we must know more about the characteristic of a
specific storage type. This thesis is concerned with the
different possibilities for thermal energy storage.

1.3   Thermal Energy Storage

The major characteristics of a thermal energy storage
are:

- storage energy density

- temperature range over which heat is added or removed

- temperature difference associated with addition or
  removal of heat

- temperature stratification in the storage unit

- power requirements for addition or removal of heat

- amount of losses from the storage system

- cyclic durability of the storage

The storage must be connected to other components of the
energy system. For this interaction between components,
factors must be considered as follows:

- period of time for which energy is stored or rate of energy losses

- transportability of stored energy

Heat may be stored by means of sensible heat or latent heat in a material. <u>Sensible heat</u> requires a temperature change; whereas <u>latent heat</u> requires a phase change or chemical reaction. The match between the energy source and the task, or load, is an important criterion in the selection of storage size and type. If large excursions in storage temperature are permitted, sensible-heat storage may be used. If in contrast delivery to load must be in a narrow temperature range, isothermal phase-change storage using latent heat may be required. The type, size, and cost of a heat exchanger associated with the storage are closely related to storage thermal properties. For example, a relatively small heat exchanger can be used if a high-temperature storage supplies a low-temperature demand. If the storage temperature is only slightly higher than the temperature demand, a large expensive heat exchanger will be required. If furthermore the energy is stored below the temperature of the demand system, a heat pump and hence even additional power is needed.

1.4 Sensible Heat Storage

The best sensible heat storage materials have

- high specific heat

- high density

- low cost

- low toxicity

- low inflammability

- low chemical activity

Sensible heat can be stored in liquids or in solids.

1.4.1 Sensible Heat Storage in Liquids

Water is the most common medium for storing sensible heat for the use with low- and medium-temperature systems. Water is cheap and abundant and has a number of particularly desirable properties. The storage of water at temperatures above its normal boiling point requires expensive pressure vessels and is rarely cost-effective. Without a pressure vessel other liquids can be used for thermal storage above 100 $^{\circ}$C. Examples are Butanol, Octane, and Isopropanol with boiling points at 118 $^{\circ}$C, 126 $^{\circ}$C, and 148 $^{\circ}$C respectively. Unfortunately these liquids have

lower density and specific heat with higher inflamma-
bility and viscosity than water.

1.4.2 Sensible Heat Storage in Solids

For some applications sensible-heat storage in solids
is advantageous. Hot air, for example, is often stored in
storage beds formed from solid particles like river rocks.
The storage bed acts thereby as both a storage
medium and heat exchanger. Storage in beds has desirable
thermal stratification capability arising from the
poor particle-to-particle thermal contact in a bed of rock
storage. It is rarely economical to use a single
large mass of a solid material for sensible-heat storage
because a large mass has a very low surface-to-volume
ratio, and hence the heat transfer from and to the storage
is too small.

1.5 Latent-Heat Storage

Latent heat exchange can occur as solid-solid, solid-
liquid, and liquid-gas phase change. Phase changes involv-
ing gases should generally be avoided since the large
volume of gas precludes compact storage.

Solid-solid phase change usually involves hydration
and dehydration. $Na_2SO_4 \cdot 10H_2O$ (Glauber's salt) was the
earliest phase-change storage material to be studied

experimentally for house heating applications. At a temperature below 32 $^{\circ}$C, the hydration point, the anhydrate becomes hydrate and crystalline with the evolution of heat. When the hydrate is heated above 32 $^{\circ}$C the crystal dissolves in the water and absorbs heat with a heat of fusion of 241 kJ/kg (compare with heat of fusion of water of 333 kJ/kg). The problem with salt hydrates is that the fusion temperature does not remain at the same temperature over several cycles. The cycle is not durable. After many cycles, the rehydration reaction requires progressively more subcooling to reach completion, thereby canceling the beneficial effects of isothermal phase change.

Solid-liquid phase change materials should have similar properties as those mentioned for sensible-heat storage materials above. In addition characteristics as follows should be present:

- high latent heat

- an appropriate and well-defined melting point

- high thermal conductivity

- good repeatability of the freeze-thaw temperature

- low costs

- low coefficient of thermal expansion

- negligible phase change expansion

If the material has not the last two mentioned characteristics, special care has to be taken for the design of the storage tank. Solid-liquid phase change materials generally have low conductivity especially in the liquid phase. As a result, energy flow into and out of storage is slow. This is also true for water. However, metal shavings in the water help to increase the conductivity of the storage medium because of the high conductivity of the metal. The storage system nearly keeps its energy density because the metal shavings have a high porosity which means that the volume of the phase change material nearly stays the same.

1.6   Objectives and Strategy of the Study

Objectives and strategy are structured into four parts and are:

1. to find a method to determine the conductivity of a porous medium represented by metal shavings saturated with water or ice, respectivly.

    In this work a method is used for the first time where conductivities of porous media with water are measured by observing the water displacement due to freezing and melting. This measurement technique which

observes the integral effect of the phase change requires only to measure or to specify the temperature of the wall of the container in which the phase change occurs.

2. to define and find quality criteria (Chap. 3.4) for these porous media and conclude media with high performance.

From basic equations quality criteria are determined which show the capability of a medium to store energy and yield the energy density. With knowledge of the conductivity these quality values can be calculated. From comparisons a porous media material of high performance can be found.

3. to report about calculation methods for design of actual latent heat-of-fusion thermal energy storage (LHTES) systems.

In practical applications mostly tube-in-shell heat exchangers are used. Equations will be given for a single tube as well as tube banks.

4. to show the effects of a storage system with different shavings in residential space heating application on the annual energy costs

A computer simulation of a solar heated house

with a LHTES unit is used to show how different storage media can influence the annual heating costs.

1.7 Background

Investigations with heat pumps which use coils in the soil as the heat source have shown that during the winter ice is formed around the coils. This ice is formed in the soil saturated with water because the coolant temperature is below 0 $^{\circ}$C. Low temperatures are necessary in order to achieve a high temperature gradient required to meet the energy demand. However, the frozen soil has to thaw during the summer, and problems arise when the summer is too short to thaw the soil. It has been proposed to use the ice built up by a heat pump in the winter for air conditioning in the summer. In this way the melting process would be completed in a shorter time and in addition surplus summer heat would be stored for heating in the winter. The melting process can be enhanced furthermore by using materials of higher conductivity than soil, like water and metal shavings as discussed above.

Many studies have been undertaken to investigate the behavior of the solid-liquid phase change of water. Herrmann (1982) [3] and White (1984) [4] worked on 'Melting and Freezing of Water around a Horizontal, Isothermal Cylinder', representing one type of a tube-in-

shell heat exchanger. Weaver (1985) [5] studied ´Solid-Liquid Phase Change Heat Transfer in Porous Media´. He worked with aluminum and glass beads in water. From his work there exists a cylindrical test cell and a program to calculate the freezing and melting process in the test cell. Both of these were used in the current research efforts. From the literature he reviewed he found five formulas which use different models to calculate the conductivity of a porous medium. Weaver found that these formulas give satisfying results for a porous medium consisting of water and glass but not for a porous medium with highly different thermal conductivities like aluminum and water.
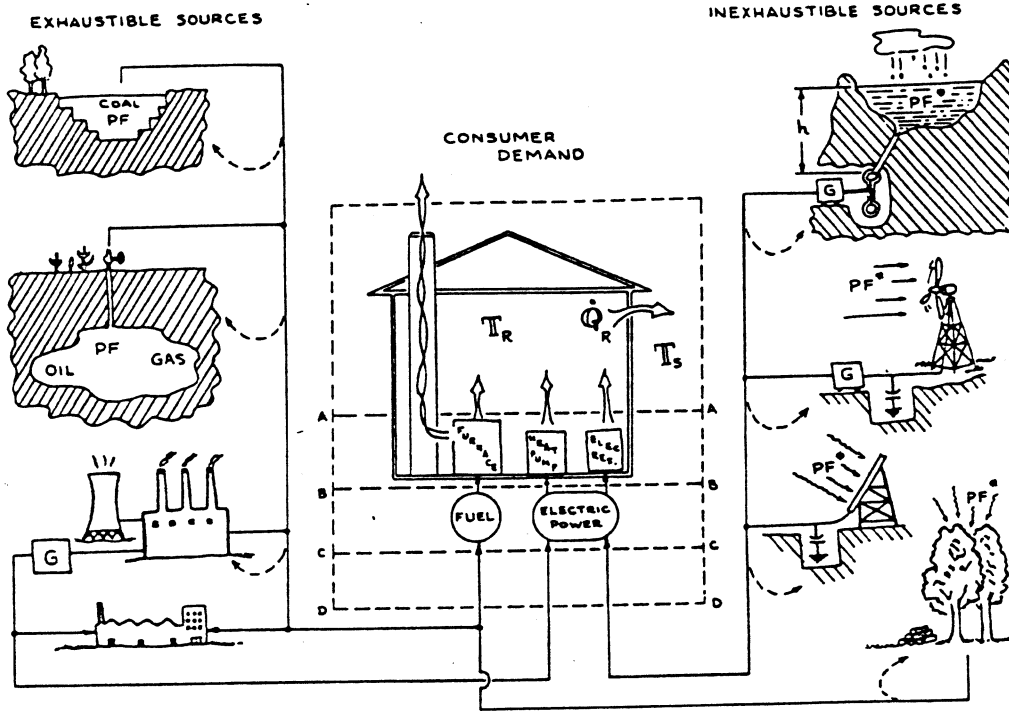
Figure 1.1   Energy sources for space heating.   [1]
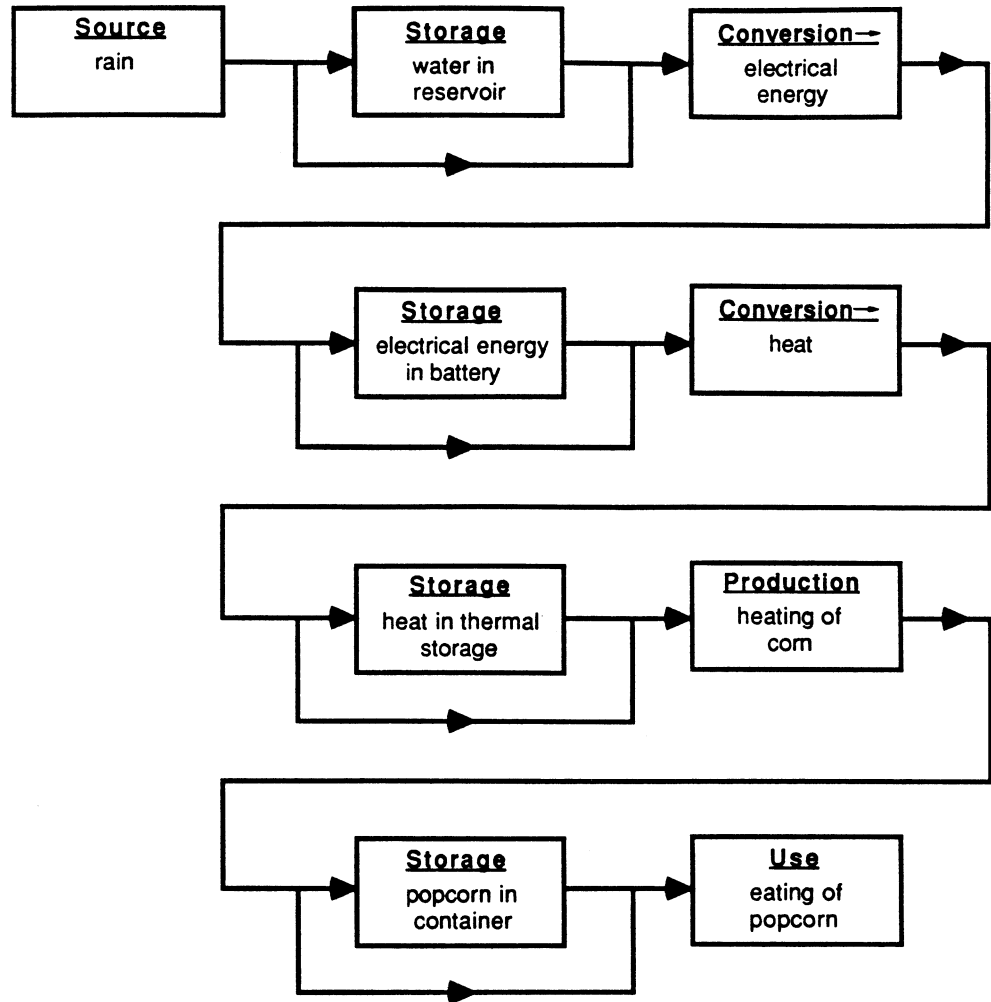
Figure 1.2   Example of popcorn production from hydro-
power used to demonstrate the many existing
storage possibilities for energy on the way
from the source to its final use.

CHAPTER 2 - EXPERIMENTAL APPARATUS AND PROCEDURE

The first objective of this thesis is to measure conductivities of porous media represented by metal shavings saturated with water or ice, respectively. The conductivities are measured by applying a melting and freezing process. This measurement method is unusual; nevertheless it is most similar to the melting and freezing in LHTES. The measurement techniques can be characterized like any other of the methods introduced in the next chapter.

2.1   Conductivity Measurement Methods

Experimental study of the thermal conductivity was started in the eighteenth century. Since that time various methods have been suggested for different ranges of temperature and for various classes of materials having different ranges of thermal conductivity values. Accordingly no method exists that would have optimum performance of conductivity measurements. Methods for the measurement of thermal conductivity fall into several categories:

In the steady-state method of measurement, the test material is subjected to a steady temperature profile. The

thermal conductivity is determined directly by measuring the rate of heat flow per unit area and the temperature gradient.

In the nonsteady-state method, the temperature distribution varies with time, and hence, the unsteady term in the heat equation, $\frac{1}{\alpha} \frac{\partial T}{\partial t}$, is involved. With knowledge of density and specific heat the conductivity can be obtained from the diffusivity α. The nonsteady-state methods are further subdivided into periodic and transient heat flow methods.

The heat flow has to be controlled in a prescribed direction such that the actual boundary conditions agree with those assumed in the experiment. There are two possible directions; and hence methods can further be subdivided into longitudinal and radial heat flow methods.

There are two ways to obtain the rate of heat flow. In an absolute method, the rate of heat flow into a specimen is directly determined, usually by measuring the electrical power input to a heater. In order to distinguish between actual conducted heat and heat loss, the heat flow out of the specimen has to be measured. In a comparative method, the rate of heat flow is usually calculated from the temperature gradient over a reference sample of known conductivity, which is placed in series with the specimen and in which hopefully the same heat flow occurs.

All methods are based on an experiment which can be modeled and mathematically described with high accuracy. An advantage is to have conditions in the experiment as they will occur in the application because additional errors resulting, for instance, from temperature dependence of the conductivity can be avoided. [6]

2.2 Experimental Set-up

The experimental set-up is used to measure conductivities of porous media saturated with water respectively ice. It consists of the following three major components introduced below: the test cell with heat exchanger, a constant temperature bath (CTB), and equipment used to observe the experiment. The integral effect of freezing and melting is observed by water displacement due to phase change expansion and contraction.

The test cell, designed by Weaver, represents the model of a cylinder with an assumed adiabatic top surface and bottom and has uniform temperature on the circumference. The test cell is described in detail by Weaver in [5] and shown in Fig. 2.2.1. The capsule consists of a brass cylinder (158.8 mm long, 73.0 mm ID) which is capped on both ends by discs. They are pressed on the cylinder by five threaded rods and are made of acrylic plastic which has a low thermal conductivity (0.195 W/mK) which helps

reducing heat losses at the ends. Two joints are placed in the top cap to enable water flow in and out of the test section due to phase change expansion. Excess water leaves the enclosure through the joint in the center when the phase change material (PCM) freezes with inward interface motion. This water reenters through the joint near the wall when the PCM melts due to a wall temperature above freezing point.

The counter flow <u>heat exchanger</u> consists of copper tubes wrapped and soldered around the outside of the brass cylinder which gives a uniform wall temperature. The test cell is insulated with Styrofoam fitted around the heat exchanger and the bottom cap. The top cap is insulated by a piece of black insulation foam, which can easily be removed for observations of the phase change process. Most important is the insulation of the caps for the approximation of the theoretical model which assumes an adiabatic top cap and bottom. The additional insulation around the heat exchanger helps to avoid unnecessary heat losses.

To supply the heat exchanger with cold or hot heat exchanger fluid, a <u>constant temperature bath</u> (CTB) Brinkmann-Lauda, RC 203 and another CTB Haake A82 were used. The CTB circulates, with an internal pump, a water ethanol mixture consisting of 50% water and 50% ethanol through the heat exchanger.

Fig. 2.2.2 - 2.2.5 show the experimental set-up inclu-
ding the _measuring instruments_. The main water displa-
cement, due to phase change expansion and contraction, can
be measured in the burette. During the process of freezing
water moves from the opening at the center of the cell,
through the capillary and into the burette. Similarly
during melting water flows from the burette, through the
capillary and into the test cell at the opening closest to
the wall. The burette allows a reading error of 0.2 ccm.
Smaller volume changes can be determined by observing the
migration of an air bubble in the capillary. The air bubble
is injected into the capillary with a syringe which can be
stabbed through a septum. The septum is made from soft rub-
ber and seals the puncture water-tightly after the syringe
is removed. A septum is installed on either end of the
capillary. The two septa on either end make sure that the
air bubble can be moved to every location within the capil-
lary by adding or removing distilled water with the
syringe. The capillary has an inner diameter D of about
1.5 mm. The volume change V can be determined from the
traveled distance 1 of the air bubble by $V = \frac{1}{4} \pi D^2 1$.
The wall temperature can be measured with five copper-
constantan thermocouples placed on the outside of the brass
cylinder.

In addition to the observations made with the burette
and the capillary, direct visual observations are also

possible by looking through the transparent top cap of the test cell. When these visual observations indicate that the ice-water interface reached the center of the test cell, this fact is also indicated by a sudden change of the voltage of the thermocouples located at the center of the test cell. These observations are used to control and to verify the displacement measurements. Measurements of the temperature distribution in the test section are made by copper-constantan thermocouples arranged in four rakes with five thermocouples each. Radial and axial position of the rakes are shown in Fig. 2.2.1, position four and five. The thermocouples are connected with a digital thermometer which has a reading error of 0.1 $^\circ$C.

2.3 Conductivity Measurements with the Test Cell

The test cell is used to perform experiments which can serve to measure conductivities for solid and liquid porous media. From PCM-freezing the conductivity of the solid porous medium (that means porous material with ice in the pores) can be determined. The wall temperature and the freezing time have to be recorded. This method (compare with Chap. 2.1) is a

- nonsteady-state, transient

- radial

- absolute

method. The temperature distribution in the solid phase varies with time when heat is removed, and the solid-liquid interface moves inward. Liquid porous medium is still present in the center of the test section until the end of the freezing process. The heat flows radially outward through the solid porous medium, and the absolute amount of heat is directly dependent on the frozen mass and on the latent heat; hence measurements of power input are not necessary although the method is direct and not comparative.

From PCM-melting the conductivity of the liquid porous medium (that means porous material with water in the pores) can be determined. The wall temperature and the melting time have to be recorded. The procedure is basically the same as described for PCM-freezing.

2.4 Standard Test Procedure

In preparing for an experiment, the test cell was filled with the respective porous medium. Moreover distilled water had to be degasified by boiling for approximately fifteen minutes and then cooled to the fusion temperature while under vacuum. This insured that the phase change process was not influenced by impurities from air bubbles in the test section. The water was then carefully siphoned

into the test cell with the porous medium already in it to avoid turbulent mixing which would enhance the absorption of air.

The liquid PCM was then cooled down to a temperature of about 0 $^{\circ}$C using one CTB. In the mean time, the second constant temperature bath was cooled down to the freezing temperature selected for this experiment. The freezing experiment started when the pump of the CTB was switched on and the cold water-ethanol mixture started flowing through the heat exchanger. Freezing temperatures in the range of -25 $^{\circ}$C to -5 $^{\circ}$C were chosen. During the experiment, a representative wall temperature and the displacement were read in intervals, depending on how fast freezing occurred. The monitoring of changes in the water level in the burette, due to phase change expansion, and in some cases, observation of an air bubble in the capillary, made it possible to determine the time when all of the water in the PCM was frozen. In addition, temperature measurement in the test section and visual observations through the cap were made. From 25 available thermocouples, only ten temperatures were read with a digital thermometer. Those ten temperatures were two wall temperatures from representative spots, five temperatures from the center thermocouple rake, and one temperature in the middle of each of the other three thermocouple rakes.

Similarly to the freezing experiment two melting experiments were carried out, one with horizontal and the other with vertical test cell position. The temperature of solid PCM was brought near to 0 $^{\circ}$C using one CTB. In the mean time, the second CTB was heated up to the melting temperature in question for this experiment. This CTB was then connected with the heat exchanger of the test cell to start the melting experiment. Melting temperatures in the range of 10 $^{\circ}$C to 30 $^{\circ}$C were chosen. Wall temperature and melting time were measured as described for freezing.

2.5 Porous Media and Water/Ice Properties

All relevant porous media properties are given in Table 2.5.1. For the experiment, beads and different shavings were used. In the ´shape´ column the diameter of the beads and the cross-section of the spirals is indicated. The value va is the ratio of volume and surface area of the porous medium.

$$va = \frac{v}{a} \qquad (2.5.1)$$

The aluminum beads are made from aluminum type 1100 with not more than 1% iron. The aluminum shavings were produced on a lathe from Al 6061 T4. Due to the different properties of aluminum, copper, steel, and brass it was not possible to produce the curls with identical geometry. Properties of water and ice are summerized in Table 2.5.2. and 2.5.3.
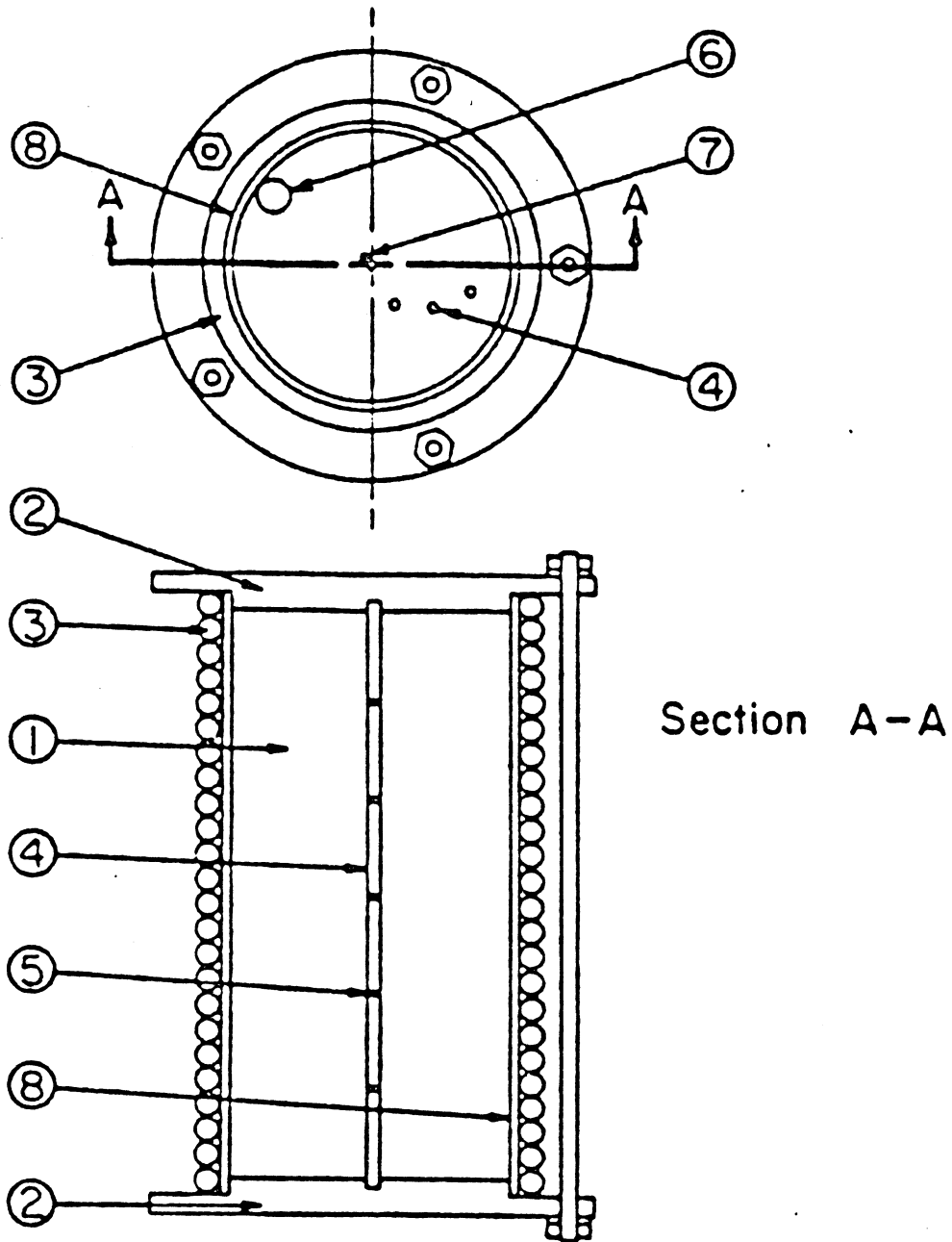
Section A-A

Schematic of test cell; 1-test section; 2-acrylic end caps; 3-copper heat exchanger; 4-thermocouple rake; 5-thermocouple position on rakes; 6-fill tube; 7-overflow tube; 8-brass cylinder.

Figure 2.2.1   Schematic of test cell.   [5]

1 – Test Cell
2 – Bifilar Coil for Thermostated Fluid
3 – Septum
4 – Capillary
5 – Burette
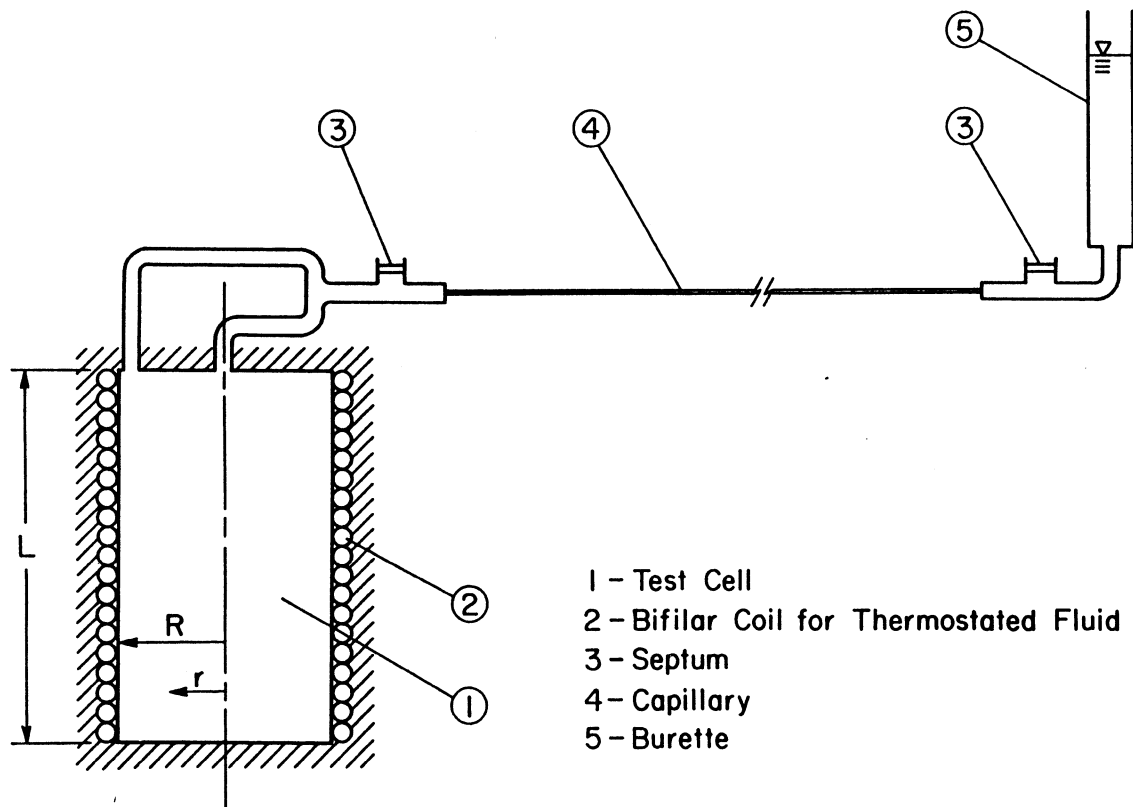
Figure 2.2.2   Device for measurements of the water displacement.
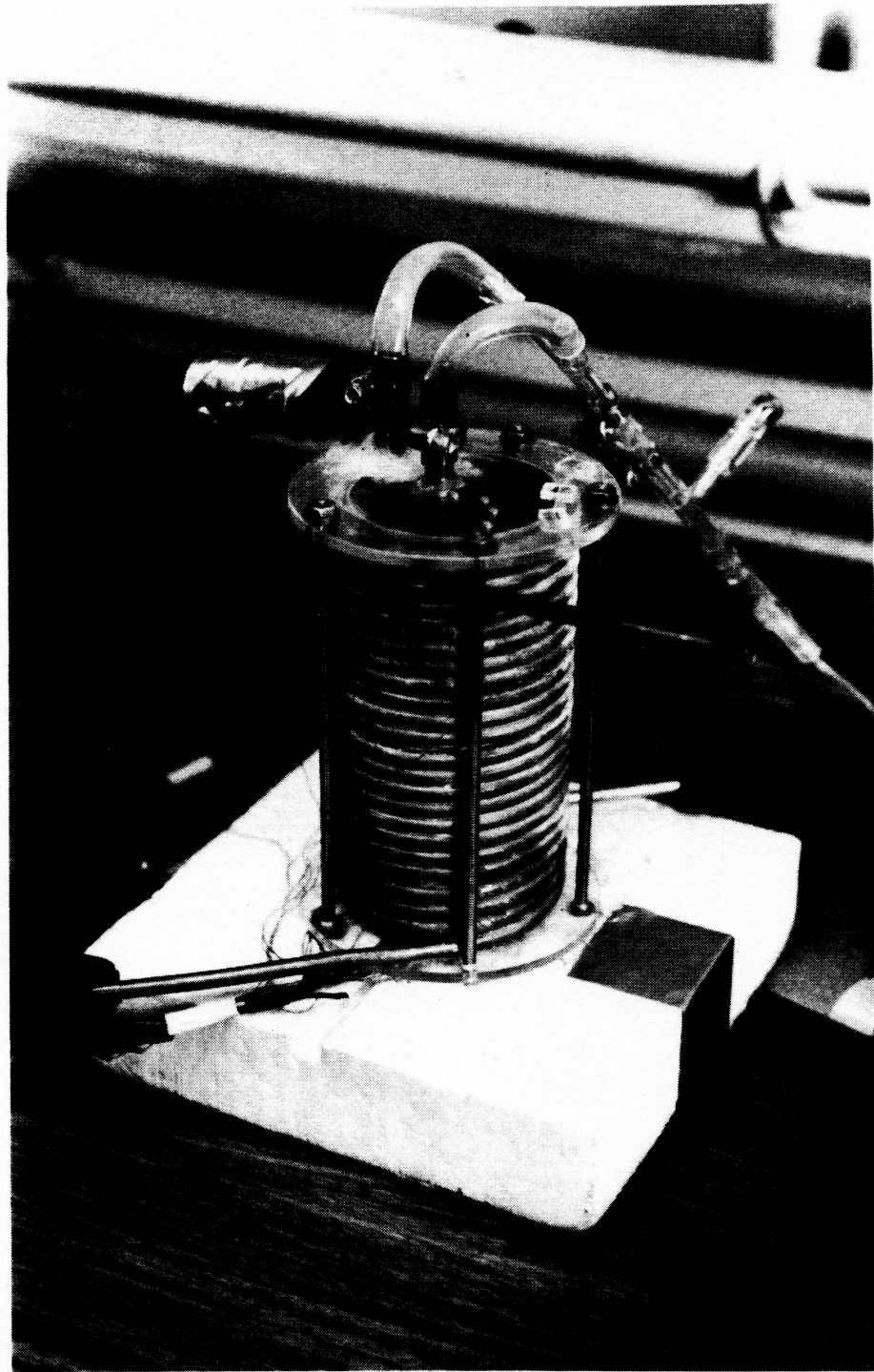
Figure 2.2.3   Test cell resting on bottom insulation.
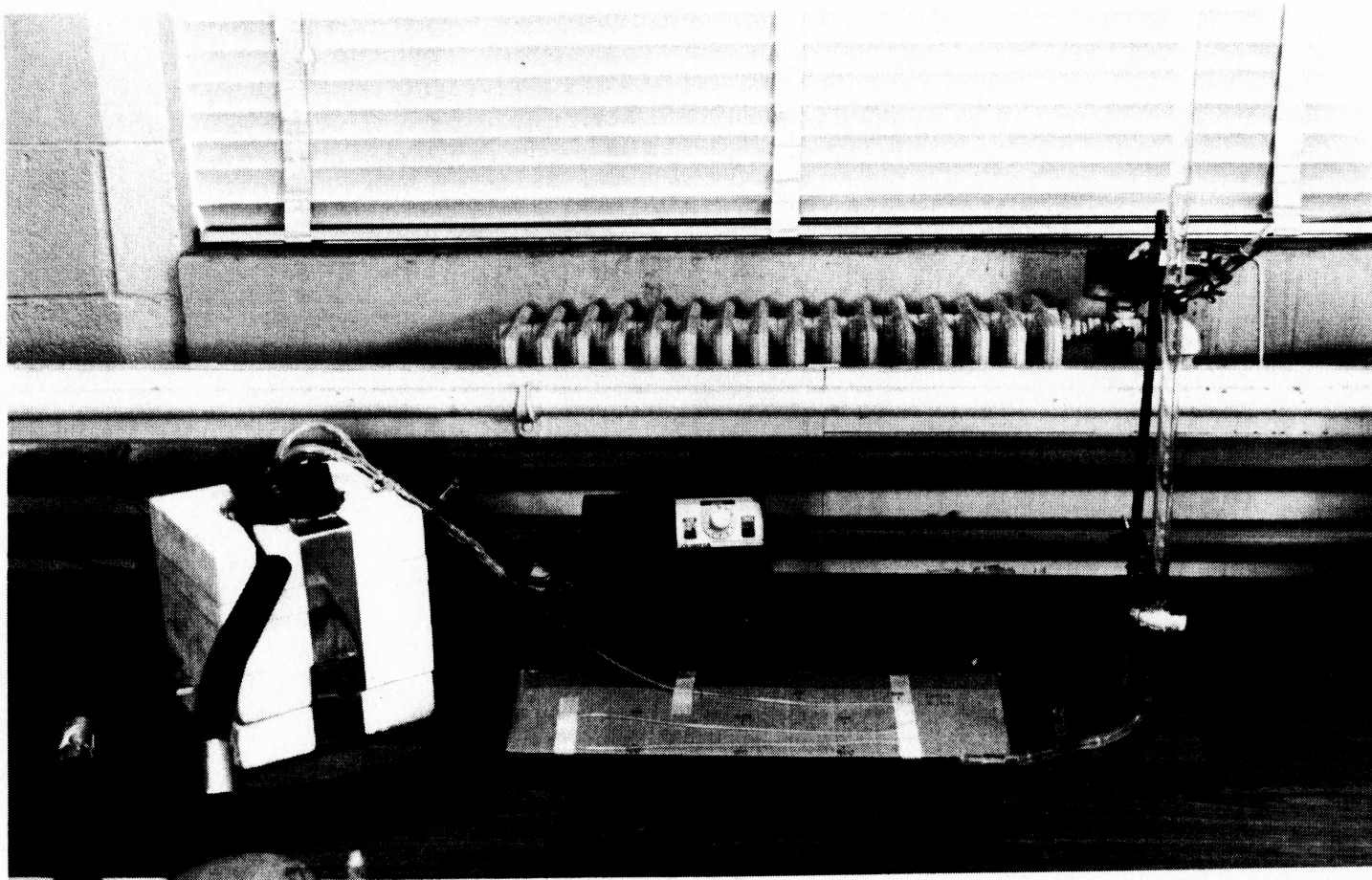
Figure 2.2.4   Insulated test cell with connection tubes to
constant   temperature   bath   (CTB),   digital
thermometer, capillary, and burette.
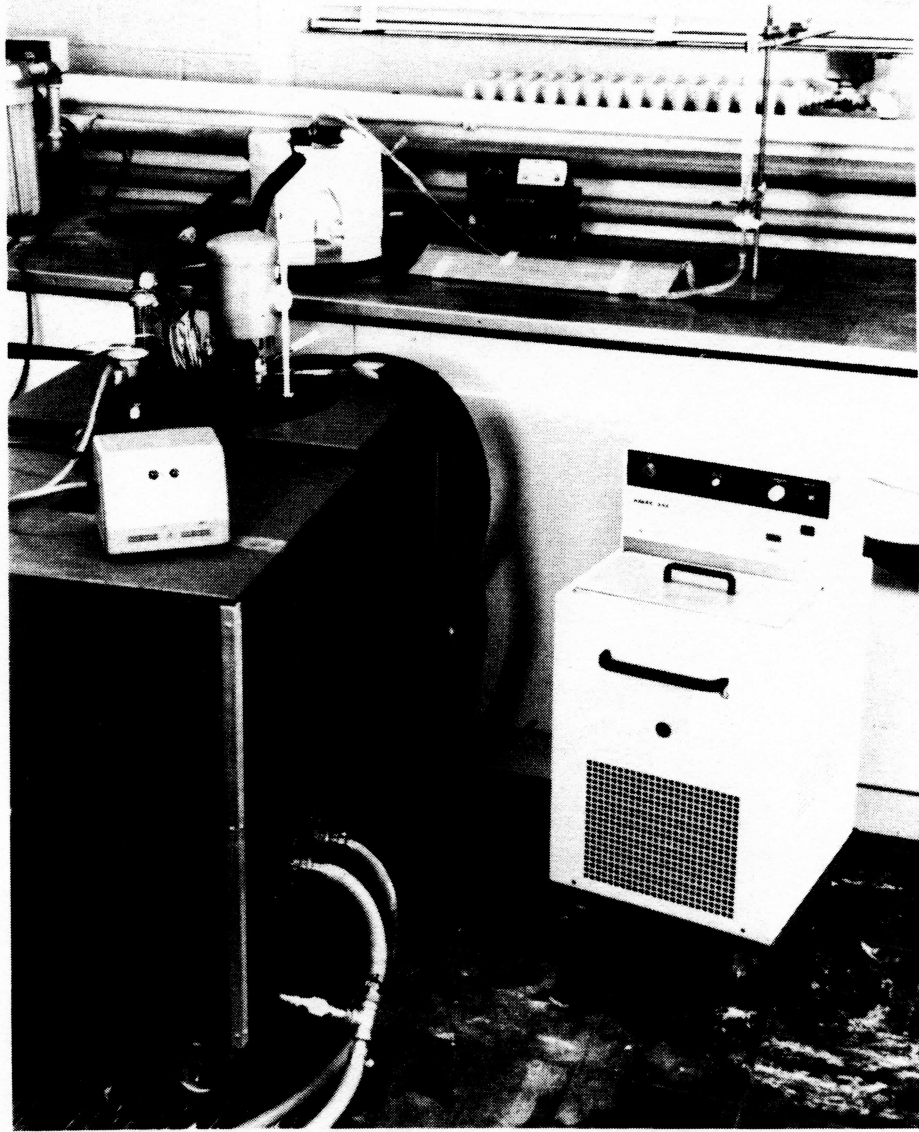
Figure 2.2.5   The complete experimental set-up.

Table 2.5.1   Porous media properties.

I.D.#	metal	Fig.#	shape	va	ρ	k_m	c_m	Φ
			mm	mm	kg/m^3	W/mK	J/kgK	
	aluminum	–	beads diameter:3.2	0.533	2702	220	880	0.424
	aluminum	–	beads diameter:12.	2.0	2702	220	880	0.532
1	aluminum	2.5.1	wool 0.5x0.05	0.0231	2700	155	880	0.989
2	aluminum	2.5.2	chips 5.84x0.15	0.0743	2700	155	880	0.903
3	aluminum	2.5.3	curls 0.0508x5.84	0.0252	2700	155	880	0.974
	copper	2.5.4	curls 0.5x4.0	0.5	8933	410	377	0.940
	brass	2.5.5	70%Cu,30%Zn;curls	0.0484	8530	106	375	0.956
	stainless steel	2.5.6	AISI 304;curls 0.1x3	0.0484	7900	14.3	457	0.959

Table 2.5.2   Properties of water.

T	ρ	k	c	$\alpha \times 10^9$
C	kg/m^3	W/m K	J/kg K	m^2/s
-10.0	998.156	0.530	4272.6	124.24
-5.0	999.291	0.544	4240.2	128.29
-4.0	999.447	0.546	4235.0	129.03
-3.0	999.582	0.549	4230.2	129.76
-2.0	999.696	0.551	4225.7	130.47
-1.0	999.792	0.554	4221.5	131.16
0.0	999.868	0.556	4217.6	131.83
1.0	999.927	0.558	4214.0	132.49
2.0	999.968	0.561	4210.7	133.13
3.0	999.992	0.563	4207.7	133.76
4.0	1000.00	0.565	4204.9	134.37
5.0	999.991	0.567	4202.3	134.97
6.0	999.968	0.569	4199.9	135.56
7.0	999.929	0.571	4197.7	136.14
8.0	999.876	0.573	4195.7	136.70
9.0	999.806	0.576	4193.9	137.26
10.0	999.727	0.578	4192.2	137.80
11.0	999.632	0.580	4190.7	138.34
12.0	999.525	0.581	4189.3	138.87
13.0	999.404	0.583	4188.0	139.38
14.0	999.272	0.585	4186.8	139.90
15.0	999.127	0.587	4185.8	140.40
16.0	998.971	0.589	4184.8	140.90
17.0	998.803	0.591	4184.0	141.39
18.0	998.624	0.593	4183.2	141.87
19.0	998.435	0.594	4182.5	142.35
20.0	998.234	0.596	4181.9	142.82
25.0	997.077	0.605	4179.6	145.11
30.0	995.678	0.613	4178.5	147.28
35.0	994.061	0.620	4178.2	149.36
40.0	992.249	0.627	4178.6	151.32

Table 2.5.3   Properties of ice.

T	ρ	k	c	α
C	kg/m^3	W/m K	J/kg K	m^2/s
-20.0	920.300	2.277	1961.3	1.261E-06
-19.0	920.154	2.270	1969.1	1.253E-06
-18.0	920.006	2.263	1976.9	1.244E-06
-17.0	919.854	2.257	1984.7	1.236E-06
-16.0	919.699	2.250	1992.5	1.228E-06
-15.0	919.541	2.244	2000.3	1.220E-06
-14.0	919.380	2.238	2008.1	1.212E-06
-13.0	919.216	2.232	2015.9	1.205E-06
-12.0	919.047	2.226	2023.7	1.197E-06
-11.0	918.876	2.221	2031.5	1.190E-06
-10.0	918.700	2.216	2039.3	1.183E-06
-9.0	918.521	2.210	2047.1	1.176E-06
-8.0	918.337	2.206	2054.9	1.169E-06
-7.0	918.149	2.201	2062.7	1.162E-06
-6.0	917.957	2.196	2070.5	1.155E-06
-5.0	917.761	2.192	2078.3	1.149E-06
-4.0	917.560	2.188	2086.1	1.143E-06
-3.0	917.355	2.184	2093.9	1.137E-06
-2.0	917.145	2.180	2101.7	1.131E-06
-1.0	916.930	2.176	2109.5	1.125E-06
0.0	916.710	2.172	2117.2	1.119E-06

The latent heat of fusion is given in [3] as

$$h_f = 333.432 \; kJ/kg$$

Figure 2.5.1   Aluminum wool.
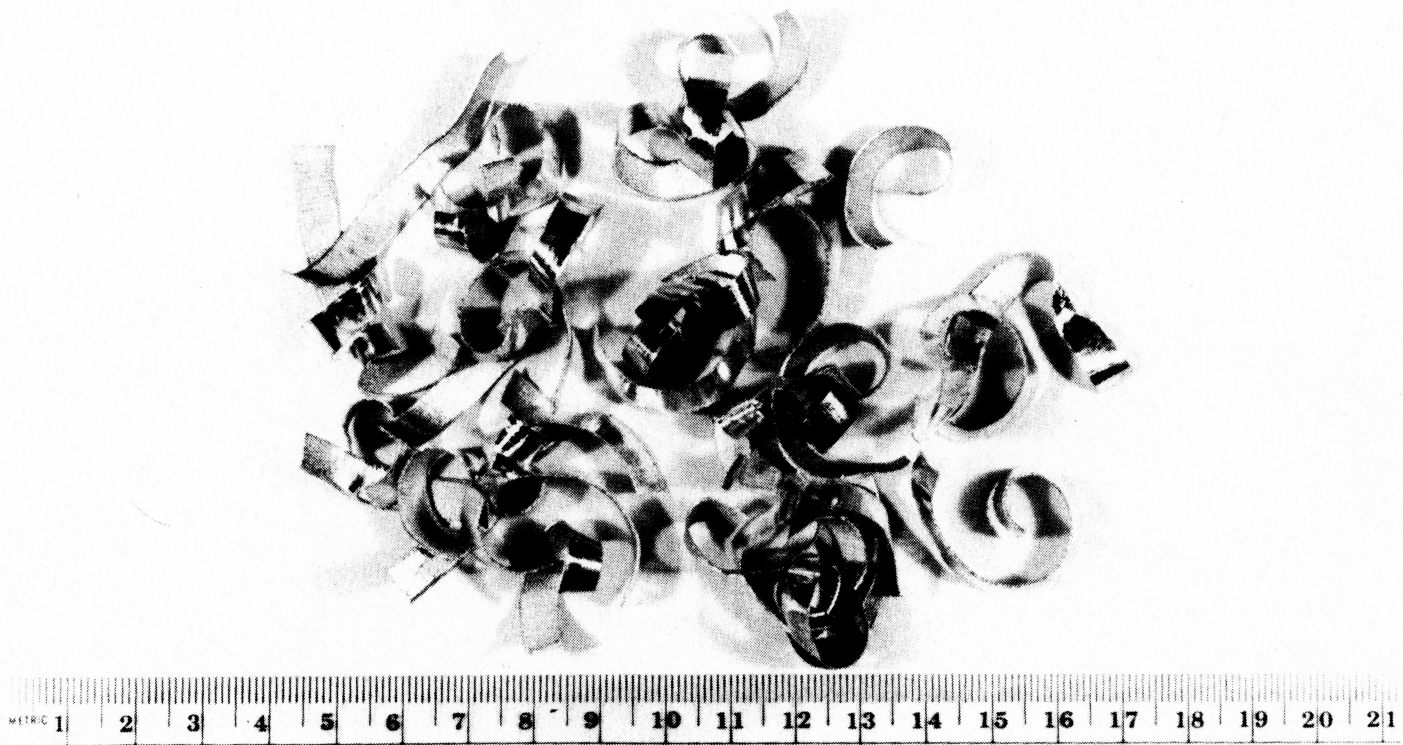
Figure 2.5.2   Aluminum chips.
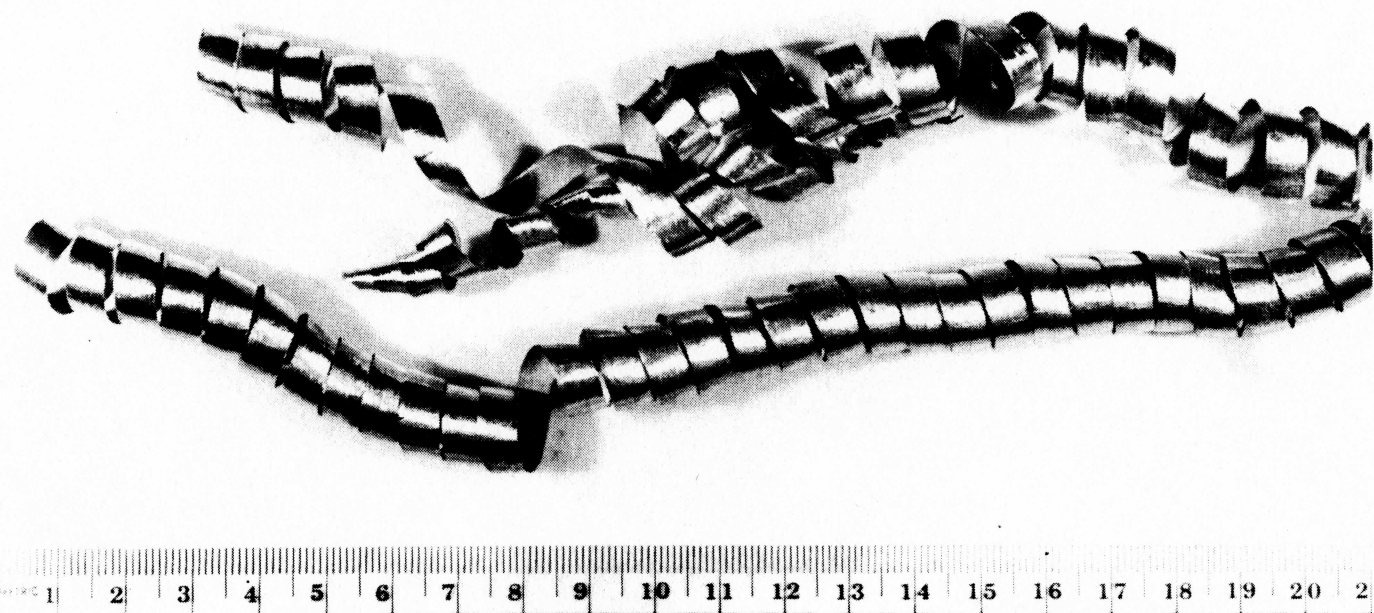
Figure 2.5.3   Aluminum curls.
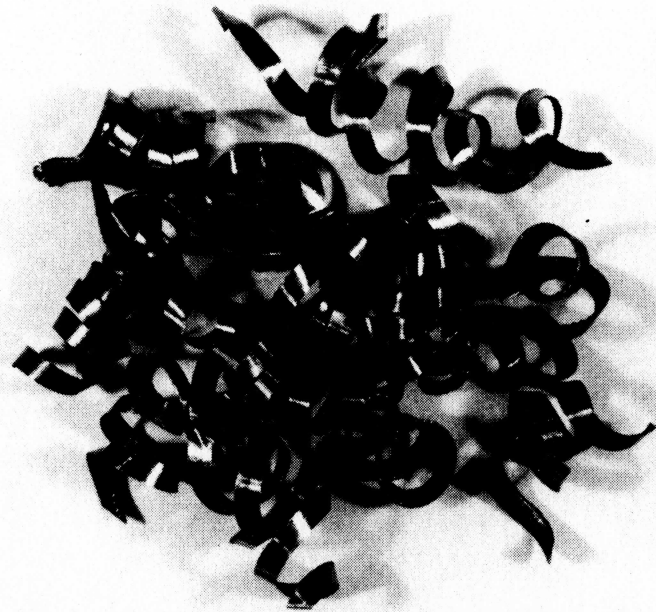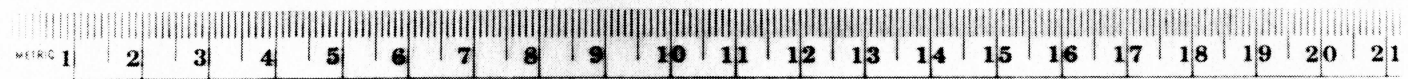
Figure 2.5.4   Copper.
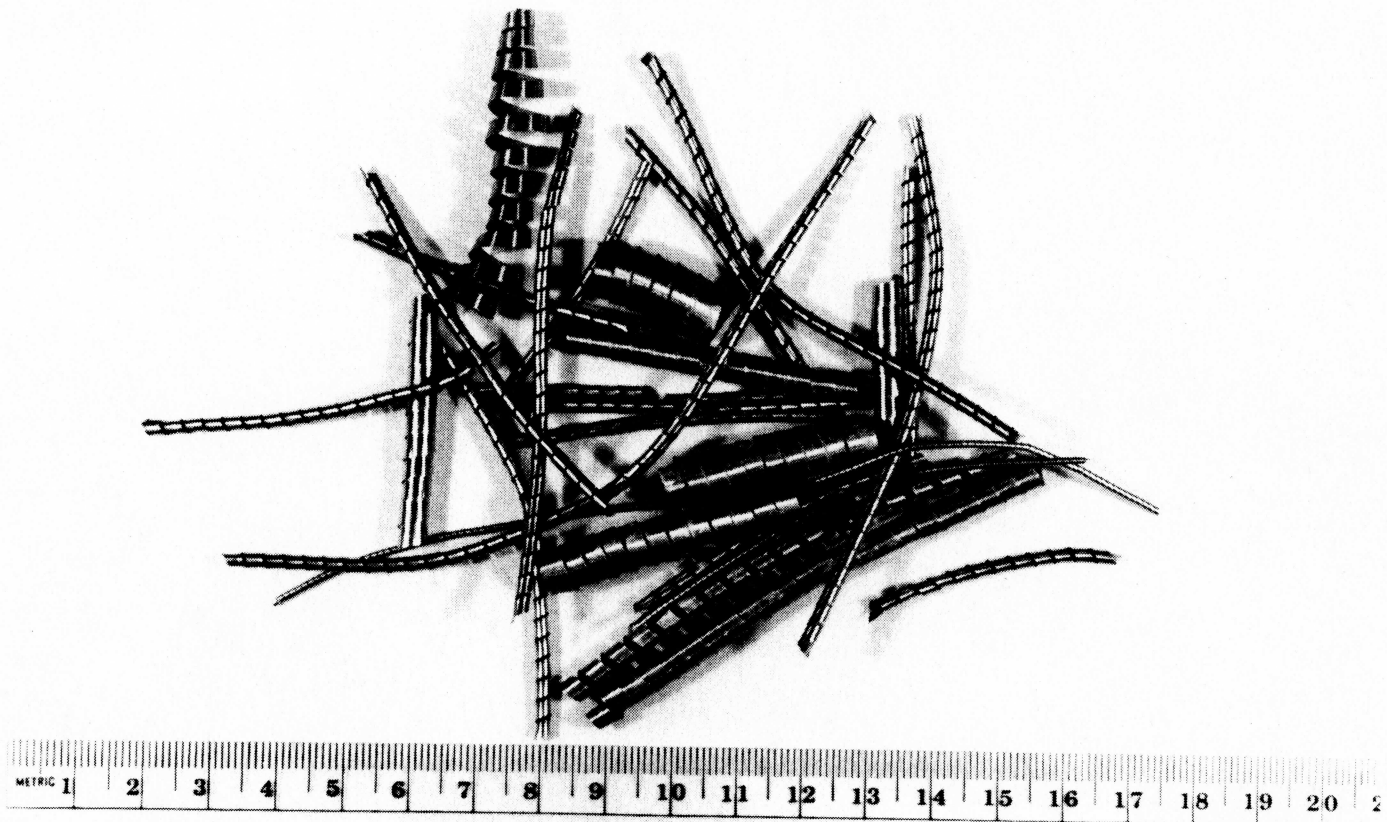
Figure 2.5.5   Brass.
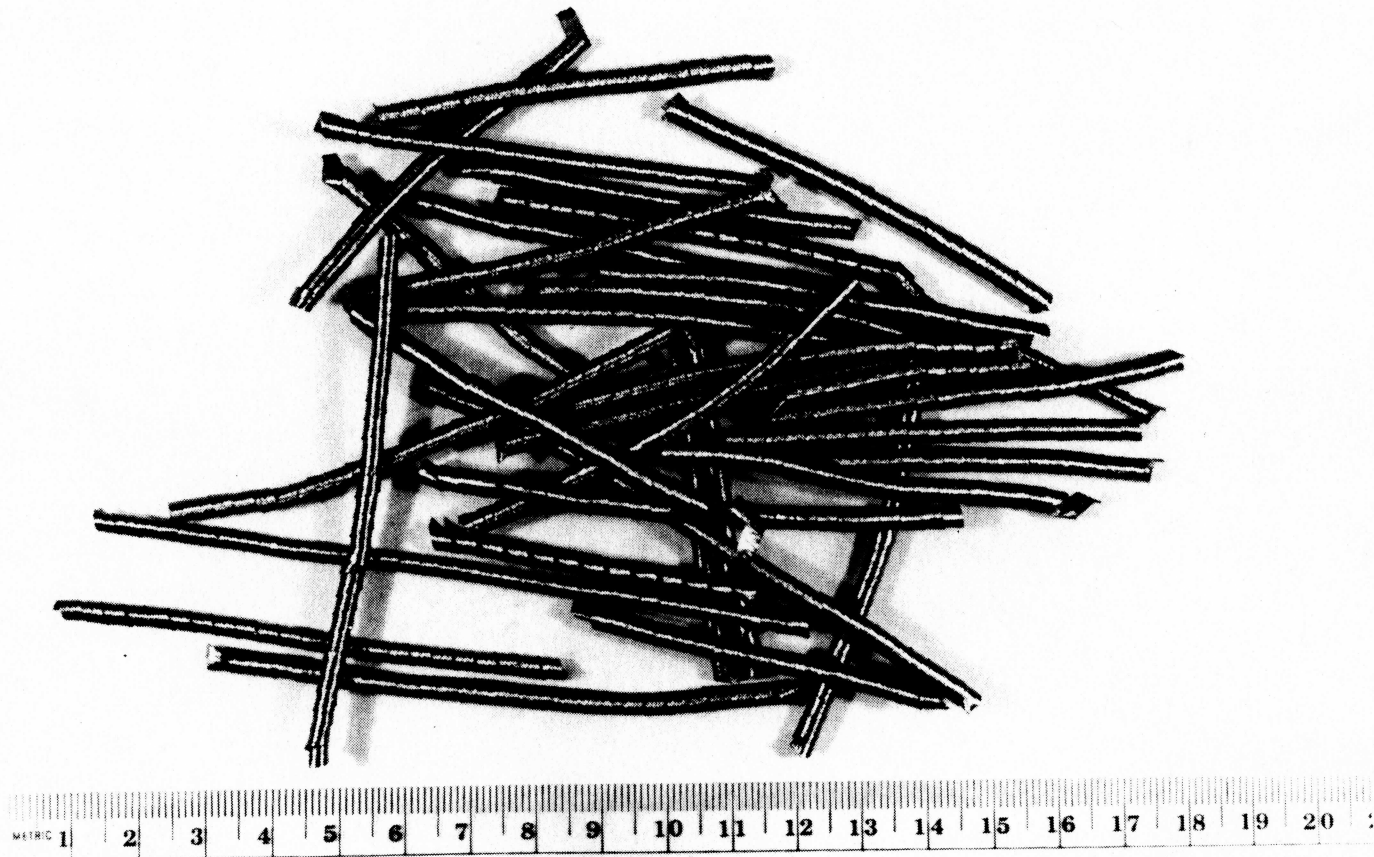
Figure 2.5.6   Stainless steel.

CHAPTER 3 - ANALYSIS

The resistance method is one of many which can be used to calculate freezing and melting. This method is applied to calculate the freezing and melting time in the test cell. The conductivity can then be calculated from the predicted and measured time for freezing and melting.

3.1 Calculation Methods

All methods used for measurements of thermal conductivity are based on an experiment which can be modeled and mathematically described. The first step for this description is to calculate the freezing and melting process which is done by calculating the fusion front position as a function of time.

An exact analytical closed form solution can not be obtained for the geometry of freezing or melting in a cylinder because nonlinearities introduced by the boundary conditions preclude exact solutions in a closed domain. However, in cases like this two methods commonly used yield a solution: the integral method and the finite difference method.

"The application of _integral_ _methods_ to the solution of problems involving the solidification of liquids initially at fusion temperature" is shown in [7]. Here formulas for a cylinder are given. The "Karman-Pohlhausen method" [7] assumes a simple one-parameter temperature profile and yields a simple formula for the freezing time as a function of the interface position. Unfortunately this method appears to fail when applied to the circular cylinder. The "Tami method" [7] assumes a two-parameter quadratic profile which makes the solution much more involved requiring numerical integration. This method still has only an accuracy of about 10 %.

The _finite-difference_ _method_ is applied by Weaver in his program for the cylinder. A finite-difference method is accurate to the extent allowed by the assumptions on which the method is based. Therefore the finite-difference method is used here to show the accuracy of the simple _resistance_ _method_.

3.2 The Resistance Method

The resistance method [8] analyzes freezing and melting on the basis of a variable resistance analog to account for the motion of the interface and the varying thickness of the solid or liquid phase, respectively.
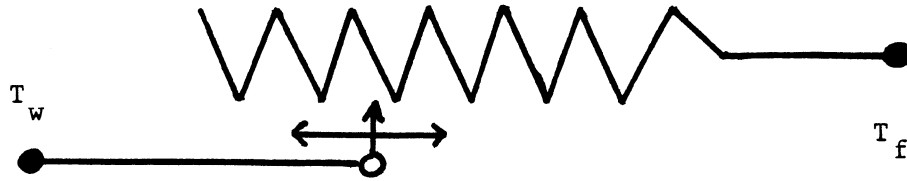
Fig. 3.2   The resistance method uses a variable resistance
            analog.

3.2.1   Calculation of Freezing and Melting Time

        Fig. 3.2.1 shows a schematic diagram of the test cell.
The cylinder is uniformly filled with porous medium and
liquid initially at uniform temperature of 0 ^{o}C. The fusion
front starts moving radially inward when a uniform wall
temperature T_w less than fusion temperature T_f for freezing
or $T_w > T_f$ for melting is imposed on the cylinder inside
surface.

        The assumptions made in the calculation are as fol-
lows:

1. Initial temperature is 0 ^{o}C.

2. The porous medium is isotropic (properties are not
    dependent on directions).

3. The porous medium is homogeneous and properties are constant in space.

4. Conduction is the dominant mode of heat transfer in both the solid and the liquid.

5. There is no bulk fluid motion due to the difference in density between the solid and liquid phase and natural convection is absent.

6. The porosity is constant.

7. The local temperatures of the phase in the voids and the porous medium are the same (i.e., there is no heat transfer between the porous medium and void phase constituent).

8. The fusion front movement is quasi steady and the temperature profile changes only slightly with time.

9. The sensible heat is negligible compared to the latent heat ($h_f \gg c_p^{\cdot} [T_f - T_w]$).

Freezing will be developed first. With the above assumptions we have a temperature distribution in the solid porous medium as in a hollow cylinder with a thermal resistance due to conduction

$$R_{t,cond} = \frac{\ln (R/r)}{2 \pi l k_{sm}} \qquad (3.2.1)$$

where l is the length of the cylinder and k_{sm} the conductivity of the solid phase of the porous medium. When the contact resistance at the interface formed by the wall and the ice layer is neglected, the total resistance is

$$R_t = \frac{1}{\dfrac{1}{R_{t,cond}} + \dfrac{1}{R_{t,conv}}} \qquad (3.2.2)$$

but with $R_{t,conv} = \infty$ in a solid we get

$$R_t = R_{t,cond}$$

Hence the heat rate flowing through the solid is

$$q = -\frac{T_f - T_w}{R_{t,cond}} \qquad (3.2.3)$$

where the minus sign indicates heat release. The heat rate leaving the cylinder can also be calculated from the latent heat multiplied by the rate of mass which is undergoing the phase change

$$q = h_f \frac{dm}{dt}$$

$$q = h_f \rho_{i,0} \; 2\pi r \; l \; \frac{dr}{dt} \; \Phi \qquad (3.2.4)$$

Note that h_f is defined for the density of ice $\rho_{i,0}$. Since the interface is at $0\ ^{o}C$, the density has to be determined at this temperature. Substituting Eq. (3.2.1) into Eq. (3.2.3) and realizing that Eq. (3.2.3) is equal to Eq.

(3.2.4) yields with separation of variables and integration

$$\int (T_f - T_w) \, dt = - \frac{h_f \, \rho_{i,0} \, \Phi}{k_{sm}} \int r \ln(R/r) \, dr$$

The wall temperature is often not constant in real application. For instance in the experiments for conductivity measurements (see Chap. 4) a transient wall temperature was observed. From the integration of the left hand side we get

$$\int (T_f - T_w) \, dt = \int T_f \, dt - \int T_w \, dt$$
$$= T_f \, t - T_{w,a} \, t$$
$$= (T_f - T_{w,a}) \, t$$

where $T_{w,a}$ is defined as the average wall temperature

$$T_{w,a} \equiv \frac{1}{t} \int T_w \, dt \qquad\qquad (3.2.5)$$

After the integration is performed the time t required for freezing to a radius r can be found.

$$t = \frac{- h_f \, \rho_{i,0} \, \Phi}{k_{sm}(T_f - T_{w,a})} \left(\frac{1}{2} r^2 \ln R - r^2 \left[\frac{1}{2} \ln r - \frac{1}{4} \right] \right) + C$$

The integration constant is obtained from the initial condition

$$r(t=0) = R$$

which yields the integration constant

$$C = \frac{h_f \, \rho_{i,0} \, \Phi}{k_{sm}(T_f - T_{w,a})} \frac{R^2}{4}$$

with which finally

$$t = \frac{h_f \, \rho_{i,0} \, \Phi}{k_{sm}(T_f - T_{w,a})} \left(\frac{1}{2} r^2 \ln(r/R) + \frac{1}{4}(R^2 - r^2) \right) \qquad (3.2.6)$$

or with

$$r/R \equiv x \qquad (3.2.7)$$

$$t = \frac{h_f \, \rho_{i,0} \, \Phi \, R^2}{k_{sm}(T_f - T_{w,a})} \left(\frac{1}{2} x^2 \ln x + \frac{1}{4}(1 - x^2) \right) \qquad (3.2.8)$$

The total freezing time $t_t = t(r=0)$ for freezing of the whole cylinder volume is obtained for the limit of t as r goes to zero. With the law of l´ Hospital

$$\lim_{r \to 0} r^2 \ln(r/R) = 0$$

$$t_t = \lim_{r \to 0} t = \frac{h_f \, \rho_{i,0} \, \Phi \, R^2}{4 \, k_{sm}(T_f - T_{w,a})} \qquad (3.2.9)$$

The derivation for <u>melting</u> is similar except that the heat of fusion has to be transported through the liquid porous medium. In contrast to the freezing case we have for the melting case convection as well as conduction heat transfer. The total resistance is again

$$R_t = \frac{1}{\frac{1}{R_{t,cond}} + \frac{1}{R_{t,conv}}} \qquad (3.2.2)$$

Unfortunately $R_{t,conv}$ is unknown for a porous medium in an enclosure of arbitrary shape. Therefore we define

$$R_t \equiv \frac{\ln(R/r)}{2\pi \, 1 \, k_{eff}} \tag{3.2.10}$$

Where k_{eff} is an effective conductivity including both the influence of conduction and convection. However k_{eff} is also not known yet but will be obtained from experiments. In contrast to the conductivity k_{sm} for the solid porous medium, the effective conductivity k_{eff} depends on the special geometry. We now follow the same procedure as done already for freezing. Heat has to be supplied to the system and hence we get a change of sign in the equation corresponding to Eq. (3.2.3) where heat was released. In the equation which corresponds to Eq. (3.2.4), ρ is still the density of ice at $0\,^{o}$C. Following the same steps further we obtain

$$t = \frac{h_f \, \rho_{i,0} \, \Phi}{k_{eff}(T_{w,a}-T_f)} \left(\frac{1}{2} \, r^2 \, \ln(r/R) + \frac{1}{4}(R^2-r^2) \right) \tag{3.2.11}$$

$$t = \frac{h_f \, \rho_{i,0} \, \Phi \, R^2}{k_{eff}(T_{w,a}-T_f)} \left(\frac{1}{2} \, x^2 \, \ln x + \frac{1}{4}(1-x^2) \right) \tag{3.2.12}$$

$$t_t = \frac{h_f \, \rho_{i,0} \, \Phi \, R^2}{4 \, k_{eff}(T_{w,a}-T_f)} \tag{3.2.13}$$

3.2.2 <u>Check of the Resistance Method with the Finite-Difference Program</u>

Weaver's program [5] for freezing in porous media in a cylinder was used to check the resistance method. The

assumptions on which this program is based are assumptions 2 through 7 from Chapter 3.2.1. The program solves the heat equation for the solid and liquid phase, respectively, using boundary conditions at the wall, the interface, and the center line together with the initial condition for the temperature of the porous medium (PM). The problem is that the location of the interface is not known a priori; therefore the heat equation has to be solved for small time steps repeatedly as the interface moves inward until the whole volume is frozen.

For the check of the resistance method, freezing of water (porosity: ϕ = 1.0) at an initial temperature T_i = 0 ^{o}C in the test cell was calculated. The results are shown in Table 3.2.2.

Table 3.2.2   Comparison of freezing time for resistance method and finite-difference method for water initially at 0 ^{o}C.

$T_{w,a}$	t_t Resistance Method	t_t Finite-Difference Method	Δ %
Freezing Time			
-20 ^{o}C	43.6 min	46.4 min	6.0
-10 ^{o}C	87.1 min	89.7 min	2.9
-5 ^{o}C	174.2 min	175.4 min	0.7

The error of the resistance method seems to be smaller or at least comparable to the error of the Tami method [7] (about 10 %) which requires many more calculations. The error of the resistance method is small if the wall temperature is close to 0 $^{\circ}$C because assumptions 8 and 9 match much better with reality. The total freezing time calculated from the resistance method is always less than the freezing time from the finite difference method because the former neglects the fact that the ice must be cooled down.

3.2.3 Conductivity Obtained from Average Wall Temperature and Freezing Time

The instantaneous wall temperature is known from the experiments at certain intervals and the freezing, respectively melting time is recorded. The average wall temperature $T_{w,a}$ is calculated from Eq. (3.2.5) which can practically be done with time weighted averaging, trapezoidal rule, or Simpson's 1/3 rule. The conductivities can now be calculated from Eq. (3.2.9) and Eq. (3.2.13). For freezing

$$k_{sm} = \frac{h_f \, \rho_{i,0} \, \Phi \, R^2}{4 \, t_t (T_f - T_{w,a})} \tag{3.2.14}$$

and for melting

$$k_{eff} = \frac{h_f \, \rho_{i,0} \, \Phi \, R^2}{4 \, t_t (T_{w,a} - T_f)} \tag{3.2.15}$$

3.3 Approximating the Conductivity for the Liquid Porous Medium

In contrast to the effective conductivity k_{eff} is the true conductivity k_{lm} not influenced by convection. This conductivity can be obtained from a first order approach based on two melting experiments: melting in a vertical cylinder and melting in a horizontal cylinder.

It is possible to calculate the conductivity k_{lm} from k_{eff} and a correction factor F.

$$k_{lm} = k_{eff} \ F \qquad\qquad (3.3.1)$$

We define the time ratio

$$c \equiv \frac{t_{t,h}}{t_{t,v}} \qquad\qquad (3.3.2)$$

In this equation is $t_{t,h}$ the total time for melting in the horizontal cylinder and $t_{t,v}$ the total time for melting in the vertical cylinder. The convection influence is of course different for these two geometries and therefore also the melting times will differ. The correction factor F depends on the amount of convection and this can be seen in the time ratio c. We assume F = F(c) to be linear. Two points of this function are already known.

First, for the time ratio c of water F must be chosen so that F corrects k_{eff} to $k_{lm} = k_{H_2O}$, the conductivity of

water which is known from tables. Hence

$$F(c=c_{H_2O}) = \frac{k_{H_2O}}{k_{eff_{H_2O}}}$$

Second, for c = 1 no convection is present (if there would be convection there would also be a difference between horizontal and vertical total melting time) and thus

$$F(c=1.0) = 1.0$$

Now the function F(c) can easily be drawn.
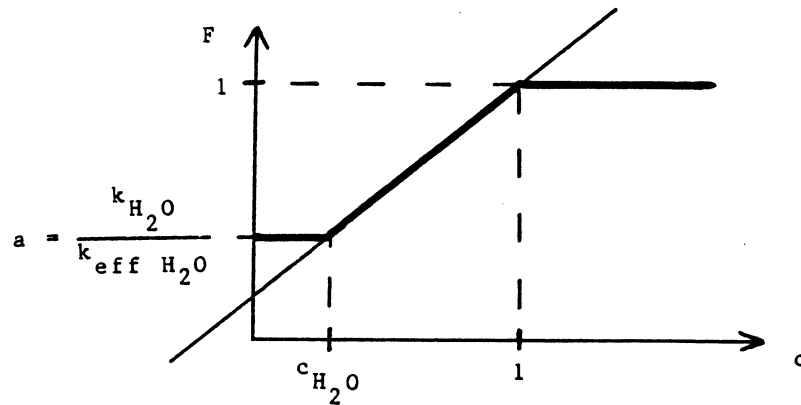
Fig. 3.3   The correction factor F as a function of the time ratio c.

$$F(c) = \begin{cases} 1.0 & \text{if } c > 1.0 \\ A\ c+B & \text{if } c_{H_2O} < c < 1.0 \\ a & \text{if } c < c_{H_2O} \end{cases} \qquad (3.3.3)$$

where

$$a \equiv \frac{k_{H_2O}}{k_{eff_{H_2O}}} \qquad (3.3.4)$$

$$A = \frac{1 - a}{1 - c_{H_2O}} \qquad (3.3.5)$$

$$B = 1 - \frac{1 - a}{1 - c_{H_2O}} \qquad (3.3.6)$$

3.4 Quality Criteria for Porous Media

There are several requirements for energy storage in a porous medium. These are previously mentioned in Chap. 1.4 and 1.5. Some requirements are influenced especially by the liquid in the PM; others are influenced by the PM itself. This thesis gives its attention to the PM and considers only water as the material undergoing phase change in the porous medium. Three new dimensions will be defined to quantify the storage behavior of the PM.

The heat storage power P shows the capability of a medium to store heat in a freezing or a melting process. High energy transfer Q in a short time gives a favorable high power P. As reference value we take the energy transfer necessary for total freezing of a volume and the related total freezing or melting time.

$$P = \frac{Q_t}{t_t} \qquad (3.4.1)$$

$$Q_t = ([c_m \rho_m (1-\Phi) + c_{ice} \rho_{ice} \Phi] T_m + h_f \rho_{i,0} \Phi) V \qquad (3.4.2)$$

with volume V, porosity ϕ, and mean temperature

$$T_m = \frac{1}{2} (T_w + T_f) \qquad (3.4.3)$$

For the cylinder we can take the results from the resistance method for the total freezing or melting time t_t, Eq. (3.2.9) or Eq. (3.2.13), and substitute them together with Eq. (3.4.2) into Eq. (3.4.1).

$$P = ([c_m \rho_m (1-\Phi) + c_{ice} \rho_{ice} \Phi] T_m + h_f \rho_{i,0} \Phi) \frac{k}{h_f \rho_{i,0} \Phi}$$
$$4\pi l \quad ABS(T_f - T_w) \qquad (3.4.4)$$

The first line in this equation is a first quality value, the _performance_ _factor_

$$pf = ([c_m \rho_m (1-\Phi) + c_{ice} \rho_{ice} \Phi] T_m + h_f \rho_{i,0} \Phi) \frac{k}{h_f \rho_{i,0} \Phi} \qquad (3.4.5)$$

The performance factor pf is independent of geometry which is described with the geometry factor (here for example $4 \pi l$ for the cylinder) and independent of the driving potential $ABS(T_f - T_w)$. ABS is the absolute value function. The conductivity k is the solid porous media conductivity k_{sm} for freezing and the effective conductivity k_{eff} for melting. For phase change in a sphere the geometry factor would be $8 \pi R$ where R is the radius of the sphere, and $2 A/x$ would be the geometry factor for the plane wall, where A is the area of the wall and x the fusion front dis-

tance from the wall. The performance factor has units of conductivity W/mK.

The _energy density_ Q''' is a second quality value.

$$Q''' = \frac{Q_t}{V} = [c_m \rho_m (1-\Phi) + c_{ice} \rho_{ice} \Phi] \, T_m + h_f \, \rho_{i,0} \, \Phi \qquad (3.4.6)$$

Since we are looking for a number showing the overall suitability of a porous medium, we multiply pf and Q''' to get a number which we call the _storage factors_

$$s = pf \quad Q''' \qquad (3.4.7)$$

For the evaluation of the experimental data $T_m = -10 \, ^{\circ}C$ was taken for freezing and $T_m = 10 \, ^{\circ}C$ for melting.

3.5   Calculated Conductivities of Porous Media

For a system with a single phase occupying the void and a single porous medium, different models can be found to calculate the overall thermal conductivity.

The _series model_ assumes that the porous medium behaves like a set of alternate layers of fluid and solid perpendicular to the mean heat flow. This assumption gives the thermal conductivity

$$k_{1m} = \frac{1}{\dfrac{1 - \Phi}{k_m} + \dfrac{\Phi}{k_1}} \qquad (3.5.1)$$

where the subscript 1m, m, and 1 refer to the effective

liquid property influenced by the porous media, the porous medium and the liquid phase occupying the void, respectively. Similarly, the corresponding equation for a solid phase occupying the void is obtained by merely replacing the subscript lm and l with sm and s, respectively, which refer to the effective solid property influenced by the porous medium and the solid phase occupying the void.

The _parallel_ _model_ also concerns a set of layers, but the mean heat flux is parallel to the direction of the layers.

$$k_{lm} = k_m (1-\Phi) + k_l \Phi \qquad (3.5.2)$$

The _Lichteneker_ _geometrical_ _model_ is listed in [9]

$$k_{lm} = k_l \frac{2-\Phi-(1-\Phi)^{1/3} + \frac{k_l}{k_m}((1-\Phi)^{1/3}-(1-\Phi))}{1 - (1-\Phi)^{1/3} + \frac{k_l}{k_m}(1-\Phi)^{1/3}} \qquad (3.5.3)$$

Also listed in [11] is the _empirical_ _model_ which can be obtained from dimensional analysis.

$$k_{lm} = k_l^{\Phi} k_m^{(1-\Phi)} \qquad (3.5.4)$$

Veinberg [10] proposed a _model_ which claims to be universally applicable for a medium with randomly distributed spherical inclusions. The nonlinear implicit equation is

$$k_{lm} + \Phi \frac{k_m - k_l}{k_l^{1/3}} k_{lm}^{1/3} - k_m = 0 \qquad (3.5.5)$$

In [11] is the <u>Zehner</u> <u>and</u> <u>Schluender</u> <u>model</u> set out.

$$\frac{k_{1m}}{k_1} = [1 - \sqrt{1-\Phi}] + \frac{2\sqrt{1-\Phi}}{1-\lambda G}$$

$$\left[\frac{(1-\lambda)G}{(1-\lambda G)^2} \cdot \ln(\frac{1}{\lambda G}) - \frac{G+1}{2} - \frac{G-1}{1-\lambda G} \right] \qquad (3.5.6)$$

where

$$G = H \left[\frac{1-\Phi}{\Phi}\right]^{10/9}$$

and

$$\lambda = \frac{k_1}{k_m}$$

The geometry factor H is 1.25 for spheres and 1.4 for broken particles. This formula is not defined for all combinations of k_m, k_1, and Φ because for

$$k_m = 1.25 \ k_1 \ \left[\frac{1-\Phi}{\Phi}\right]^{10/9}$$

the denominator $1-\lambda G$ becomes zero. For this special case a formula is given in [11]. In order to illustrate the first five formulas and to show the different behavior of the functions, these formulas are plotted for a water metal system and an ice metal system, respectively. The plots are three-dimensional plots showing the conductivity k_m and the porosity Φ in the horizontal plane and the result, the effective PM conductivity, on the z-axis vertical. The related Figures are Fig. 3.5.1 through Fig. 3.5.10.

The parallel and the series model are the limits of a possible effective PM conductivity. The other models mentioned above have different shapes lying embedded within these limits.

Comparison of experimental data with the Zehner and Schluender formula shows that the formula overpredicts for shavings by about 50 % and underpredicts for the beads by about 60 %. In the following text it is not further accounted for the Zehner and Schluender formula. The validity of the other formulas is checked in Chapter 4 and Appendix A.
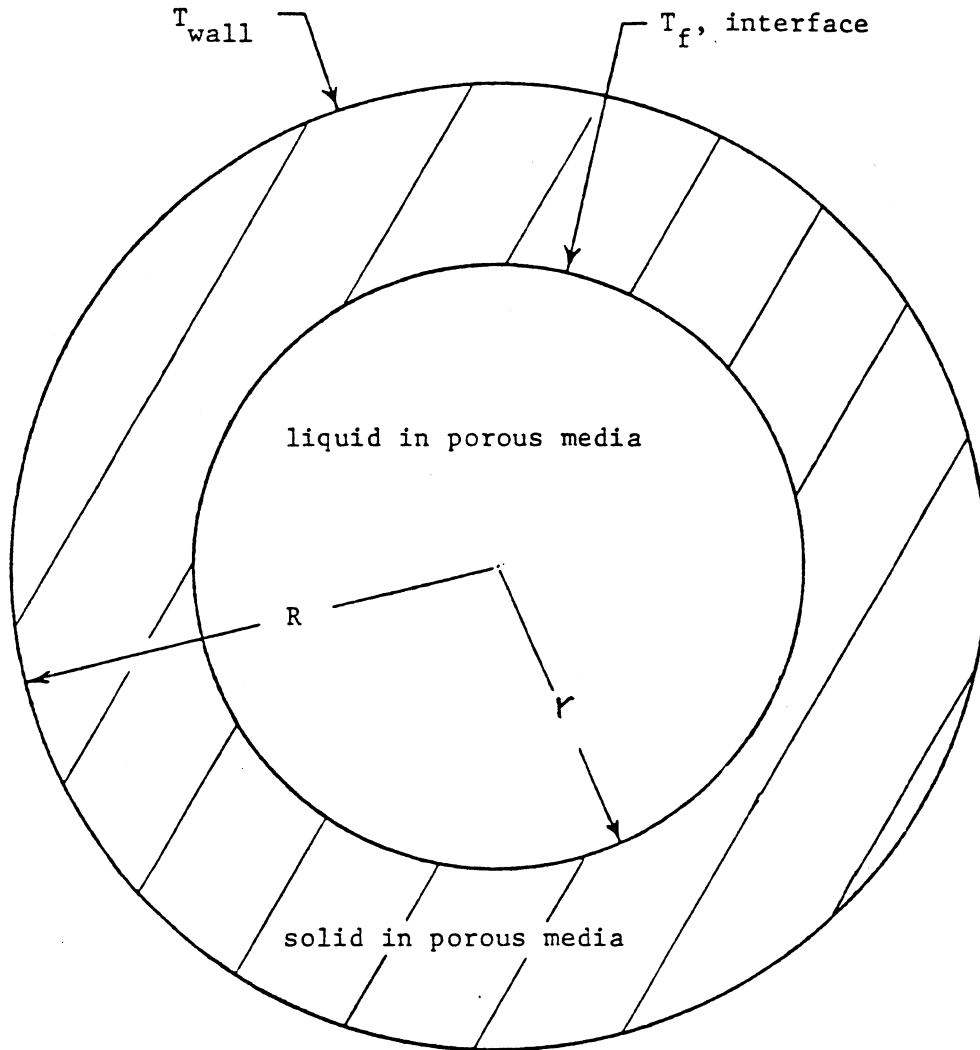
Figure 3.5.1   Schematic of the test cell. Freezing   with
                inward interface motion. [5]
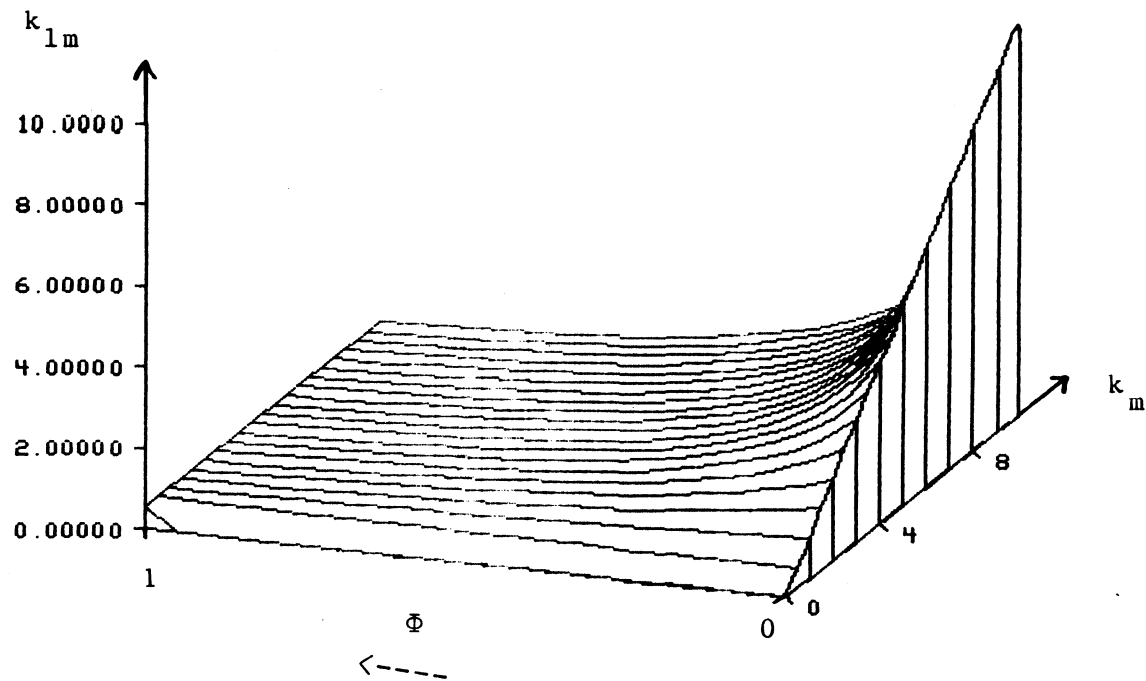
Figure 3.5.2   Thermal conductivity   of   water   and   porous
medium calculated by using the series model.
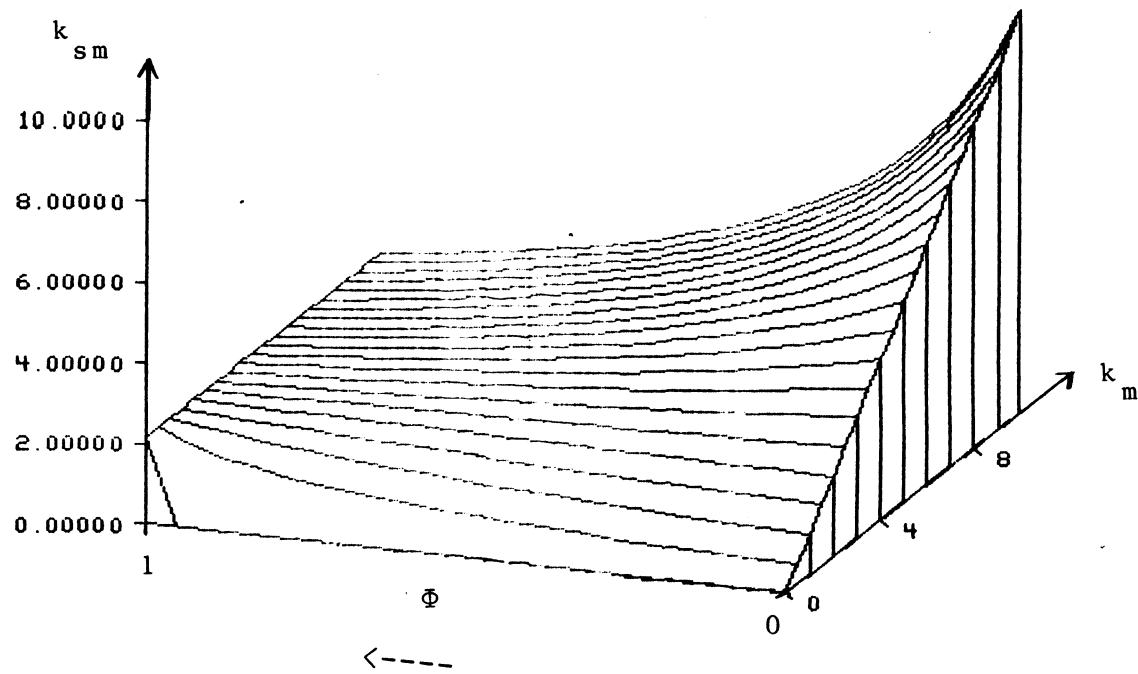
Figure 3.5.3   Thermal   conductivity   of   ice   and   porous
medium calculated by using the series model.

k_{1m}

10.0000

8.00000

6.00000

4.00000

2.00000

0.00000

k_m

8

4

0

Φ

$\longleftarrow ----$

1

0
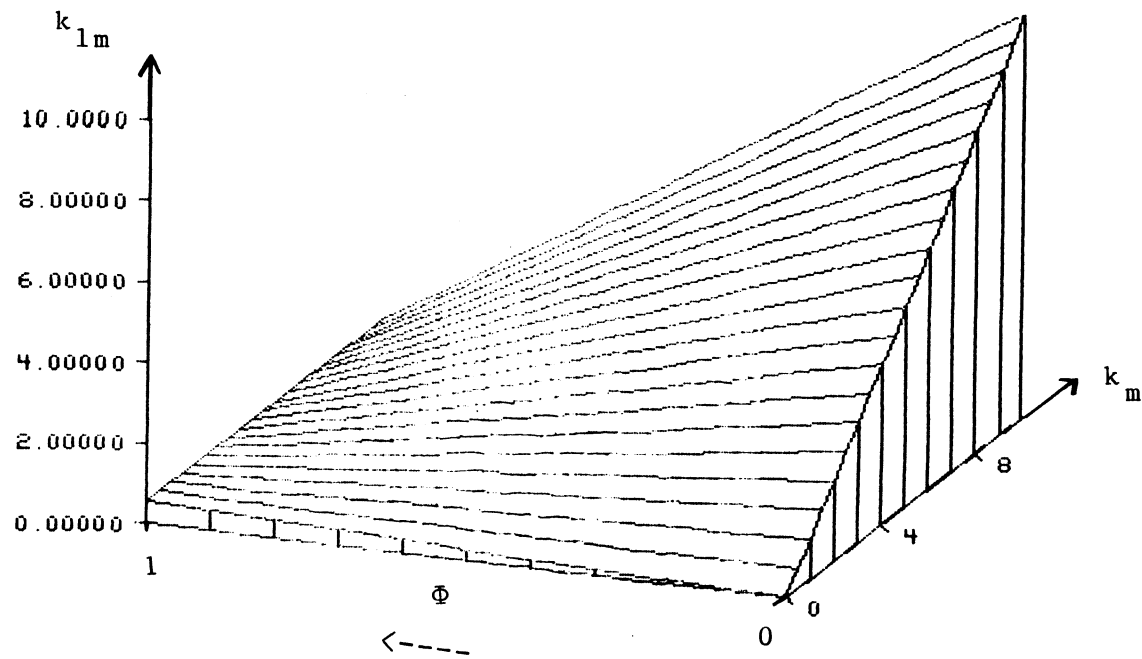
Figure 3.5.4   Thermal conductivity of water and porous medium calculated by using the parallel model.
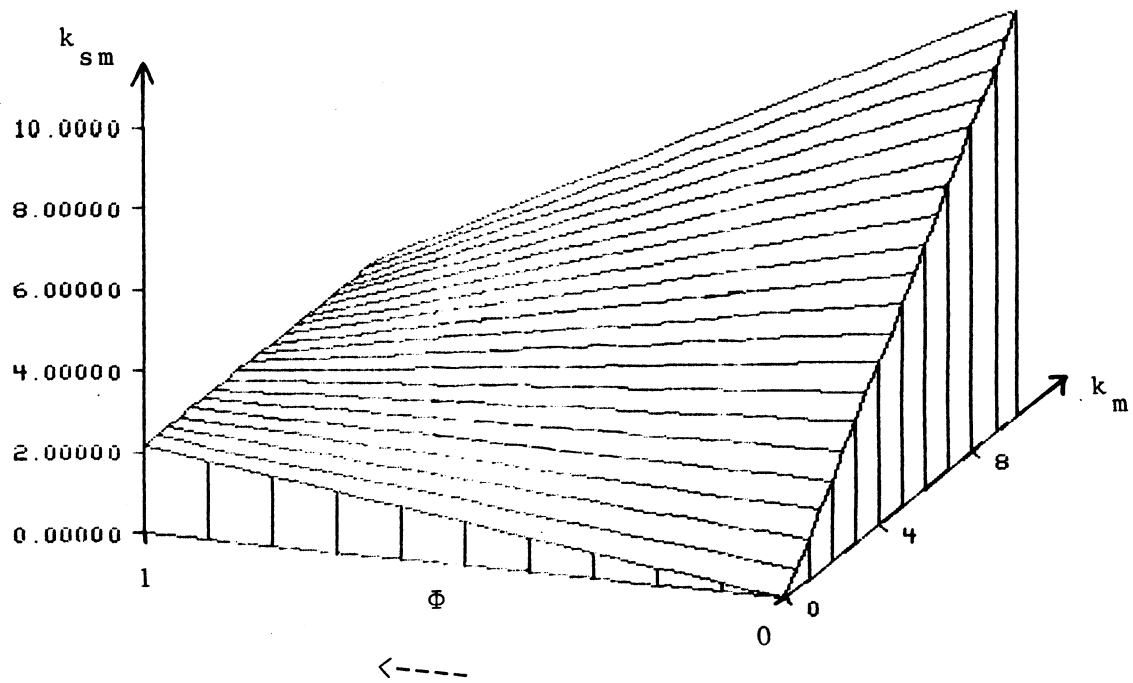
Figure 3.5.5   Thermal conductivity of ice and porous
medium calculated by using the parallel
model.
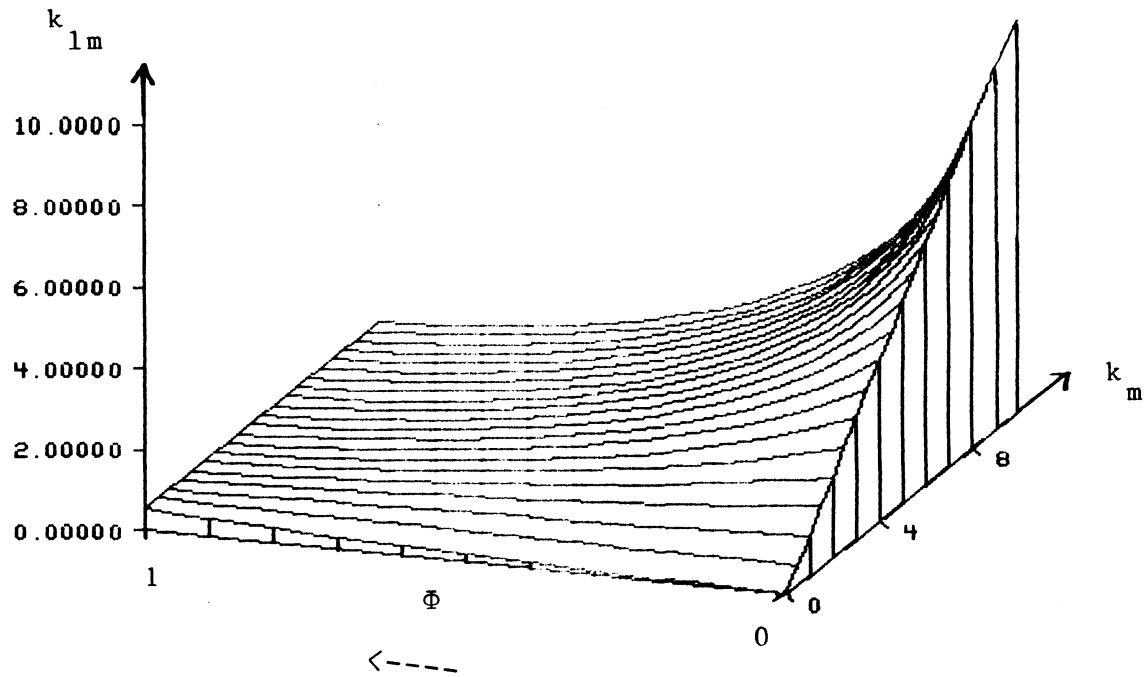
Figure 3.5.6　　Thermal conductivity of water and porous medium calculated by using the Lichteneker geometrical model.
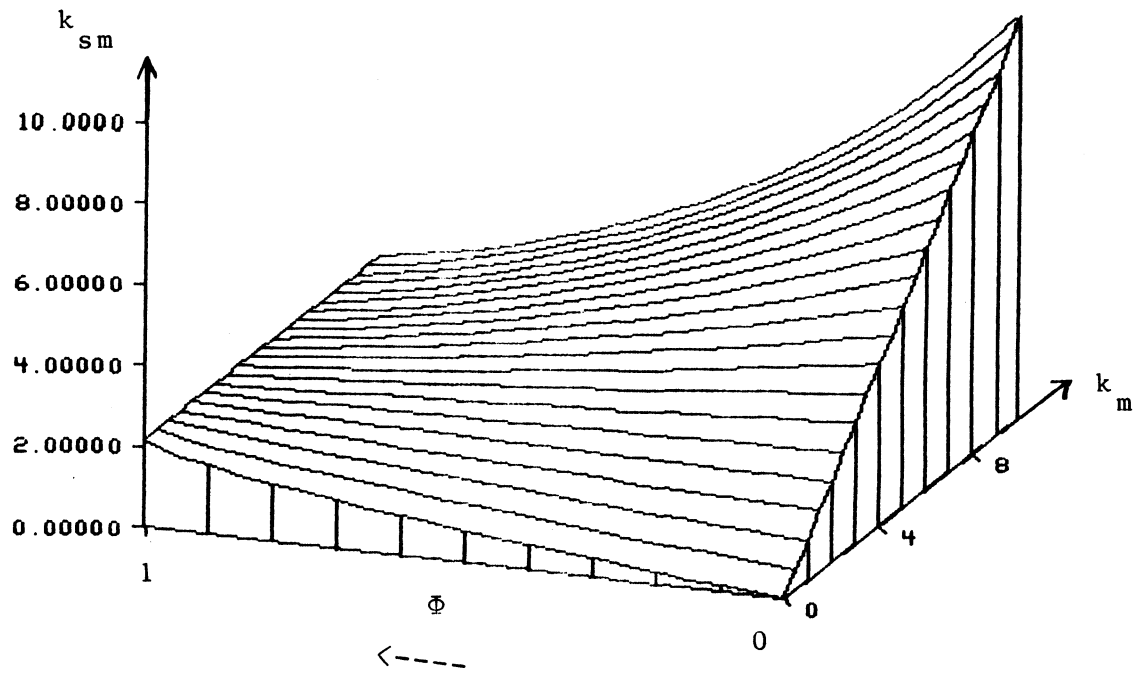
Figure 3.5.7   Thermal conductivity of ice and porous medium calculated by using the Lichteneker geometrical model.
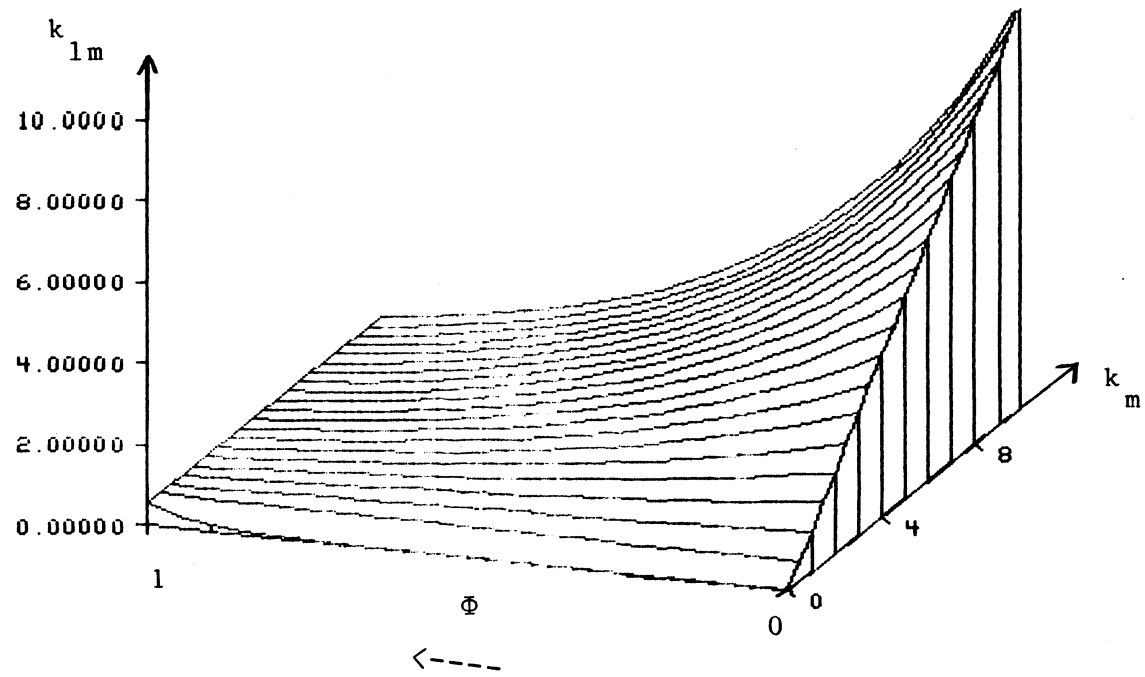
Figure 3.5.8   Thermal conductivity of water and porous
medium calculated by using the empirical
model.
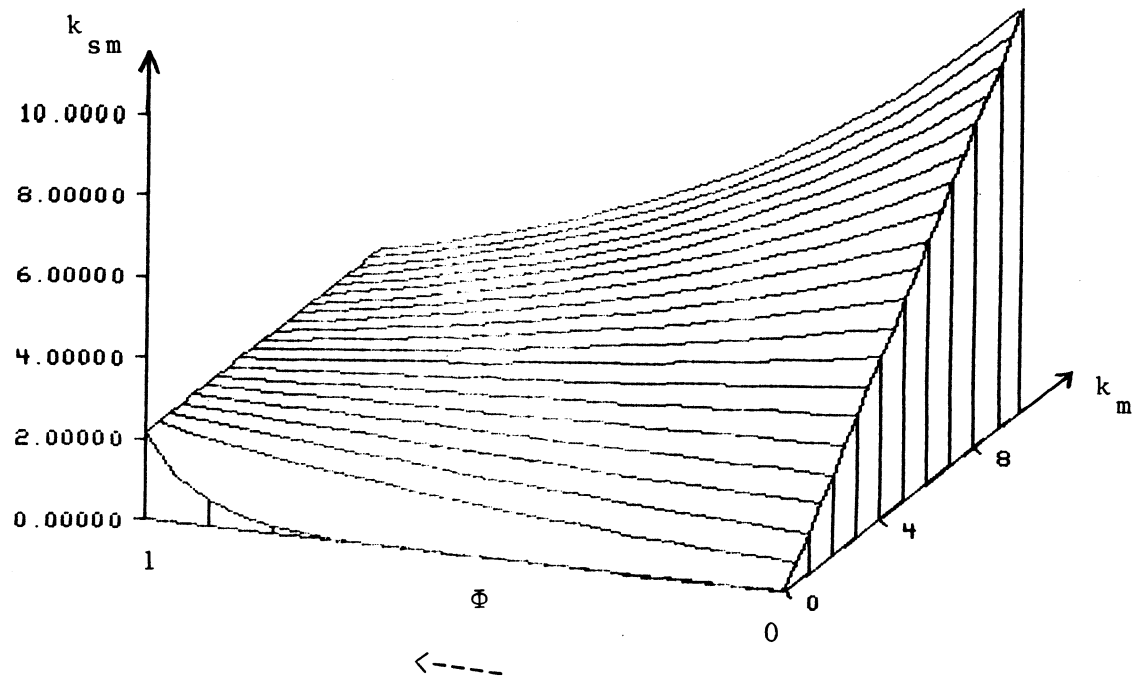
Figure 3.5.9   Thermal   conductivity   of   ice   and   porous
medium   calculated   by   using   the   empirical
model.
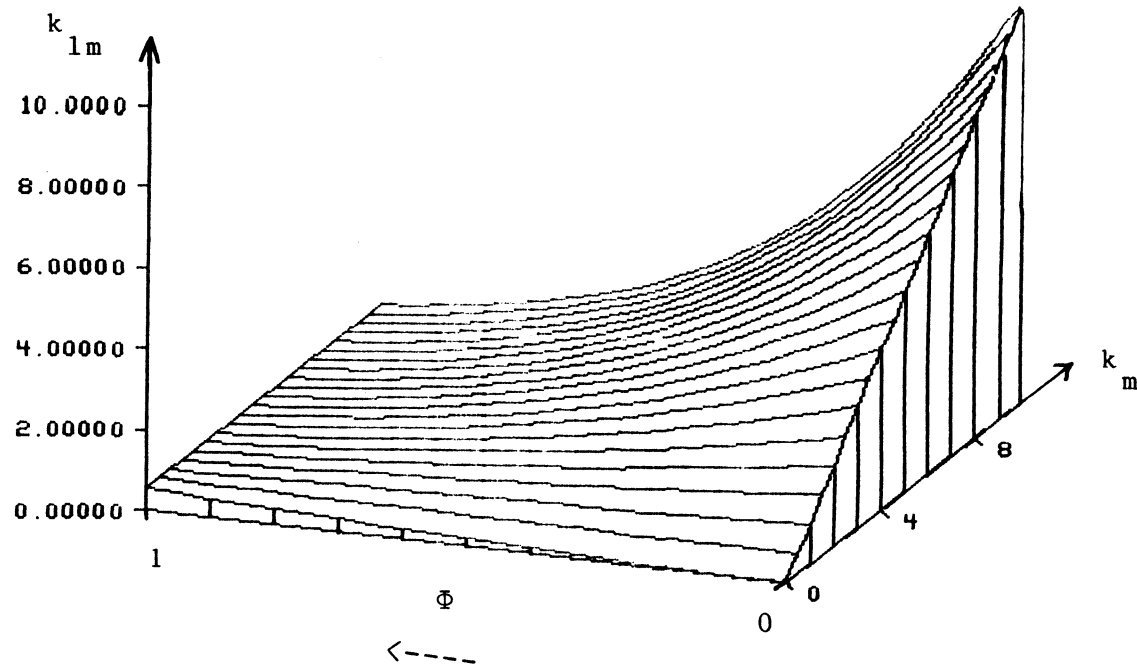
Figure 3.5.10   Thermal conductivity of water and porous
medium   calculated   by   using   the   Veinberg
model.
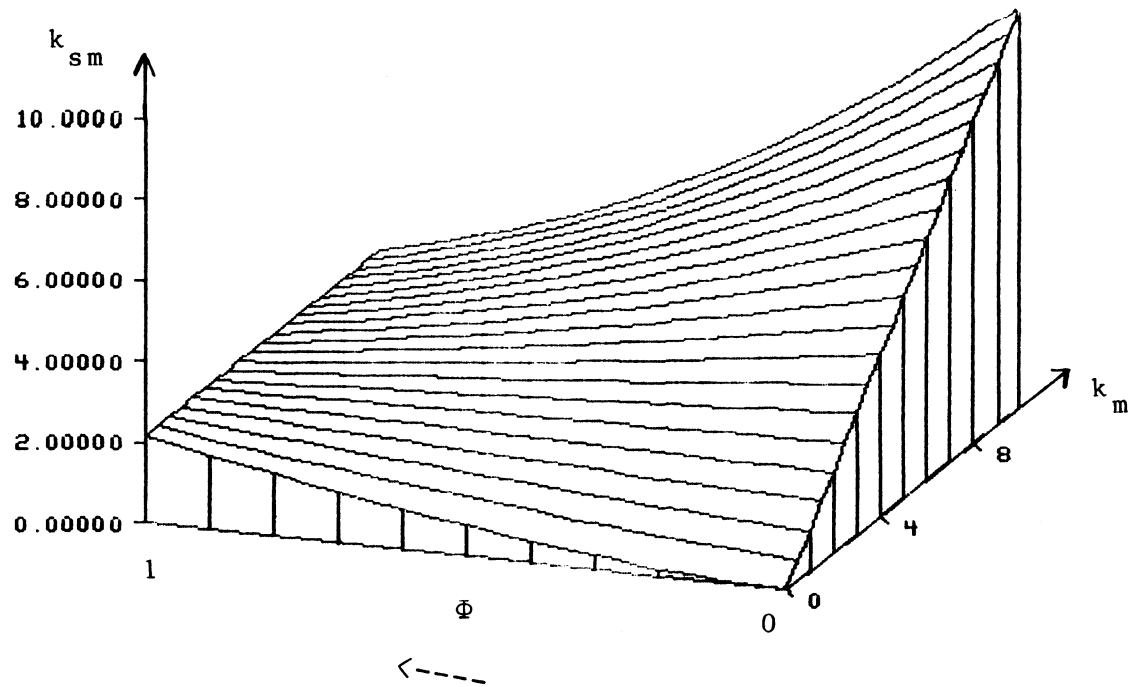
Figure 3.5.11   Thermal   conductivity   of   ice   and   porous
medium   calculated   by   using   the   Veinberg
model.

CHAPTER 4 - EXPERIMENTS

Previous to measurements of the conductivity of porous media, experiments were performed only with distilled water in order to check, the apparatus, the method, and the accuracy of the measurements.

4.0.1 Experimental Data

Thirty-five experiments were performed for the thesis. The data of these experiments were evaluated by a computer program. The output of this program is given in the Appendix A. Each experiment covers two pages in the Appendix. The first page describes the porous medium, melting or freezing conditions, total time for phase change, measured conductivities, conductivities for comparison, especially those obtained from five conductivity models, and values of the three defined quality criteria. On the second page a plot of the phase change as a function of time is shown. The solid line shows the observed phase change process. Every star on the line marks one measured value. The dashed and dotted lines show the phase change process calculated with the resistance method and average wall

temperature from Eq. 3.2.8, Eq. 3.2.12. The percentage of phase change is calculated from the radius of the interface by

$$\text{percentage of phase change} = (1-x^2) \cdot 100 \ \%$$

The dashed line uses the true conductivities without convection influence. Only for melting a dotted line is plotted which shows the phase change as it would be with a constant effective conductivity for the whole experiment. The dotted line for melting and the dashed line for freezing always lie above the solid line because the actual wall temperature in the first part of the experiment is closer to $0 \ ^{o}C$ than the average wall temperature. This means that the actual driving potential in the beginning is smaller than assumed, because using the average wall temperature throughout the whole experiment yields less phase change. For comparison, values of interest are taken from Appendix A and are given in tables incorporated in this text.

4.0.2 Determination of Beginning and End of Phase Change

For accurate measurements, the exact freezing and melting time has to be determined which means that the beginning and the end of the phase change has to be ascertained exactly. This was done by observing the movement of the air bubble in the capillary. After the flow of the coolant through the heat exchanger was initiated for a

freezing experiment, the air bubble first moved quickly towards the test cell because the test cell shrank when the wall was suddenly cooled. Thereafter, the same movement continued when the water cooled down. When the ice formation started, the air bubble jumped towards the burette where it left the system. However, when freezing experiments having an average wall temperature of about $-10\ ^{\circ}C$ or less were performed, it was observed that ice was already formed a few seconds after the coolant flow was initiated. This means that for low temperatures, observations of the air bubble were not necessary. The same behavior was observed for melting experiments - the melting started nearly without any delay after the flow of the CTB-fluid through the heat exchanger was started. The end of the phase change, that is the time when everything in the test section is frozen or thawed, was more difficult to detect. The percent volume change in a cylindrical test cell is a logarithmic function of time which means that the volume change rate gets smaller and smaller with time, making it more difficult to determine the end of the phase change. Of course here also observations of the air bubble achieved a higher accuracy compared to observation of the water level in the burette. Observations with air bubble and burette were checked by temperature measurements in the test section. When a thermocouple makes contact with the fusion front, its temperature changes within a few seconds. The

thermocouples on the center rake were therefore used to check the phase change end.

4.1 Measurements with Distilled Water

4.1.1 Freezing

Freezing with temperatures of the coolant of less than $-10\,^{\circ}C$ instantly gives an ice layer on the inner cylinder wall. In the vertical test cell position this ice layer grows almost exactly cylindrically inward. For horizontal freezing however, a water volume shaped like a funnel remained unfrozen below the top cap for about four minutes so that the end of the freezing process was much less sharply defined. Thus the vertical position of the test cell was chosen for later freezing experiments.

Dendritic ice forms when water is supercooled considerably below $0\,^{\circ}C$ before nucleation occurs. It consists of crystals which form thin plates dispensed in the water. The ice growth occurs only in the supercooled region and ends at the $0\,^{\circ}C$ isotherm. The quantity of the dendritic ice that is formed can be related to the amount of subcooling

$$\frac{m_{ice}}{m_{H_2O}} = \frac{c_{H_2O}\,(T_f - T_n)}{h_f}$$

where T_n is the nucleation temperature.

Subcooling and formation of dendritic ice was observed in the freezing experiment #3 with an average wall temperature of -4.1 ^{o}C. The water initially at -0.1 ^{o}C cooled down within 43 minutes to a uniform temperature of -4.0 ^{o}C. Initiated by a hit on the test cell, nucleation occurred. Dendritic ice was instantaneously formed, shooting from the wall right into the center of the test cell since all of the water was at a temperature below 0 ^{o}C. The water in between the dendrites was again at 0 ^{o}C after the dendritic ice was formed. The burette showed a displacement due to nucleation of 3 ccm. Thereafter normal ice formation started at the cylinder wall, incorporating the ice dendrites, until the whole test section was frozen.

Subcooling and dendritic ice formation should be avoided for LHTES systems because it precludes heat transfer at a constant temperature. Furthermore, it requires a longer freezing time because water which conducts heat before nucleation has a lower conductivity than ice.

4.1.2 Melting

For melting, none of the two positions of the test cell yield exact uniform radial interface movement because of convection effects, meaning that the applied phase change model describes the melting process not fully exact.

In the _vertical_ position, the warm water moves to the top so that the ice at the top of the test cell melts faster. Accordingly, at the end of the experiment the rest of the ice is approximately shaped like a parabolic cone placed in the middle of the bottom of the test cell. For _horizontal_ melting, it could be observed that an ice rod remained in the center of the test cell diminishing in diameter. The melting did not occur concentricly but around a line below the center line of the cylinder, due to the fact that the rising warm water causes a higher melting rate on top of the rod. At the end of the experiment the center of the ice rod was approximately 10mm away from the center line of the cylinder. Nevertheless, when the remaining piece of ice finally lost its contact with the thermocouple rake, it floated up and was quickly melted due to direct contact with the warm cylinder wall. The ice rod in these melting experiments showed grooves cut into the ice-water interface in planes perpendicular to the axis of the cylinder. The grooves were deepest under the ice rod and became shallower towards the top. In experiment #6 with an average wall temperature of $25.7\ ^{o}C$, five grooves were present. The grooves show the presence of free convection which is, in an enclosure, based on convection cells, where one convection cell belongs to each groove.

4.1.3 Freezing and Melting with Initial Temperatures Different from Fusion Temperature

Three experiments were performed in which the initial temperature was different from 0 $^{\circ}$C. Table 4.1.3.1 compares freezing and melting time of these experiments with the equivalent ones which had an initial temperature of about 0 $^{\circ}$C. Comparison of experiment #2 and #9 shows that freezing of water with an initial temperature of 19 $^{\circ}$C took 9% longer. Also the finite-difference program was used to verify the measured freezing times of experiment #2 and #9. The finite-difference program calculated a total freezing time t_t of 67.7 min for experiment #2 and 76.4 min for experiment #9, hence a percentage difference of 13% which is a slightly higher difference as calculated from the measurements with 9%.

Table 4.1.3.1   Comparison of freezing and melting time for experiments with initial temperatures equal and unequal 0 $^{\circ}$C.

Exp #			T_i $^{\circ}$C	$T_{w,a}$ $^{\circ}$C	t_t min	$\Delta\%$ %	$\dfrac{c_p \Delta T_i}{h_f}$
2	f	v	0.4	-12.0	65		
9	f	v	19.0	-11.5	71	9	0.24
5	m	v	-0.4	26.8	36		
10	m	v	-15.0	26.8	40	11	0.09
6	m	h	-0.4	25.7	25		
11	m	h	-15.0	25.7	30	20	0.09

f: freezing   m: melting
v: vertical   h: horizontal

For melting, respective values of 11% and 20% were obtained. These percent values of the time difference were in the range of the values obtained from $c_p \Delta T_i / h_f$, the ratio of sensible and latent heat. For freezing in a cylinder, values for $t_t(T_i)/t_t(T_i = 0\ ^oC)$ are calculated using Weaver's finite-difference program [5]. The calculated time ratio for the cylinder is independent of size. These values listed in Table 4.1.3.2 can be used to correct freezing times obtained from methods which assume the initial temperature to be the fusion temperature.

Table 4.1.3.2   Ratio of total times for freezing in a cylinder - freezing from an initial temperature greater than 0 ^oC divided by freezing from a temperature $T_i = 0\ ^oC$.

T_i	$\dfrac{t_t(T_i)}{t_t(T_i = 0\ ^oC)}$
C	
0	1.000
5	1.033
10	1.064
15	1.094
20	1.122
25	1.149
30	1.175

4.1.4 Conductivity Measurements for Ice

Table 4.1.4.1 Comparison of measured conductivities of ice
with conductivities from tables.

Exp #		$T_{w,a}$ °C	k_{ice} W/mK	k_{table} W/mK	$\Delta\%$
1	vertical	-18.6	2.16	2.21	2.3
2	vertical	-12.0	2.18	2.20	0.9
3	vertical	-4.1	1.76	2.18	19.3
4	horizontal	-11.5	2.15	2.20	2.3

Experiments like the freezing experiment #3 where sub-
cooling occurred are not suitable for conductivity measure-
ments. Those experiments have a longer freezing time com-
pared to a similar experiment without subcooling. Hence the
measured conductivity from experiment #3 is too low. The
other conductivities measured in experiments with average
wall temperatures of less than -10 °C show only an error of
about 2 % when they are compared with conductivities from
tables evaluated at the mean temperature from Eq. 3.4.3.

4.1.5 Conductivity Measurements of Water

Table 4.1.4.2 shows the measured effective conduc-
tivity of water calculated from Eq. 3.2.15 which is not a
property of the medium but rather depends on the geometry

Table 4.1.4.2 Effective conductivity of water in the test
cell averaged over total melting time.

Exp #		$T_{w,a}$ °C	k_{eff} W/mK
5	vertical	26.8	1.76
6	horizontal	25.7	2.64
7	vertical	9.6	1.00
8	horizontal	9.5	1.43

of the vessel. The effective conductivity is not even con-
stant for one experiment because the enclosure gets bigger
when melting proceeds, and so the effective conductivity
increases. Thus a low effective conductivity is present in
the beginning of the melting process and a relatively high
conductivity is present in the end. Since there is more
convection heat transfer in the horizontal cylinder than in
the vertical cylinder, the effective conductivity is higher
in the horizontal cylinder. The experiments show also that
higher convection activity is achieved with higher wall
temperature from which also a higher effective conductivity
results. The measured true conductivity (without convection
influence) for water is the exact value because the calcu-
lations from Chapter 3.3 for the true conductivity uses
just the known conductivity of water to calibrate the equa-
tion.

Nevertheless, there is still a possibility to calcu-
late the true conductivity without the convection influ-

ence. For a Rayleigh number less than 1000, there is no convection in a cylindrical vertical or horizontal enclosure. From knowledge of the Rayleigh number, the maximal gap width of the molten region can be calculated for which the test cell has only conduction . The result shows that a water layer of 3.4 mm can be molten in the test cell without having convection. An effective conductivity calculated with Eq. 3.2.12 from the phase change right in the beginning in the gap hence yields the true conductivity k_{1m}. The true conductivity k_{1m} is a property of the medium.

Table 4.1.5   Comparison of measured conductivities of water - without convection influence - with conductivities from tables.

Exp		$T_{w,a}$	$k_{H_2O}(Ra=1000)$	k_{table}	$\Delta\%$
#		^{o}C	W/mK	W/mK	%
5	vertical	26.8	0.538	0.604	-10.9
6	horizontal	25.7	0.493	0.604	-18.4
7	vertical	9.6	0.615	0.574	7.1
8	horizontal	9.5	0.558	0.575	-3.0

Table 4.1.5 compares measured true conductivities of water with conductivities from tables. The conductivity is calculated for a gap width equivalent to that of Ra=1000. The percent error for water here is higher than the error for ice because here only values from the very beginning could be used. In the beginning the change of the wall temperature is high (see Chapter 4.1.6), and the reading of the wall temperature was limited to time increments of 30

seconds. On the other hand, the gap width of 3.4 mm was already reached after 2 to 4 minutes which means that there was not enough data present to calculate the average wall temperature (Eq. 3.2.5) with a higher accuracy and therefore, the accuracy of the true conductivity k_{lm} is limited.

4.1.6 Wall Temperature

The plot in Fig. 4.1.6 gives an example for variation of the wall temperature with time for experiment #1 - vertical freezing. When freezing starts, only a thin ice layer separates the fusion front from the wall, which means only small resistance for the energy transfer and high load, and hence, a wall temperature close to 0 ^{o}C. When the ice layer grows, the load decreases and the wall temperature converges towards the CTB temperature.
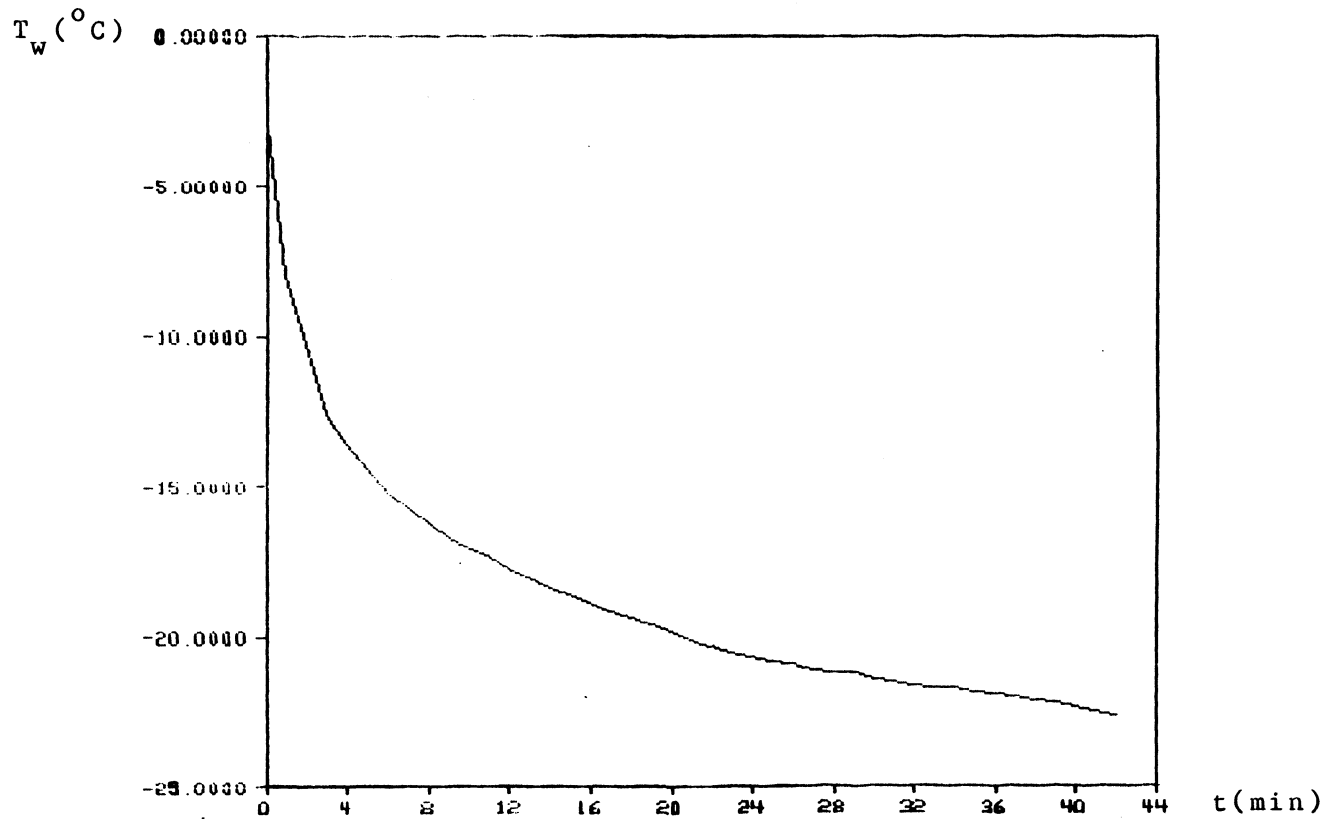
Figure 4.1.6   Wall temperature vs time. Here as example
experiment #1 — vertical freezing with a
temperature of the constant temperature bath
of -25 $^\circ$C.

4.2 Freezing and Melting in Porous Media

Freezing and melting were observed in the test cell for different porous media in order to measure their conductivity and to evaluate their performance for heat transfer enhancement, and usefulness for energy storage. Experiments with different kinds of aluminum porous media were performed to get information about the influence of the shape of the PM on the phase change. Also, the influence of the material was studied by performing experiments with copper, brass, and stainless steel in addition to the experiments with aluminum.

From temperature measurements with the thermo couples, the shape of the fusion front was observed. The fusion front for freezing in the test cell is cylindrical throughout the whole experiment. For melting, the same deviation from the cylindrical shape was observed as observed already for pure water.

Normally a clearly formed interface was observed. However, for the 12 mm aluminum beads and the copper spirals, the metal pieces reaching out from the interface act as fins. For example, during freezing, the main interface moves gradually inward while ice also builds up around the beads or spirals, acting as fins. The ice that builds up around these fins is later incorporated into the main ice mass when the main interface has moved further on. For

melting, similarly, it was observed that the ice thawed not only around the cylinder wall but also around the spheres and spirals which are in contact with the wall of the test cell. It seems that for this type of phase change, there has to be a high conductivity of the PM present, as well as a high ratio of volume to surface area, va, as in big spheres or heavy spirals. To which extent this type of phase change influences an overall conductivity measurement and calculation for a geometrically straight surface could not be determined.

Dendritic ice formation is not as likely in porous media as it is in water because the porous media yield more possibilities for nucleation than pure water does.

4.2.1 Freezing with Different Shapes of the Porous Medium

The porosity of optimal packed spheres in an infinite container is 0.26. Nevertheless, the beads with 12 mm diameter from experiment # 24 and the beads from experiment # 12 with 3.2 mm diameter have a higher porosity because the wall effect prevents the optimal arrangement for highest density of the beads.

The conductivities of the aluminum porous media increases with decreasing porosity. This is predicted by all five formulas from Chapter 3.5 which are used for

Table 4.2.1   Values obtained from freezing in aluminum porous media.

Exp #		Φ	k_{sm} W/mK	K_{emp} $\Delta\%$ %	Q''' $\cdot 10^{-9}$ J/m^3	pf W/mK	s $\cdot 10^{-9}$ JW/m^{4}K
12	beads 3.2mm	0.424	18.53	+68	0.152	21.6	3.28
24	beads 12.mm	0.532	15.90	+19	0.184	18.0	3.30
18	chips	0.903	4.69	−29	0.296	5.0	1.48
21	curls	0.974	3.93	−38	0.317	4.2	1.32
15	wool	0.989	2.73	−15	0.322	2.9	0.93

calculations and it is also evident since aluminum has a much higher conductivity than water. Amazing however is the big difference in conductivities of wool and curls although their porosity and volume to surface area ratio is almost the same.

For all experiments the empirical formula (Eq. 3.5.4) predicted the conductivity best. (Only for the beads with 3.2mm diameter the Veinberg model calculated the conductivity more accurate.) The absolute value of the error is between 15 and 68%. The highest energy density has, of course, the medium with the highest porosity because the major fraction of stored heat is stored in the form of latent heat which is achieved only in water and not in the aluminum. The performance factor, pf, follows the trend of the conductivity and is of same magnitude. The storage factor, $s = Q''' \cdot pf$, obtained by the beads is the highest. This

happens due to the fact that even a small increase of the metal volume causes a relatively big increase of the conductivity; whereas the energy density varies linearly with the porosity.

4.2.2 Melting with different Shapes of the Porous Medium

Table 4.2.2   Values obtained from melting in aluminum porous media.

Exp #		v: k_{eff} W/mK	k_{1m} W/mK	h: k_{eff} W/mK	k_{1m} W/mK	h: s JW/m^4K
13/14	beads 3.2mm	7.81	7.81	6.81	6.81	1.37
25/26	beads 12.mm	6.89	6.89	7.43	7.43	1.63
19/20	chips	3.04	1.70	4.01	1.94	1.45
22/23	curls	3.07	2.42	3.60	2.71	1.39
16/17	wool	2.02	0.68	2.95	0.68	1.16

v: vertical
h: horizontal

When melting data is discussed, it has to be recalled that conduction and convection are of importance. The true conductivities k_{1m} for water and aluminum are all lower than the conductivities k_{sm} for ice and aluminum because the conductivity of water is only about one fourth of the ice conductivity; however, the convection influence is also of importance. Convection in addition to conduction, which are both included in the term k_{eff}, increases this value in comparison to the true conductivity, k_{1m}. For the beads, however, the melting times in the vertical and horizontal

test cell position are the same, hence it follows that convection has no effect, and effective and true conductivities are the same. The effective conductivities follow the assumed pattern - the conductivity is high when the porosity is low. The convection influence can be seen in the plots in the appendix when the solid line is compared with the dotted line. Convection is present when the phase change rate is low in the beginning but high in the end (nearly no decline of the slope in the solid curve) compared to the dotted line. The ratio of k_{eff} divided by k_{lm} shows the convection influence, where a high ratio signifies high convection activity. This ratio is for curls, chips, wool, and pure water 1.3, 1.8, 2.9, and 3.0 respectively and 1.3, 2.1, 4.5, and 4.5 respectively for the horizontal position. The wool allows almost as much convection as pure water. Although the chips have a smaller porosity than the curls, convection in the chips is of greater importance. In the horizontal test cell position more convection is present. The effective conductivity of ice and aluminum is about two times the conductivity of water and aluminum. The storage factor for freezing is of the same magnitude as the storage factor for melting, only for the beads is it in the melting case considerably lower. In all but one of the melting experiments, the best results were obtained again by the empirical model for conductivity calculation.

4.2.3 Freezing of Water in Different Porous Media

Material

Table 4.2.3   Values obtained from freezing of water in copper, aluminum, brass, and steel porous media.

Exp		k_m	k_{sm}	k_{emp} $\Delta\%$	Q''' $\cdot 10^{-9}$	pf	s $\cdot 10^{-9}$
#		W/mK	W/mK	%	J/m^3	W/mK	JW/m^{4}K
27	copper	409.8	5.79	-48	0.307	6.19	1.90
21	alumi-num	155.0	3.93	-38	0.317	4.2	1.32
30	brass	106.0	3.76	-31	0.312	4.00	1.25
33	steel	14.3	2.44	-3	0.313	2.60	0.81

In addition to copper, brass, and steel, the aluminum curls from experiment # 21 are included in this table because they have a comparable shape and porosity.

The conductivity of the saturated porous media increases with increasing conductivity of the porous media. The porosity was about the same in all of these experiments. The empirical formula yielded the best results. The energy density is nearly the same for all of these experiments since the porosity does not vary a lot. The copper porous medium achieved the best results in respect to conductivity and storage factor.

4.2.4 Melting of Ice in Different Porous Media Material

Table 4.2.4   Values obtained from melting of ice in copper, aluminum, brass, and steel porous media.

Exp #		v: k_{eff} W/mK	k_{lm} W/mK	h: k_{eff} W/mK	k_{lm} W/mK	h: s JW/m^4K
28/29	copper	2.83	1.40	3.71	1.51	1.40
22/23	alumi-num	3.07	2.42	3.60	2.71	1.39
31/32	brass	2.19	1.14	2.80	1.22	1.07
34/35	steel	1.89	0.88	2.69	1.04	1.03

v: vertical
h: horizontal

The conductivities increase with increasing conductivities of the porous metal. Higher than expected, however, are the conductivities of aluminum. Copper achieved the best storage factor. The ratio of effective over true conductivity is about the same for all materials with the exception of aluminum which shows a lower ratio. The best predictions of the conductivity were obtained by the empirical model. The values of the empirical model were again too low.

4.2.5 Improvement of the Empirical Formula for Conductivity Calculation

As shown above the empirical formula is the best method for calculating true conductivities. Although this formula reasonably follows trends in variations of porosity

and conductivity of the PM, the obtained values are almost always too low. Therefore a correction factor of 1.35 is proposed to represent similar conditions as those investigated in this thesis. In this way it is obtained

$$k_{sm} = 1.35 \ k_{ice}^{\Phi} \ k_m^{(1-\Phi)} \qquad (4.2.5.1)$$

$$k_{1m} = 1.35 \ k_{H_2O}^{\Phi} \ k_{1m}^{(1-\Phi)} \qquad (4.2.5.2)$$

$$\text{for} \quad 0.7 < \Phi < 0.98$$

In this way only an error of ± 35 % has still to be expected. For the given porosity range, a lower limit for the conductivity can be obtained from the original empirical formula Eq. (3.5.4) and an upper limit, although mostly far off, from the parallel model Eq. (3.5.2). Eq. (4.2.5.1) and Eq. (4.2.5.2) should only be used for the given porosity range because due to the correction factor the known conductivities for $\Phi = 0$ and $\Phi = 1$ are not regained correctly anymore. It could not be found out how the ratio volume to surface area, the length of the spirals, and phase change with the fin effect affects the true conductivity. Nevertheless it seems that these influences are small compared to variations in the metal conductivity and especially in the change of porosity.

CHAPTER 5 -   FREEZING   AROUND   A   SINGLE   TUBE   AND   IN

TUBE-IN-SHELL   HEAT   EXCHANGERS

LHTES units normally consist of tubes in a storage tank through which the coolant flows. Such an arrangement is called tube-in-shell heat exchanger. In this chapter first calculations for freezing around a single tube in an infinite shell are presented which are then extended to calculations of tube-in-shell heat exchangers for LHTES.

The calculations from Chapter 5.1.2, 5.2.1, and 5.2.2 are also valid for melting with turbulent free convection flow. For this case k_{sm} has to be replaced by k_{eff} where k_{eff} has to be obtained then from experiments with a scale model. This is possible because the convection coefficient in turbulent buoyancy driven flow is independent of the characteristic length.

5.1   Freezing Around One Single Tube in an Infinite Shell

5.1.1   Exact Solution from Ozisik

For freezing around one single tube in an infinite shell an exact solution is given by Ozisik [12]. This solu-

tion accounts for initial temperatures of the liquid different from the fusion temperature. The solution given by Ozisik accounts only for conduction. Since initial temperatures of the liquid which are different from the fusion temperature are allowed, convection is present in the liquid phase. The convection in the liquid phase can be accounted for approximately when in Eq. (5.1.1.2) the true conductivity k_{1m} is substituted by the effective conductivity k_{eff}. The calculation is only valid for a line heat sink which could be approximated by a heat exchanger tube with a very small diameter. The position of the fusion front has to be calculated from the transcendental equation 5.1.1.1:

$$\frac{Q}{4\pi} e^{-\lambda^2} + \frac{k_{1m}(T_i - T_f)}{Ei(-\lambda^2 \alpha_{sm}/\alpha_{1m})} e^{-\lambda^2 \alpha_{sm}/\alpha_{1m}} = \lambda^2 \alpha_{sm} \rho_{i,0} h_f$$

where Q is the heat sink strength in W/m and

$$\alpha_{1m} = \frac{k_{1m}}{(\rho c)_{1m}} \qquad (5.1.1.2)$$

$$(\rho c)_{1m} = \Phi \rho_1 c_1 + (1-\Phi)\rho_m c_m \qquad (5.1.1.3)$$

Similar formulas are obtained for α_{sm} and $(\rho c)_{sm}$ if the subscript 1 is replaced by s. The similarity parameter λ is

$$\lambda = \frac{r}{2(\alpha_{sm} t)^{1/2}} \qquad (5.1.1.4)$$

-Ei(-x) is the exponential-integral-function which is defined for x > 0 as

$$-Ei(-x) \equiv \int_1^\infty \frac{e^{-xt}}{t}\, dt \qquad (5.1.1.5)$$

values for the exponential-integral-function are given in Table 5.1.1.

5.1.2 Resistance Method

The resistance method can also be used to calculate outward freezing around a cylindrical tube. The same assumptions have to be made as for inward freezing in a cylinder (Chapter 3.2.1).

$$t = \frac{h_f\, \rho_{i,0}\, \Phi}{k_{sm}(T_f - T_w)}\ [\frac{1}{2}\ r^2 \ln\frac{R}{r} + \frac{1}{4}(r^2 - R^2)\ ] \qquad (5.1.2)$$

5.2 Freezing in a Tube-in-Shell Heat Exchanger Consisting of a Tube Bank

5.2.1 NTU Method

Shamsundar et. al. [13] calculated freezing in a tube-in-shell heat exchanger with the NTU method. In these calculations is accounted for temperature variation of the coolant in the axial direction but axial heat conduction is assumed to be negligible. Further assumptions are:

- PCM initially at freezing temperature

- cocurrent flow

- tube geometry as shown in Fig. 5.2.2

- sensible heat negligible

The method accounts for forced convection in the tubes and requires therefore the Biot number which can be calculated from

$$Bi = \frac{h\ D}{k_{sm}} \qquad (5.2.1.1)$$

where D is the tube diameter, k_{sm} is the measured conductivity of the solid porous medium and h is the convection coefficient calculated from correlations for internal forced convection. It is a dimensionless time defined by

$$t_o = \frac{k_{sm}}{\rho_{i,0}\ h_f\ \Phi\ D^2} \int_0^t [T_f - T_{in}(t)]\ dt \qquad (5.2.1.2)$$

T_{in} is the inlet temperature of the coolant. Shamsundar et al. state that this definition and calculation method accounts for a time dependent inlet temperature. Another necessary value is obtained from

$$NTU = \pi\ D\ L\ h/(\dot{m}\ c)_f \qquad (5.2.1.3)$$

The fraction F_o of PCM that is frozen in a radial plane element at the inlet to the storage can be calculated by iteration from

$$t_o = J\ [\ \frac{F_o}{Bi} + \psi(F_o)\ ] \qquad (5.2.1.4)$$

with the auxiliary function $\psi(F_o)$ given in Fig. 5.2.2 and

$$J = \frac{4}{\pi} - \frac{1}{4} \text{ for aligned tubes}$$

or

$$J = \frac{1}{\pi} - \frac{1}{8} \text{ for staggered tubes.}$$

The effectiveness ε is defined as

$$\varepsilon = \frac{T_{out} - T_{in}}{T_f - T_{in}} \qquad (5.2.1.5)$$

or

$$\varepsilon = \frac{\dot{Q}}{\dot{m} c_c (T_f - T_{in})} \qquad (5.2.1.6)$$

where c_c is the specific heat of the coolant and ε can be obtained from iteration of

$$NTU = -\ln(1-\varepsilon) + Bi \, [\Omega(F_o) - \Omega[(1-\varepsilon)F_o]] \qquad (5.2.1.7)$$

where $\Omega(F_o)$ is another auxiliary function given by Fig. 5.2.2. The energy transfer rate $\dot{Q}$ can now be obtained from Eq. 5.2.1.6. The frozen PCM fraction $\overline{F}$ can finally be obtained from

$$\overline{F} = (F_o \varepsilon + Bi \, [\psi(F_o) - \psi(1-\varepsilon)F_o]) / NTU \qquad (5.2.1.8)$$

This method also applies to the counter-current flow heat exchanger over the first phase of heat recovery during which the tubes of the heat exchanger have no mutual interaction. When the tube pitch is not close to the tube diameter, this first phase forms the bulk of the freezing

time. During the remaining period, the counter current heat exchanger will be a better performer than the cocurrent one. Using the data pertaining to the latter will hence enable a conservative estimate. For other ratios of pitch and tube diameter as shown in Fig. 5.2.2 two integrals have to be solved. The input to these integrations is obtained as the result of two-dimensional finite-difference calculations in a representative plane perpendicular to the tube axes. The details of these calculations can be found in [13].

5.2.2 Resistance Method for Tube-in-Shell Heat Exchanger

As long as the fusion fronts of the different tubes do not make contact with one another the resistance method derived for a single tube is valid. When the fusion fronts then finally meet, a kind of inward freezing can be assumed to calculate the last part of the phase change. In this chapter the calculation for a staggered tube bank of the design indicated in Fig. 5.2.1 is shown.

After the fusion fronts make contact, further inward freezing of the remaining unfrozen shape is estimated to take place like freezing in a circular cylinder. This virtual cylinder has the radius

$$R_v = 3^{-1/2} L - R \qquad (5.2.2.1)$$
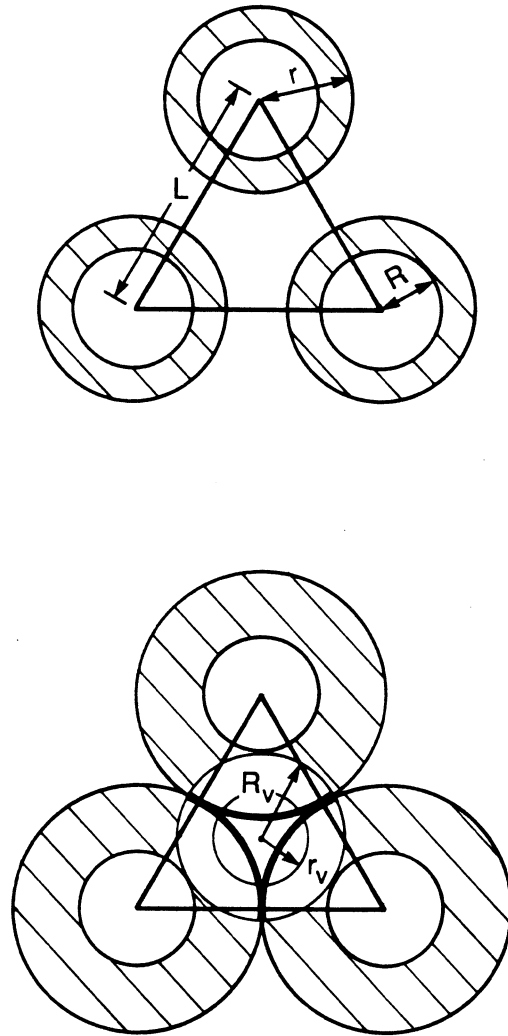
Fig. 5.2.1   Freezing around staggered tubes

which is the distance from the center of the triangle to

the outer radius of a heat exchanger tube. For calculations

of the freezing time from a given frozen fraction

$$\overline{F} = \frac{V(t)}{V_{all}}$$

it must be distinguished if a certain amount of solid phase (and hence frozen fraction $\overline{F}$) will form before or after the fusion fronts meet. The frozen fraction $\overline{F}$ at the time when the fusion fronts meet is

$$\overline{F}_{meet} = \frac{\frac{1}{4} L^2 - R^2}{\frac{3^{1/2}}{2\pi} L^2 - R^2} \qquad (5.2.2.2)$$

When $\overline{F} < \overline{F}_{meet}$ the interface radius r can be calculated from the given frozen fraction $\overline{F}$ with

$$r = R \left(\left[\frac{3^{1/2}}{2\pi} \left(\frac{L}{R} \right)^2 - 1 \right] \overline{F} + 1 \right)^{1/2} \qquad (5.2.2.3)$$

the freezing time t can now be calculated from Eq. 5.1.2. When $\overline{F} > \overline{F}_{meet}$ the radius of the interface in the virtual cylinder is

$$r_v = \left[\left(\frac{3^{1/2}}{4\pi} L^2 - \frac{1}{2} R^2 \right) (1 - \overline{F}) \right]^{1/2} \qquad (5.2.2.4)$$

and

$$t = t(\overline{F}_{meet}) + [t(r_v) - t(r_{v,i})] \qquad (5.2.2.5)$$

$r_{v,i}$ is the radius of a cylinder with the same volume as the volume of the liquid phase in a triangular unit when the fusion fronts meet. Therefore $r_{v,i} = r_v(\overline{F}_{meet})$ from Eq. (5.2.2.4) which yields

$$r_{v,i} = \frac{L}{2} \left(\frac{3^{1/2}}{\pi} - \frac{1}{2} \right)^{1/2} = 0.11328 \, L$$

From the equation for outward freezing

$$t(\overline{F}_{meet}) = t(\frac{L}{2}) = \frac{h_f \, \rho_{i,0} \, \Phi}{k_{sm}(T_f - T_w)} \left[\frac{1}{8}L^2 \ln\frac{2R}{L} + \frac{1}{4}(\frac{1}{4}L^2 - R^2)\right] \quad (5.2.2.6)$$

from the equation for inward freezing

$$t(r_v) = \frac{h_f \, \rho_{i,0} \, \Phi}{k_{sm}(T_f - T_w)} \left[\frac{1}{2}r_v^2 \ln(\frac{r_v}{R_v}) + \frac{1}{4}(R_v^2 - r_v^2)\right] \quad (5.2.2.7)$$

and also from the equation for inward freezing

$$t(r_{v,i}) = \frac{h_f \, \rho_{i,0} \, \Phi}{k_{sm}(T_f - T_w)} \left[\frac{1}{2}r_{v,i}^2 \ln(\frac{r_{v,i}}{R_v}) + \frac{1}{4}(R_v^2 - r_{v,i}^2)\right] \quad (5.2.2.8)$$

The Eq. 5.2.2.2 / 5.2.2.3 / 5.2.2.4 are derived in Appendix B.

Table 5.1.1   Values of the exponential-integral-function.

$E_1(x)$ or $-Ei(-x)$ Function

[12]

x	$E_1(x)$	x	$E_1(x)$	x	$E_1(x)$	x	$E_1(x)$
0.00	∞	0.25	1.0442826	0.50	0.5597736	1.60	0.0863083
0.01	4.0379296	0.26	0.0138887	0.55	0.5033641	1.65	0.0802476
0.02	3.3547078	0.27	0.9849331				
0.03	2.9591187	0.28	0.9573083	0.60	0.4543795	1.70	0.0746546
0.04	2.6812637	0.29	0.9309182	0.65	0.4115170	1.75	0.0694887
0.05	2.4678985	0.30	0.9056767	0.70	0.3737688	1.80	0.0647131
0.06	2.2953069	0.31	0.8815057	0.75	0.3403408	1.85	0.0602950
0.07	2.1508382	0.32	0.8583352				
0.08	2.0269410	0.33	0.8361012	0.80	0.3105966	1.90	0.0562044
0.09	1.9187448	0.34	0.8147456	0.85	0.2840193	1.95	0.0524144
0.10	1.8229240	0.35	0.7942154	0.90	0.2601839	2.0	4.89005(−2)
0.11	1.7371067	0.36	0.7744622	0.95	0.2387375	2.1	4.26143
0.12	1.6595418	0.37	0.7554414				
0.13	1.5888993	0.38	0.7371121	1.00	0.2193839	2.2	3.71911
0.14	1.4241457	0.39	0.7194367	1.05	0.2018728	2.3	3.25023
0.15	1.4644617	0.40	0.7023801	1.10	0.1859909	2.4	2.84403
0.16	1.4091867	0.41	0.6859103	1.15	0.1715554	2.6	2.18502
0.17	1.3577806	0.42	0.6699973				
0.18	1.3097961	0.43	0.6546134	1.20	0.1584084	2.8	1.68553
0.19	1.2648584	0.44	0.6397328	1.25	0.1464134	3.0	1.30484
0.20	1.2226505	0.45	0.6253313	1.30	0.1354510	3.5	6.97014(−3)
0.21	1.1829020	0.46	0.6113865	1.35	0.1254168	4.0	3.77935
0.22	1.1453801	0.47	0.5978774	1.40	0.1162193	4.5	2.07340
0.23	1.1098831	0.48	0.5847843	1.45	0.1077774	5.0	1.14830
0.24	1.0762354	0.49	0.5720888	1.50	0.1000196	∞	0

(The figures in parenthesis indicate the power of 10 by which the numbers to the left, and those below in the same column, are to be multiplied).
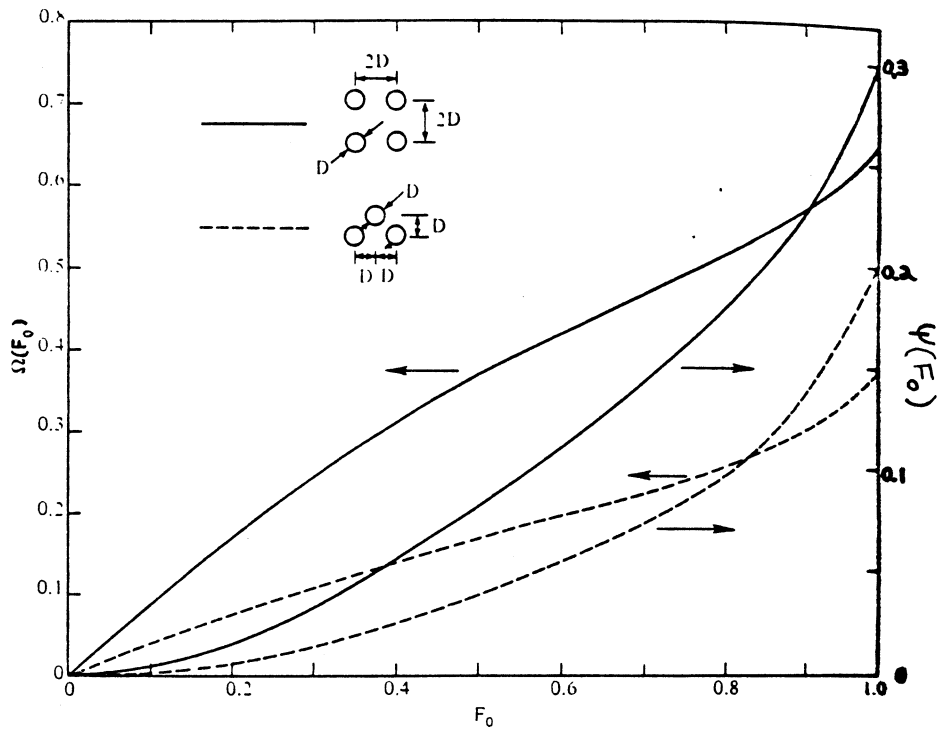
Figure 5.2.2   Auxiliary function for phase change   storage
                calculations.   [13]

CHAPTER 6 - APPLICATION OF LATENT HEAT STORAGE

Finally, the usefulness of a storage system depends not only on quality criteria like the ones defined and discussed above but also on the way a storage tank is incorporated in a system and how the parts of this system act together.

In order to find out more about these interactions, a system was modeled and analyzed by a computer program.

6.1 The Model

Fig. 6.1 shows the schematic of the model. The storage tank serves as a seasonal storage in space heating application. Cooling was not considered.

The storage tank is a cylinder with two heat exchanger tubes, one from the collector and one from the heat pump. The tubes are situated on the centerline of the cylinder. Calculations for the storage tank are performed with the resistance method. In order to avoid freezing of the storage tank from the outside during the winter, the tank is buried and placed at a location with a distance z to the

surface, where z is the largest freezing depth of the soil during the year. In this way the storage tank even receives heat from the soil; an effect which is also known from heat pumps with ground coils.

The heat losses of the house are calculated with the degree-day-method [14]. A loss coefficient-area (UA) = 463 W/K was chosen. It is assumed that the house has no capacity at all to store heat not even for short periods. For the heat pump an efficiency of 0.3 was chosen.

Collector calculations were performed as shown in [14] with collector data from Fig. 7.7.1 of [14]. Meteorological data were taken also from [14] Appendix G for a site in Madison, Wisconsin.

For the control system of the house it was decided that water from the collector is passed through the radiators of the house whenever the temperature of the water leaving the collector is higher than a minimum temperature of 35 $^{\circ}$C and heating of the house is necessary. If the temperature of the water from the collector is less than the minimum temperature, the inlet to the radiators at A (Fig. 6.1) is closed and the heat is used for energy storage (by melting the ice in the storage tank) as long as the temperature of the fluid is above 0 $^{\circ}$C. Whenever the collector power is not enough for space heating, the use of the heat pump is prefered for additional heat supply rather than

using external energy from a power plant or a conventional furnace.

The <u>program</u> simulates the heating system during one year. It starts calculating in April and assumes that the storage tank is filled by a frozen fraction $\overline{F}$ = 0.99. Approximately the same number was obtained at the end of the year. Iteration is necessary to calculate the elements of the system because the calculation result from one element has an impact also on performance calculation of other elements.

Parameters used for the simulation were as follows:

Site	Madison,Wisconsin	
	latitude	43.1°
	climate	4294 degree-days per year
House	loss coefficient-area (UA)	463 W/K
	min. required collector fluid temperature for heating	35 $^{\circ}$C
Collector	slope	63.1°
	azimuth angle	0.0°
	surface area	40 m^2
	flow rate	0.133 kg/s
Storage tank	length	50 m
	diameter	0.5 m
	depth z	2.0 m
Heat pump	efficiency	0.3

6.2 Results

The energy necessary for heating the house over the period of one year is $Q = 47.7 \cdot 10^3$ kWh. Table 6.2 shows the influence of different porous media on the performance of the system. This influence is documented by the ratio of auxiliary energy and total energy necessary to heat the house. Auxiliary energy Q_{aux} is needed to drive the heat pump or to heat the house directly. Table 6.2 shows further values of the quality criteria for horizontal melting.

Table 6.2   Results from simulation program compared with quality values for horizontal melting.

PM	$\dfrac{Q_{aux}}{Q} \cdot 100\%$	$Q''' \cdot 10^{-9}$	pf	$s \cdot 10^{-9}$
	%	J/m^3	W/mK	JW/m^4K
without storage	85			
only water (k_{eff} = 2.64 W/mK)	74	0.348	3.0	1.05
saturated porous metal				
steel	71	0.335	3.07	1.03
Al wool	69	0.345	3.35	1.16
beads 3.2	66	0.161	8.47	1.37
brass	62	0.334	3.2	1.07
Al curls	61	0.340	4.1	1.39
beads 12.	61	0.196	8.95	1.76
Al chips	57	0.317	4.59	1.45
copper	55	0.329	4.25	1.4

The simulation showed that the storage tank was too small for the beads. Already in the early summer the PCM in the tank was thawed and no more heat storage was possible. In case of the shavings, the PCM was thawed in September or November. When pure water was used, a frozen fraction of about 0.1 remained. The problem was to thaw the frozen mass from the previous winter with a reasonable collector size. Table 6.2 shows that quality criteria can give hints for storage design. However, the simple multiplication of energy density, Q'', and performance factor, pf, yields results which might put too much emphasis on the performance factor.
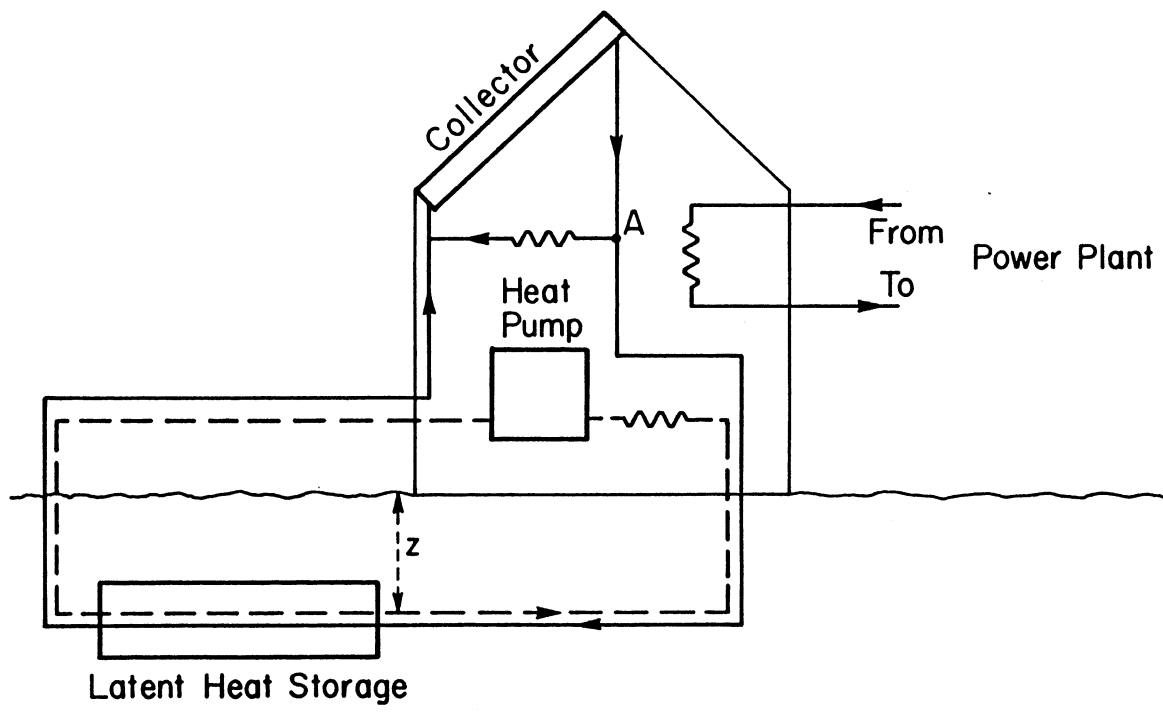
Figure 6.1   Schematic of the modeled house for simulation of latent heat storage in real application.

CHAPTER 7 - CONCLUSIONS AND RECOMMENDATIONS

7.1 Conclusions

No formula was found which predicted the conductivity correctly, but a simple apparatus was described to measure the conductivity.

Shavings used as porous media enhance the performance of a storage tank because they

- keep the nucleation temperature T_n close to 0 ^{o}C and avoid subcooling even at freezing temperatures only slightly below fusion temperature

- increase the apparent conductivity of the liquid and solid phase

- increase the performance factor pf and therefore increase the added or removed heat rate

- reduce the energy density only very little due to the high porosity.

From the experiments it can be concluded that the optimum porosity Φ for a LHTES with water as PCM should be between

0.6 and 0.9, where a value of about 0.6 is appropriate for high heat rates that have to be added or removed. A value of about 0.9 should be chosen when energy density is more important than heat transport. A porous medium with a high conductivity yields the best results. However, the conductivity of the water-metal or ice-water mixture does not increase proportionally with an increase of the metal conductivity. Hence it can be economical to use a cheaper metal and to increase the heat transfer rate by other means.

When the conductivity is known from any experiment freezing in a tube-in-shell heat exchanger can be calculated from the NTU-method. For melting, on the other hand, the effective conductivity has to be known from experiments with a scale model; and this procedure is only valid for turbulent flow in the melt region.

7.2 Recommendations

Further research should address three problems:

1. Find an accurate formula to predict the conductivity of a mixture consisting of a PCM and a porous medium.

2. Find a calculation method for the melting process of ice filling the voids of a porous medium.

3. Perform experiments with tube-in-shell heat exchangers and determine the accuracy of the NTU-method and the resistance method.

The procedure for 2. would be as follows:

- Calculate heat transfer due to free convection in an enclosure filled only with the PCM ($\Phi=1.0$).

- Account for the obstructions of the porous medium. (Introduce the permeability of the porous medium).

- Account for the enlargement of the liquid region when melting progresses and its influence on free convection.

- Account for the irregular shape of the fusion front which is formed due to convection when melting proceeds.

LIST OF REFERENCES

LIST OF REFERENCES

[1]   Leidenfrost,W. "The Use of Heat Pumps in Reducing Fuel Consumption for Nonsolar Climate Control of Buildings," Energy, Vol. 3, pp.83-93, Pergamon Press, 1978.

[2]   Kreith,F. and Kreider, J.F., Principles of Solar Engineering, Hemisphere Publishing Corporation, 1978.

[3]   Herrmann, J.F., Experimental Study on Melting of Ice and Freezing of Water Around a Horizontal Cylindrical Heat Source/ Sink, Special Project Report, Mechanical Engineering, Purdue University, West Lafayette, Indiana, 1982.

[4]   White, D.A., Melting of Ice and Freezing of Water Around a Horizontal Isothermal Cylinder, M.S. Thesis, Purdue University, West Lafayette, Indiana, 1984.

[5]   Weaver, J.A., Solid-Liquid Phase Change Heat Transfer in Porous Media, M.S. Thesis, Purdue University, West Lafayette, Indiana, 1985.

[6]   Touloukian, Y.S., Powell, P.W., Ho, C.Y., and Klemens, P.G., Thermophysical Properties of Matter, Volume 1: Thermal Conductivity, Metallic Elements and Alloys, IFI/Plenum, New York-Washington, 1970.

[7]   Poots, G., "On the Application of Integral-Methods to the solution of Problems Involving the Solidification of Liquids Initially at Fusion Temperature," Int. J. Heat Mass Transfer, Vol. 5, pp. 525-531, Pergamon Press, 1962.

[8]   Wolf, H., Heat Transfer, pp. 432-441, Harper & Row, Publisher, New York, 1983.

[9]   Combarnous, M.A. and Bories, S.A., "Hydrothermal Convection in Saturated Porous Media," Advances in Hydroscience, Chow, V.T., Editor, Academic Press, Vol. 10, pp.231-307, 1975.

[10]   Veinberg, A.K., "Permeability, Electical Conductivity, Dielectric Constant and Thermal Conductivity of a Medium with Spherical and Ellipsoidal Inclusions," Soviet Physics-Doklady, Vol. 2, No. 7, pp. 593-595, 1967.

[11]   Zehner, P and Schluender, E.U., Waermeleitfaehigkeit von Schuettungen bei maessigen Temperaturen, Chemie-Ing.-Techn., v.42, pp. 933-941,1970.

[12]   Osizik, M.N., <u>Heat</u> <u>Conduction</u>, John Wiley and Sons,
        New York,1980.

[13]   Shamsundar, N. and Srinivasan, R.,   "Effectiveness-
        NTU Charts for Heat Recovery from Latent Heat
        Storage Units," <u>Journal</u> <u>of</u> <u>Solar</u> <u>Engineering</u>,   Vol.
        102, pp. 263-271, 1980.

[14]   Duffie, J.A. and Beckman, W.A., <u>Solar</u> <u>Engineering</u> <u>of</u>
        <u>Thermal</u> <u>Processes</u>,   John   Wiley and Sons, New York,
        1980.

A P P E N D I C E S

Appendix <u>A</u>. <u>Experimental Data</u>

Explanation to Appendix A are given in Chapter 4.0.1.

Experiment #   1

metal   : no metal only DISTILLED WATER
porosity   : phi = 1.000
discribtion   :   —
vol./area   : va = ****** mm
density   : rhom= ******** kg/m**2
specific heat: cm   = ******** J/kg*K

FREEZING in a VERTICAL cylinder

temperature of bath .... : Tb = -25.0 C
ambient temperature .... : Tsur= 21.0 C
average wall temperature .... : Tw,a= -18.6 C
initial temperature of liquid phase: Ti =   0.6 C
average temperature of solid phase : Tsm = -9.3 C

total time for freezing: tt = 42.3 min

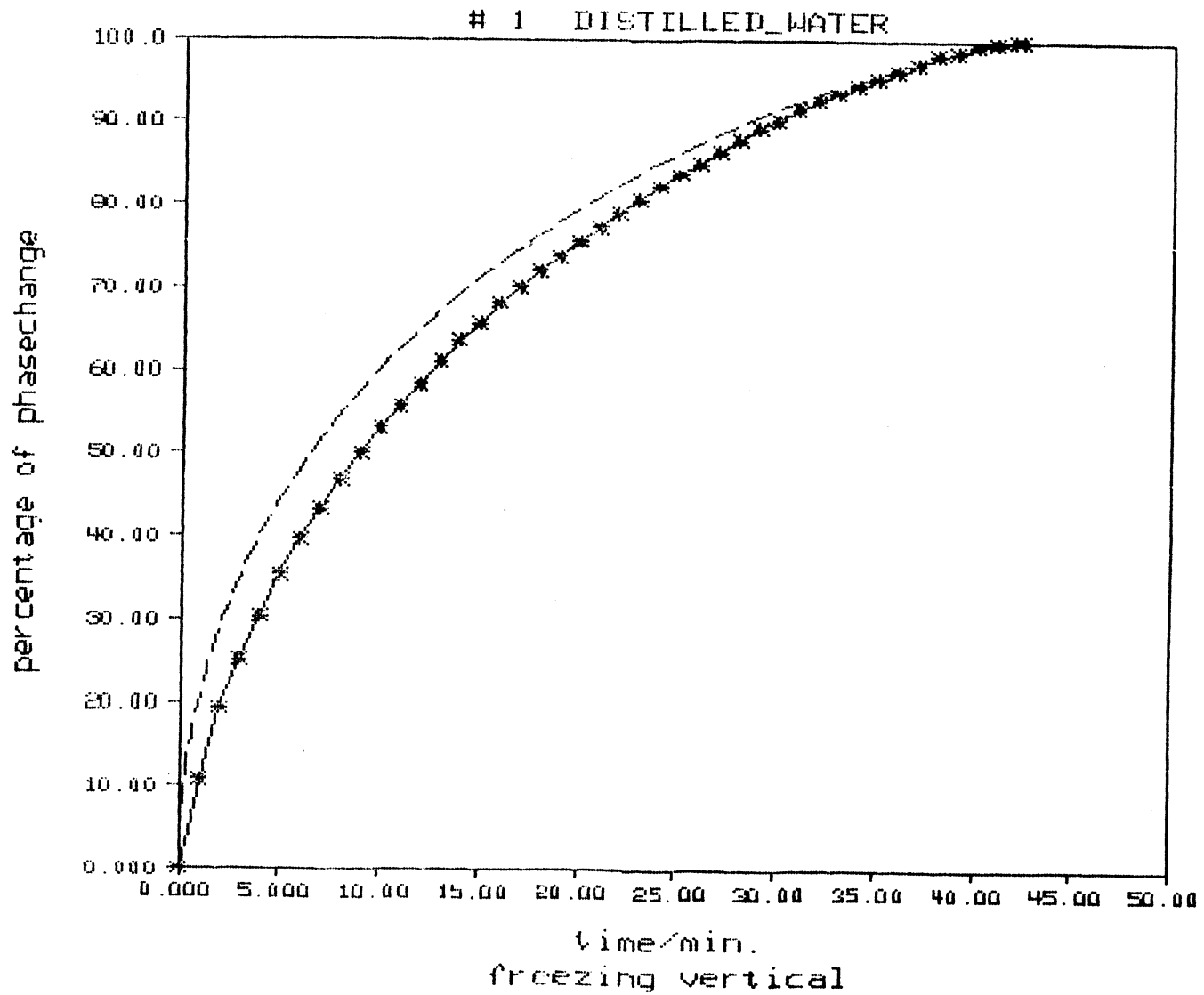CONDUCTIVITY for solid phase at Tsm = -9.3 C

****
*   ksm=   2.16 W/m*K   *
****

compare with these conductivities at Tsm= -9.3 C

metal   : km   = ****** W/m*K
ice   : kice =   2.21 W/m*K
series   : kser =   2.21 W/m*K
parallel   : kpar =   2.21 W/m*K
empirical   : kemp =   2.21 W/m*K
geometrical: kgeo =   2.21 W/m*K
Veinberg   : kvein=   2.21 W/m*K

energy density   : Q'''= 0.325e+09 J/m**3
performance factor: pf = 2.29   W/m*K
storage factor   : s   = 0.743e+09 J*W/m**4*K

1   DISTILLED_WATER

percentage of phasechange

time/min.
freezing vertical

112

Experiment #   2


```
metal          : no metal only DISTILLED WATER
porosity       : phi = 1.000
discribtion    :   -
vol./area      : va  = ****** mm
density        : rhom= ******** kg/m**2
specific heat: cm  = ******** J/kg*K
```


FREEZING in a VERTICAL cylinder

```
temperature of bath ............. : Tb   = -15.0 C
ambient temperature ............. : Tsur=  21.0 C
average wall temperature ........ : Tw,a= -12.0 C
initial temperature of liquid phase: Ti  =   0.4 C
average temperature of solid phase : Tsm =  -6.0 C


total time for freezing:        tt  =  65.0 min
```
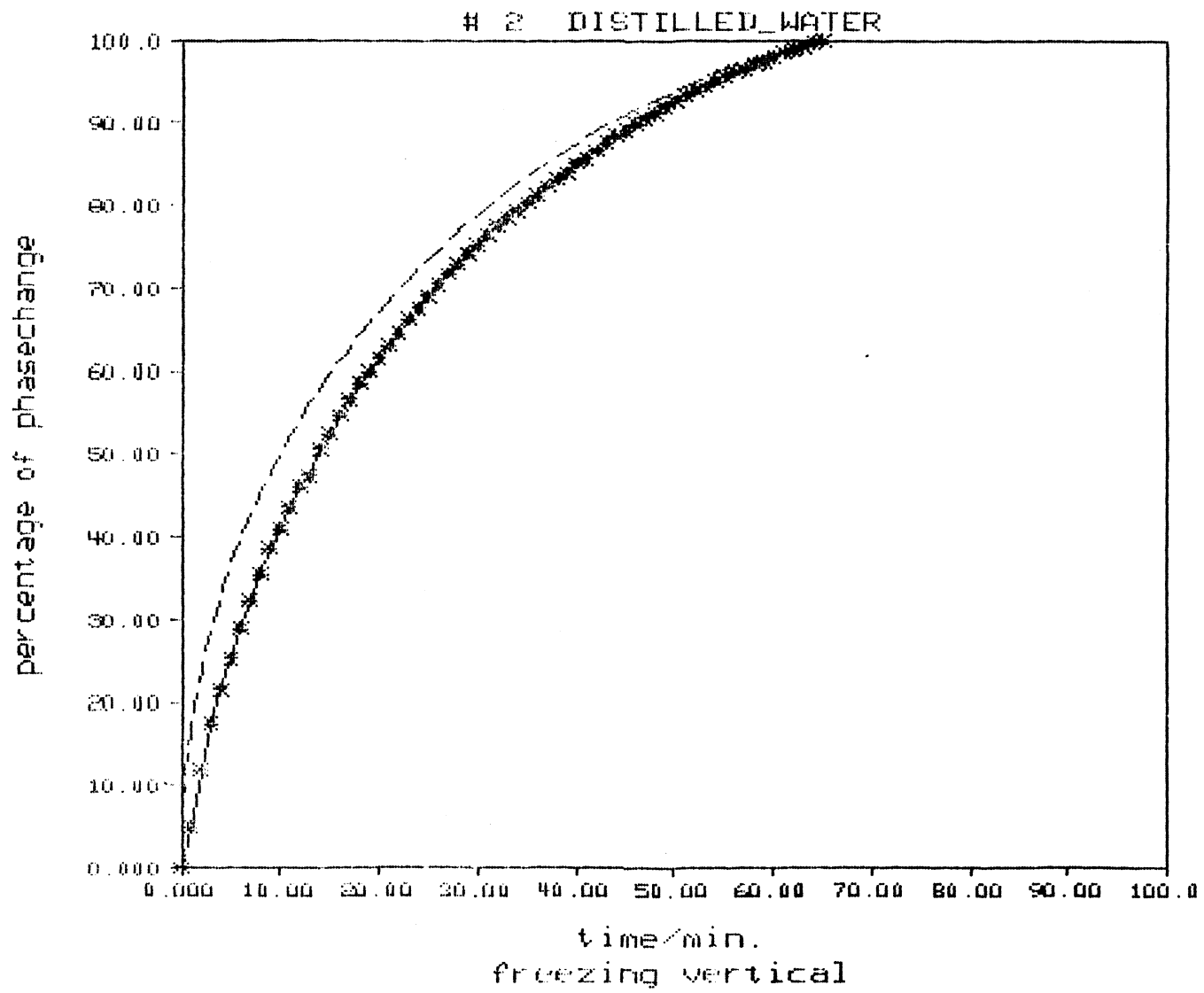
CONDUCTIVITY for solid phase at Tsm =   -6.0 C

```
*************************
*   ksm=   2.18 W/m*K   *
*************************
```

compare with these conductivities at Tsm=   -6.0 C

```
metal        : km   = ****** W/m*K
ice          : kice =   2.20 W/m*K
series       : kser =   2.20 W/m*K
parallel     : kpar =   2.20 W/m*K
empirical    : kemp =   2.20 W/m*K
geometrical: kgeo =   2.20 W/m*K
Veinberg     : kvein=   2.20 W/m*K

energy density   : Q'''=  0.325e+09 J/m**3
performance factor: pf  =   2.32      W/m*K
storage factor   : s   =  0.753e+09 J*W/m**4*K
```

2   DISTILLED_WATER

percentage of phasechange

time/min.
freezing vertical

114

Experiment #   3

metal   : no metal only DISTILLED WATER
porosity   : phi = 1.000
discribtion   :   --
vol./area   : va = ****** mm
density   : rhom= ******* kg/m**2
specific heat: cm = ******* J/kg*K

FREEZING in a VERTICAL cylinder

temperature of bath .... : Tb   = -5.0 C
ambient temperature .... : Tsur= 21.0 C
average wall temperature .... : Tw,a= -4.1 C
initial temperature of liquid phase: Ti   = -0.1 C
average temperature of solid phase : Tsm = -2.0 C

total time for freezing: tt = 235.0 min

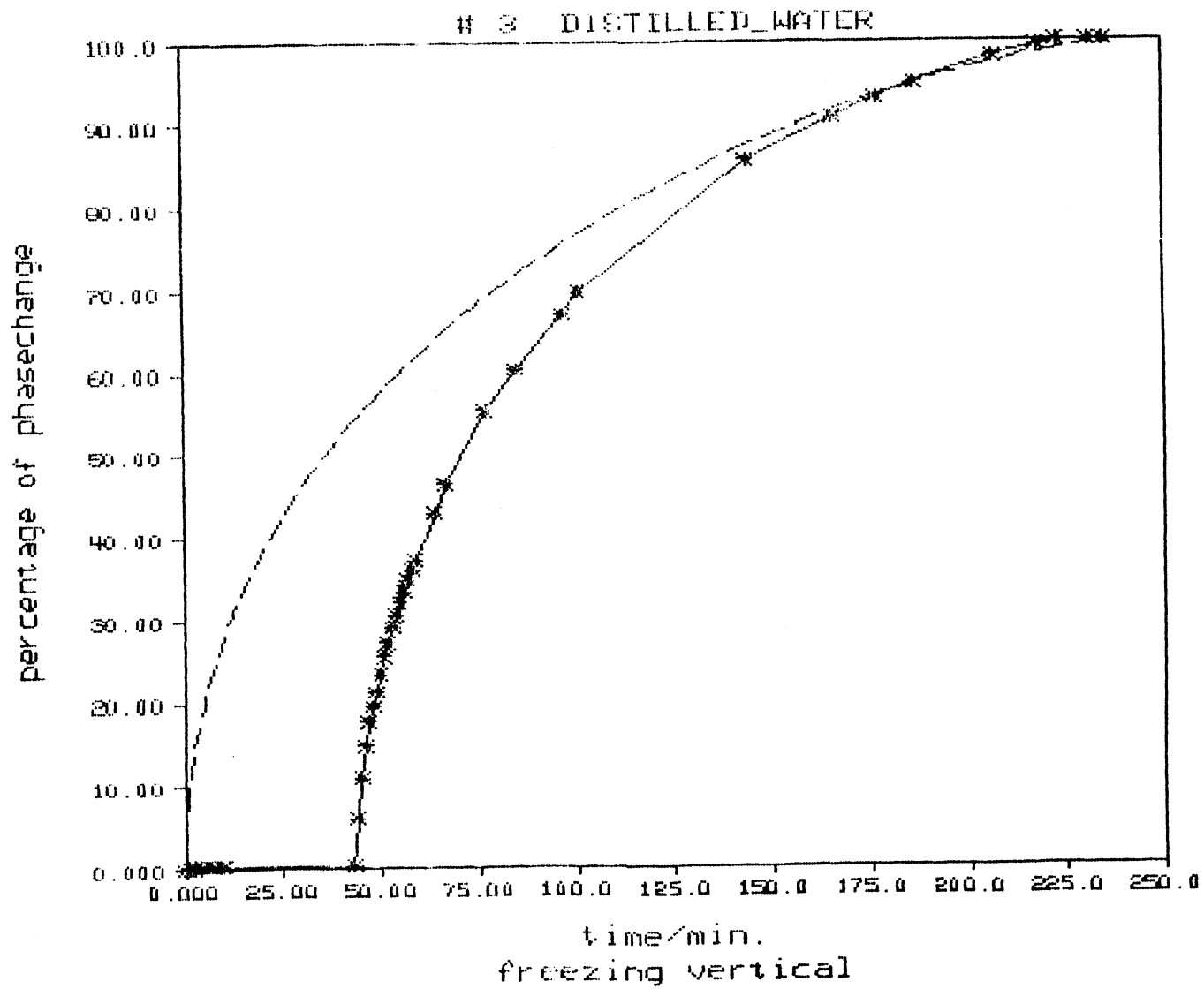CONDUCTIVITY for solid phase at Tsm = -2.0 C

****
*   ksm= 1.76 W/m*K   *
****

compare with these conductivities at Tsm= -2.0 C

metal   : km   = ****** W/m*K
ice   : kice = 2.18 W/m*K
series   : kser = 2.18 W/m*K
parallel   : kpar = 2.18 W/m*K
empirical   : kemp = 2.18 W/m*K
geometrical: kgeo = 2.18 W/m*K
Veinberg   : kvein= 2.18 W/m*K

energy density   : Q'''= 0.325e+09 J/m**3
performance factor: pf =   1.87   W/m*K
storage factor   : s   = 0.608e+09 J*W/m**4*K

2   DISTILLED_WATER

percentage of phasechange

time/min.
freezing vertical

116

Experiment #   4

```
metal          : no metal only DISTILLED WATER
porosity       : phi = 1.000
discribtion    :   -
vol./area      : va  = ****** mm
density        : rhom= ******** kg/m**2
specific heat: cm  = ******** J/kg*K
```

FREEZING in a HORIZONTAL cylinder

```
temperature of bath .............. : Tb   = -15.0 C
ambient temperature .............. : Tsur=  21.0 C
average wall temperature ......... : Tw,a= -11.5 C
initial temperature of liquid phase: Ti   =   0.3 C
average temperature of solid phase : Tsm  =  -5.7 C
```

total time for freezing: tt = 69.0 min

CONDUCTIVITY for solid phase at Tsm =   -5.7 C

```
*************************
*   ksm=   2.15 W/m*K   *
*************************
```

compare with these conductivities at Tsm=   -5.7 C

```
metal          : km   = ****** W/m*K
ice            : kice =   2.20 W/m*K
series         : kser =   2.20 W/m*K
parallel       : kpar =   2.20 W/m*K
empirical      : kemp =   2.20 W/m*K
geometrical:   kgeo =   2.20 W/m*K
Veinberg       : kvein=   2.20 W/m*K
```

```
energy density    : Q''' =   0.325e+09 J/m**3
performance factor: pf  =   2.28      W/m*K
storage factor    : s   =   0.740e+09 J*W/m**4*K
```

4   DISTILLED_WATER

freezing horizontal

118
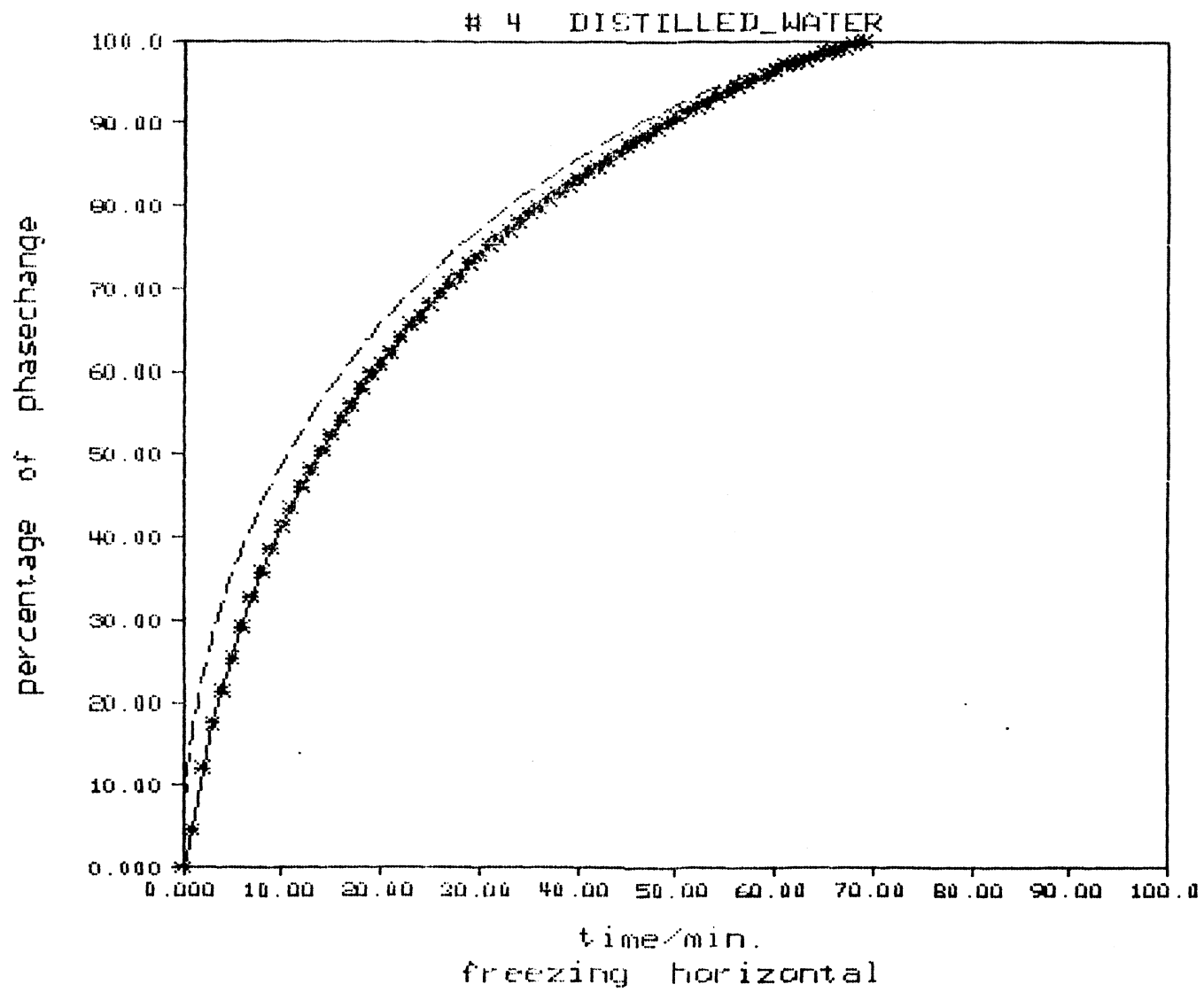
Experiment #   5


```
metal            : no metal only DISTILLED WATER
porosity         : phi = 1.000
discribtion      :   -
vol./area        : va  = ****** mm
density          : rhom= ******** kg/m**2
specific heat:   cm  = ******** J/kg*K
```


MELTING in a VERTICAL cylinder

```
temperature of bath .............. : Tb   =  30.0 C
ambient temperature .............. : Tsur=  21.0 C
average wall temperature ......... : Tw,a=  26.8 C
initial temperature of solid phase : Ti   =  -0.4 C
average temperature of liquid phase: Tlm  =  13.4 C
```

total time for melting: tt =   36.0 min
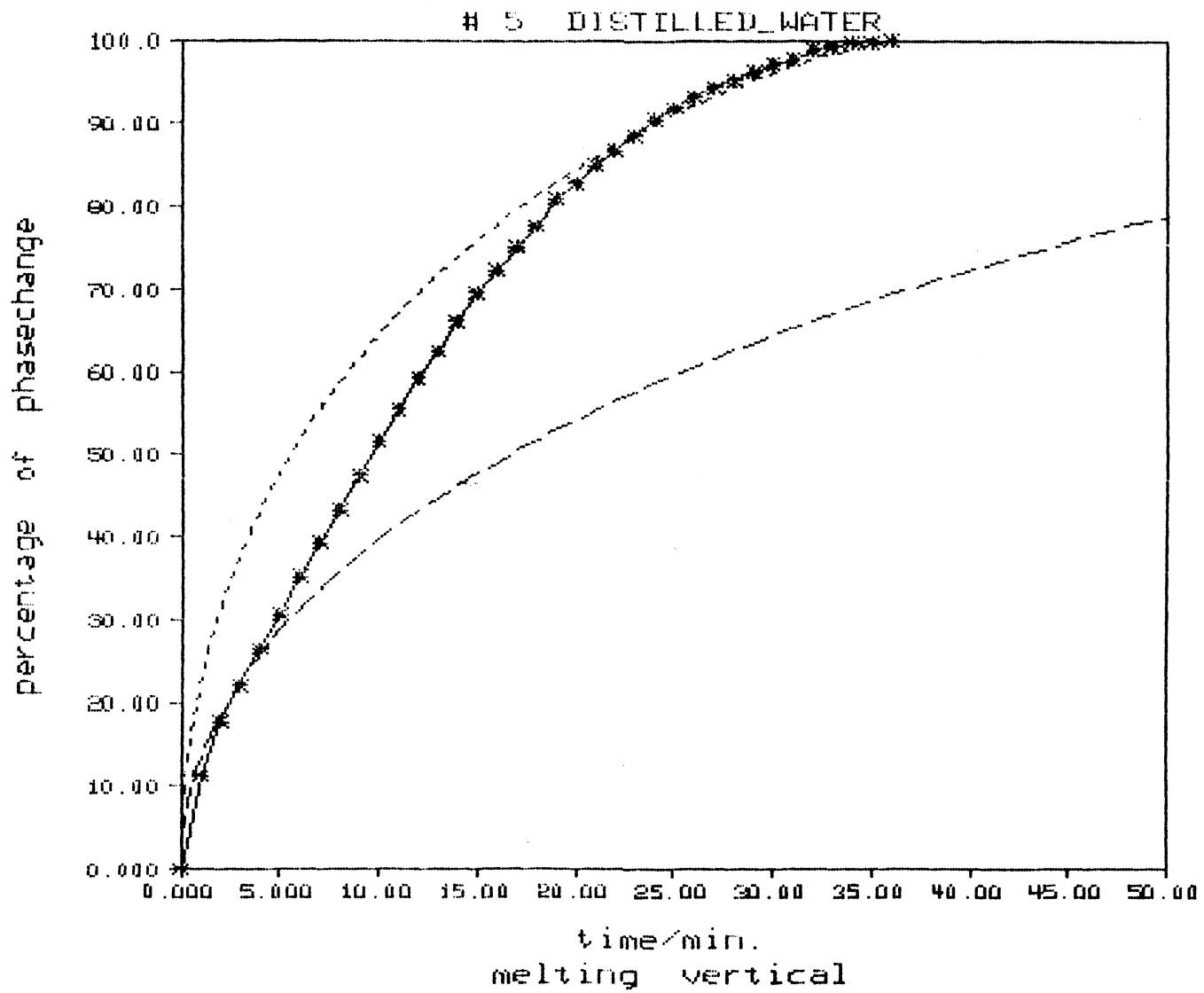
CONDUCTIVITY for liquid phase at Tlm =   13.4 C

```
     keff=    1.76 W/m*K
```

```
*************************
*   klm=   0.58 W/m*K   *
*************************
```

compare with these conductivities at Tlm=   13.4 C

```
metal        : km   = ****** W/m*K
water        : kh2o =   0.58 W/m*K
series       : kser =   0.58 W/m*K
parallel     : kpar =   0.58 W/m*K
empirical    : kemp =   0.58 W/m*K
geometrical: kgeo =   0.58 W/m*K
Veinberg     : kvein=   0.58 W/m*K
```

```
energy density   : Q''=  0.348e+09 J/m**3
performance factor: pf  =   2.00      W/m*K
storage factor   : s   =  0.696e+09 J*W/m**4*K
```

5   DISTILLED_WATER

percentage of phasechange

time/min.
melting vertical

120

Experiment #   6

metal   : no metal only DISTILLED WATER
porosity   : phi = 1.000
discribtion   :   —
vol./area   : va = ****** mm
density   : rhom= ******** kg/m**2
specific heat: cm = ******** J/kg*K

MELTING in a HORIZONTAL cylinder

temperature of bath .... : Tb   =   30.0 C
ambient temperature .... : Tsur=   21.0 C
average wall temperature .... : Tw,a=   25.7 C
initial temperature of solid phase : Ti   =   -0.4 C
average temperature of liquid phase: Tlm =   12.9 C

total time for melting: tt   =   25.0 min

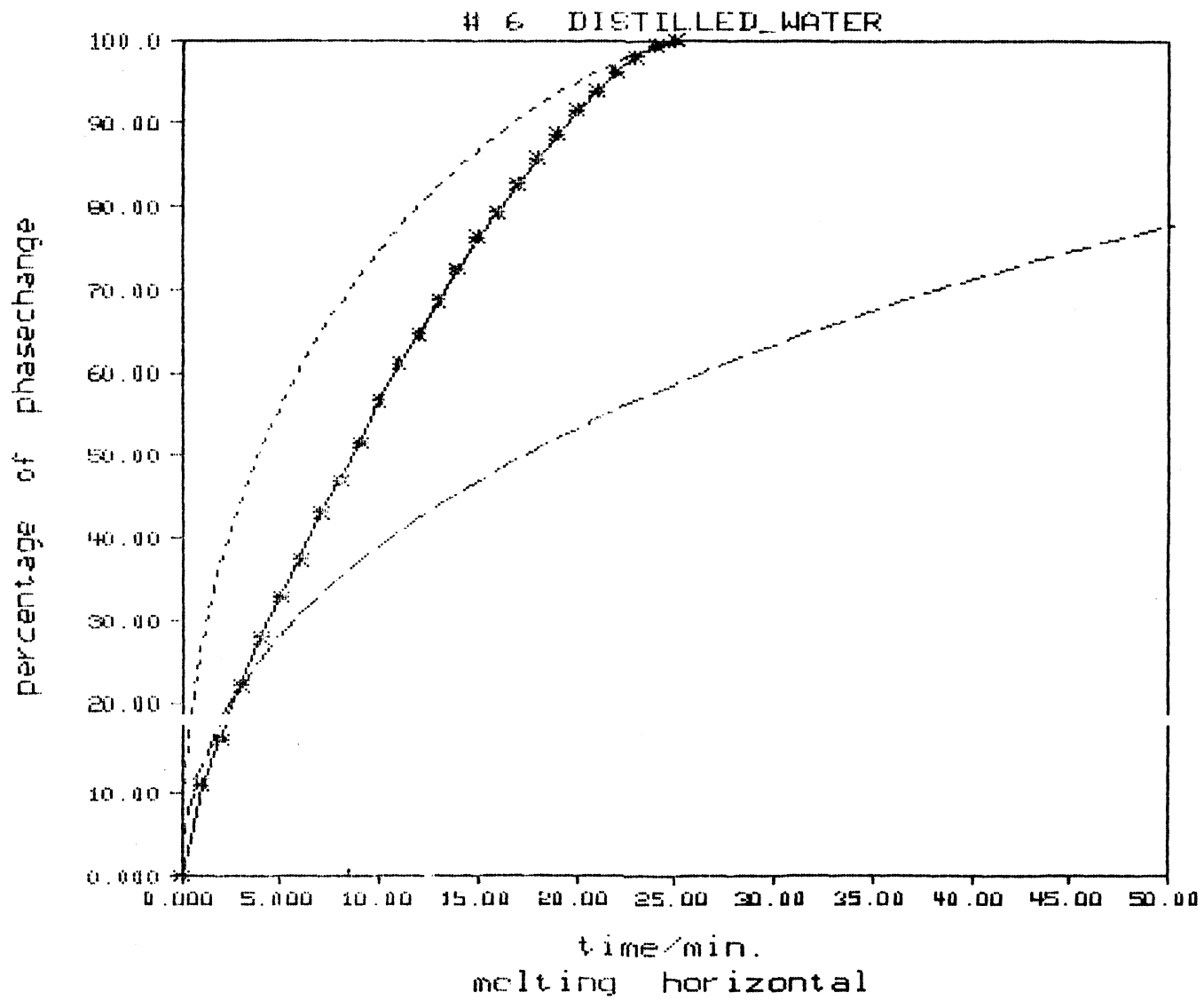CONDUCTIVITY for liquid phase at Tlm =   12.9 C

    keff=   2.64 W/m*K

****
*   klm=   0.58 W/m*K   *
****

compare with these conductivities at Tlm=   12.9 C

metal   : km   = ****** W/m*K
water   : kh2o =   0.58 W/m*K
series   : kser =   0.58 W/m*K
parallel   : kpar =   0.58 W/m*K
empirical   : kemp =   0.58 W/m*K
geometrical: kgeo =   0.58 W/m*K
Veinberg   : kvein=   0.58 W/m*K

energy density   : Q''''= 0.348e+09 J/m**3
performance factor: pf =   3.00   W/m*K
storage factor   : s. = 0.105e+10 J*W/m**4*K

6   DISTILLED_WATER

melting horizontal

time/min.

percentage of phasechange

122

Experiment #   7

metal   : no metal only DISTILLED WATER
porosity   : phi = 1.000
discribtion   :   -
vol./area   : va   = ****** mm
density   : rhom= ******** kg/m**2
specific heat: cm   = ******** J/kg*K

MELTING in a VERTICAL cylinder

temperature of bath .... : Tb   =   10.0 C
ambient temperature .... : Tsur=   21.0 C
average wall temperature .... : Tw,a=   9.6 C
initial temperature of solid phase : T1   =   -0.3 C
average temperature of liquid phase: Tlm =   4.8 C

total time for melting: tt   = 177.0 min

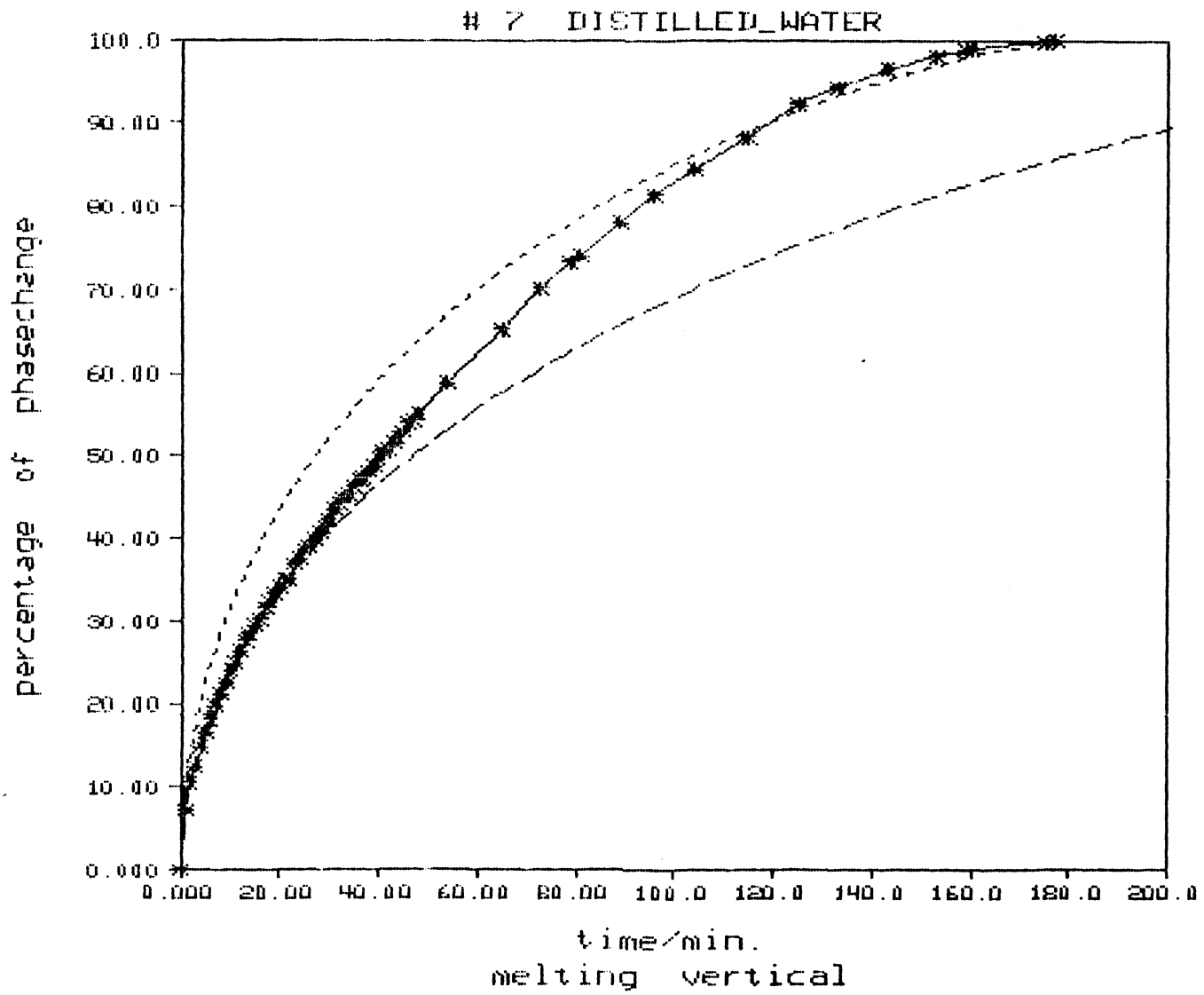CONDUCTIVITY for liquid phase at Tlm =   4.8 C

    keff=   1.00 W/m*K

****
*   klm=   0.58 W/m*K   *
****

compare with these conductivities at Tlm=   4.8 C

metal   : km   = ****** W/m*K
water   : kh2o =   0.57 W/m*K
series   : kser =   0.57 W/m*K
parallel   : kpar =   0.57 W/m*K
empirical   : kemp =   0.57 W/m*K
geometrical: kgeo =   0.57 W/m*K
Veinberg   : kvein=   0.57 W/m*K

energy density   : Q'''=   0.348e+09 J/m**3
performance factor: pf =   1.14   W/m*K
storage factor   : s   =   0.396e+09 J*W/m**4*K

7   DISTILLED_WATER

percentage of phasechange

time/min.
melting vertical

124

Experiment #   8

metal   : no metal only DISTILLED WATER
porosity   : phi = 1.000
discribtion   :   -
vol./area   : va = ****** mm
density   : rhom= ******** kg/m**2
specific heat: cm = ******** J/kg*K

MELTING in a HORIZONTAL cylinder

temperature of bath .... : Tb =   10.0 C
ambient temperature .... : Tsur= 21.0 C
average wall temperature .... : Tw,a=   9.5 C
initial temperature of solid phase : Ti = -0.2 C
average temperature of liquid phase: Tlm =   4.7 C

total time for melting: tt = 126.0 min

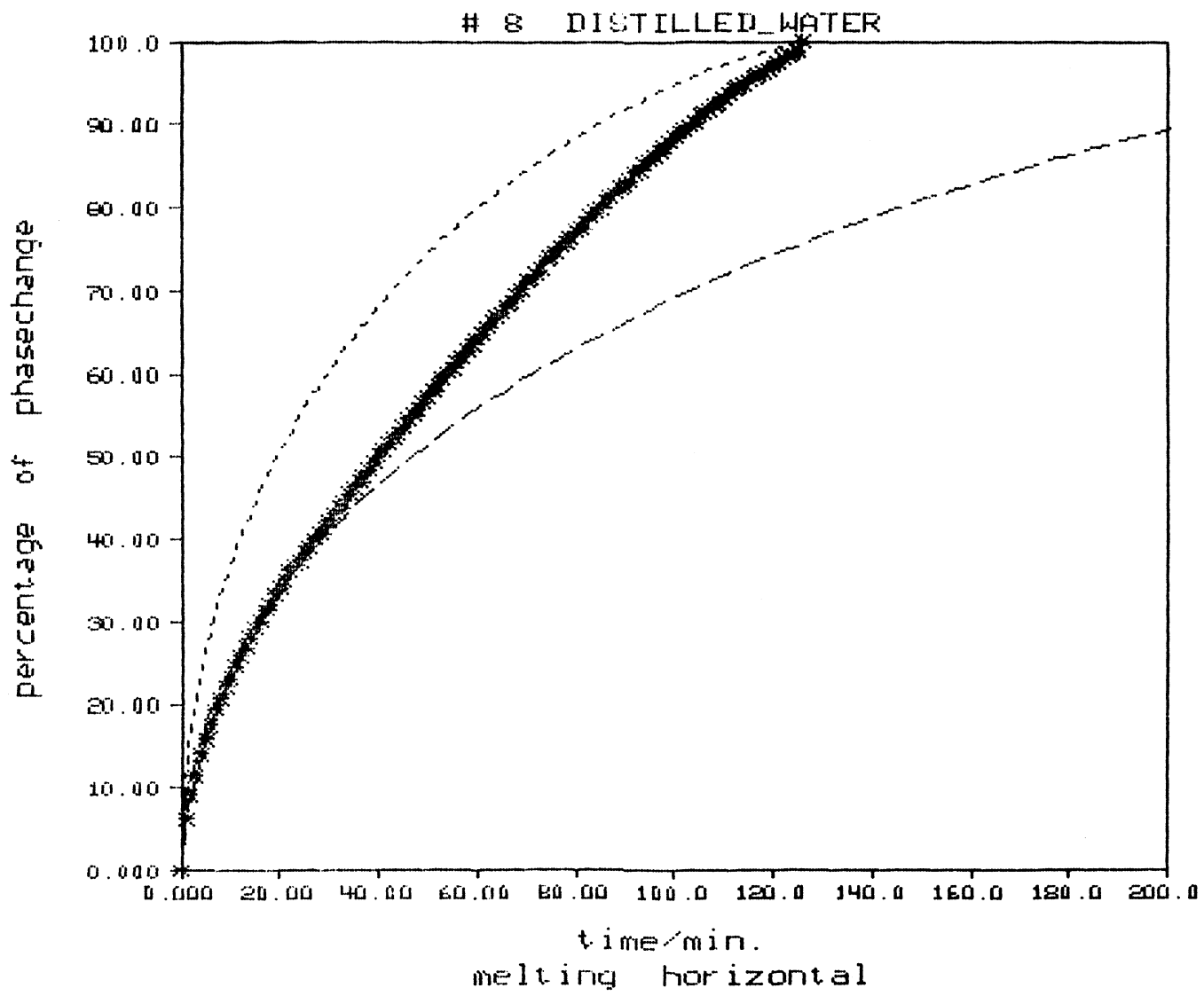CONDUCTIVITY for liquid phase at Tlm =   4.7 C

    keff=   1.43 W/m*K

****
*   klm=   0.59 W/m*K   *
****

compare with these conductivities at Tlm=   4.7 C

metal   : km   = ****** W/m*K
water   : kh2o =   0.57 W/m*K
series   : kser =   0.57 W/m*K
parallel   : kpar =   0.57 W/m*K
empirical   : kemp =   0.57 W/m*K
geometrical: kgeo =   0.57 W/m*K
Veinberg   : kvein=   0.57 W/m*K

energy density   : Q'''=   0.348e+09 J/m**3
performance factor: pf =   1.62   W/m*K
storage factor   : s   =   0.564e+09 J*W/m**4*K

8 DISTILLED_WATER

percentage of phasechange

time/min.
melting horizontal

Experiment #   9

    metal   : no metal only DISTILLED WATER
    porosity   : phi = 1.000
    discribtion   :   -
    vol./area   : va = ****** mm
    density   : rhom= ******** kg/m**2
    specific heat: cm = ******** J/kg*K

FREEZING in a VERTICAL cylinder

temperature of bath .... : Tb = -15.0 C
ambient temperature .... : Tsur= 19.0 C
average wall temperature .... : Tw,a= -11.5 C
initial temperature of liquid phase: Ti = 19.0 C
average temperature of solid phase : Tsm = -5.8 C

total time for freezing: tt = 71.0 min

CONDUCTIVITY for solid phase at Tsm = -5.8 C

****
*   ksm=   2.08 W/m*K   *
****

compare with these conductivities at Tsm= -5.8 C

metal   : km   = ****** W/m*K
ice   : kice =   2.20 W/m*K
series   : kser =   2.20 W/m*K
parallel   : kpar =   2.20 W/m*K
empirical   : kemp =   2.20 W/m*K
geometrical: kgeo =   2.20 W/m*K
Veinberg   : kvein=   2.20 W/m*K

energy density   : Q''= 0.325e+09 J/m**3
performance factor: pf =   2.21   W/m*K
storage factor   : s   = 0.718e+09 J*W/m**4*K

R 9   DISTILLED_WATER

freezing vertical

128
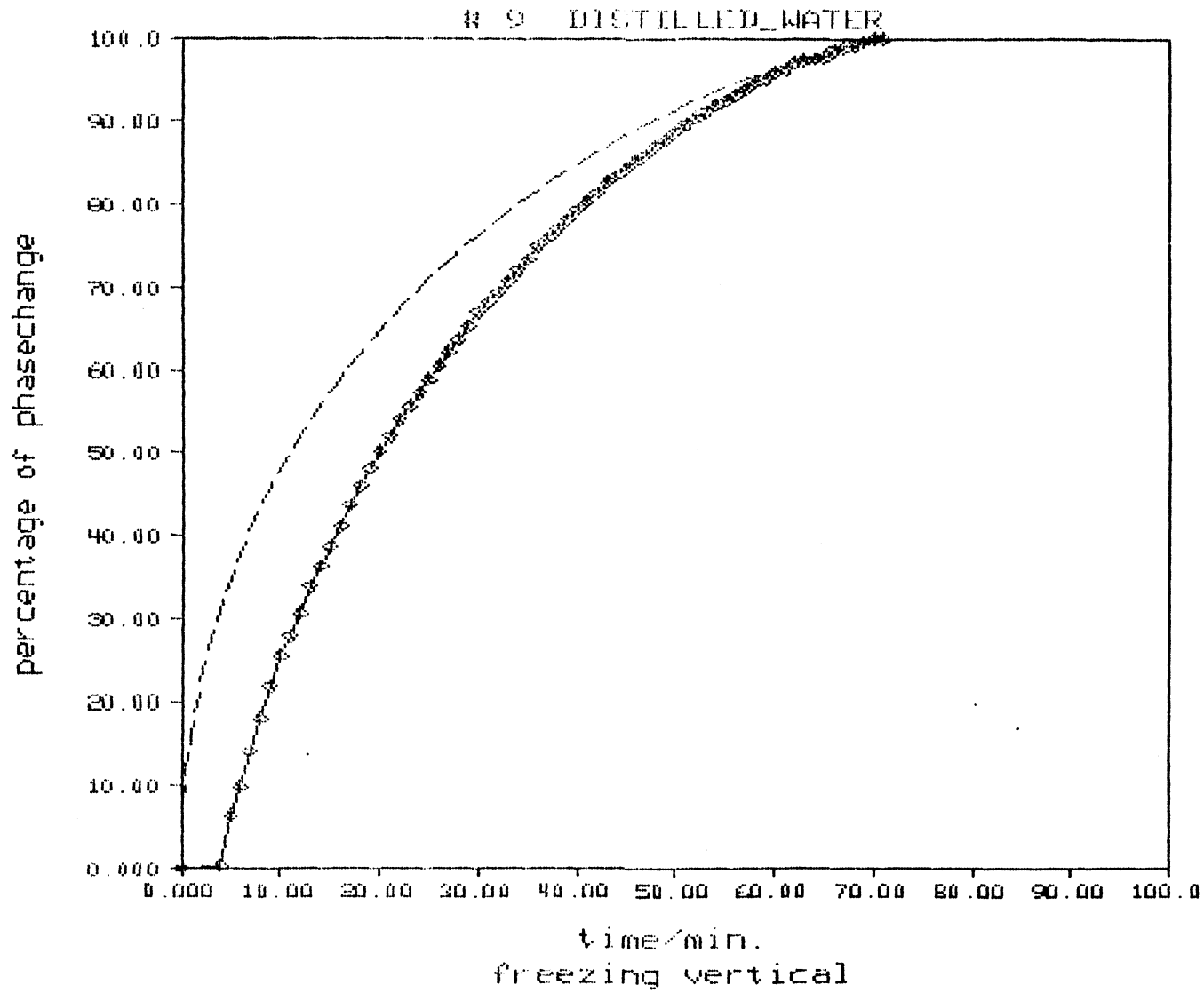
Experiment # 10

metal   : no metal only DISTILLED WATER
porosity   : phi = 1.000
description   : -
vol./area   : va = ****** mm
density   : rhom= ******** kg/m**2
specific heat: cm = ******** J/kg*K

MELTING in a VERTICAL cylinder

temperature of bath .... : Tb   = 30.0 C
ambient temperature .... : Tsur= 21.0 C
average wall temperature .... : Tw,a= 26.8 C
initial temperature of solid phase : Ti   = -15.0 C
average temperature of liquid phase: Tlm = 13.4 C

total time for melting: tt = 40.0 min
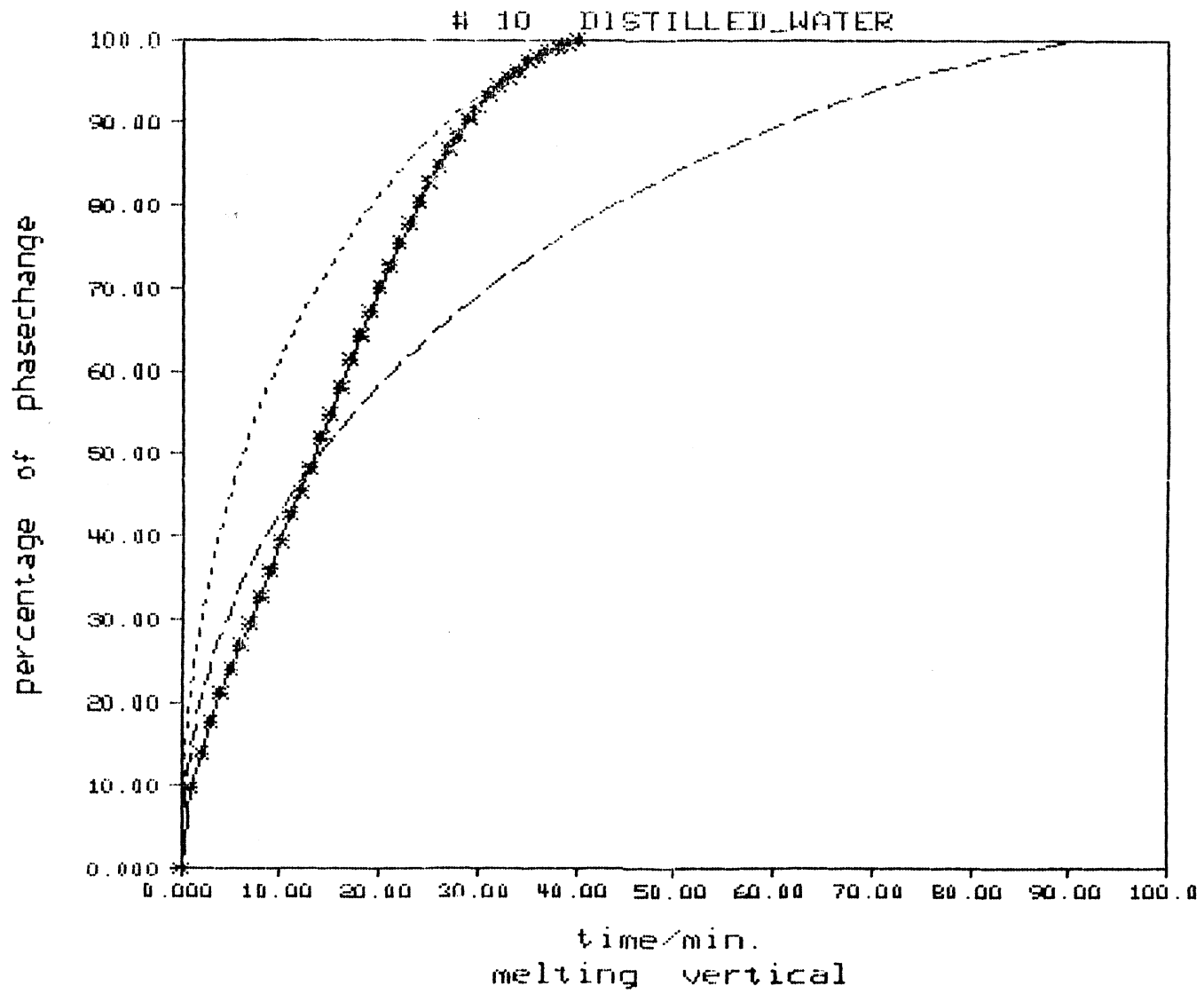
CONDUCTIVITY for liquid phase at Tlm = 13.4 C

    keff=   1.59 W/m*K

****
*   klm=   0.69 W/m*K   *
****

compare with these conductivities at Tlm= 13.4 C

metal   : km   = ****** W/m*K
water   : kh2o =   0.58 W/m*K
series   : kser =   0.58 W/m*K
parallel   : kpar =   0.58 W/m*K
empirical   : kemp =   0.58 W/m*K
geometrical: kgeo =   0.58 W/m*K
Veinberg   : kvein=   0.58 W/m*K

energy density   : Q'''=   0.348e+09 J/m**3
performance factor: pf =   1.80   W/m*K
storage factor   : s   =   0.627e+09 J*W/m**4*K

10   DISTILLED_WATER

melting vertical

Experiment # 11

metal   : no metal only DISTILLED WATER
porosity   : phi = 1.000
discribtion   :   -
vol./area   : va = ****** mm
density   : rhom= ******** kg/m**2
specific heat: cm = ******** J/kg*K

MELTING in a HORIZONTAL cylinder

temperature of bath .... : Tb   = 30.0 C
ambient temperature .... : Tsur= 21.0 C
average wall temperature .... : Tw,a= 25.7 C
initial temperature of solid phase : Ti   = -15.0 C
average temperature of liquid phase: Tlm =   12.9 C

total time for melting: tt = 30.0 min

CONDUCTIVITY for liquid phase at Tlm =   12.9 C

    keff=   2.20 W/m*K

****
* klm=   0.76 W/m*K *
****

compare with these conductivities at Tlm=   12.9 C

metal   : km   = ****** W/m*K
water   : kh2o = 0.58 W/m*K
series   : kser = 0.58 W/m*K
parallel   : kpar = 0.58 W/m*K
empirical   : kemp = 0.58 W/m*K
geometrical: kgeo = 0.58 W/m*K
Veinberg   : kvein= 0.58 W/m*K

energy density   : Q''= 0.348e+09 J/m**3
performance factor: pf =   2.51   W/m*K
storage factor   : s   = 0.872e+09 J*W/m**4*K

11   DISTILLED_WATER

melting horizontal

132
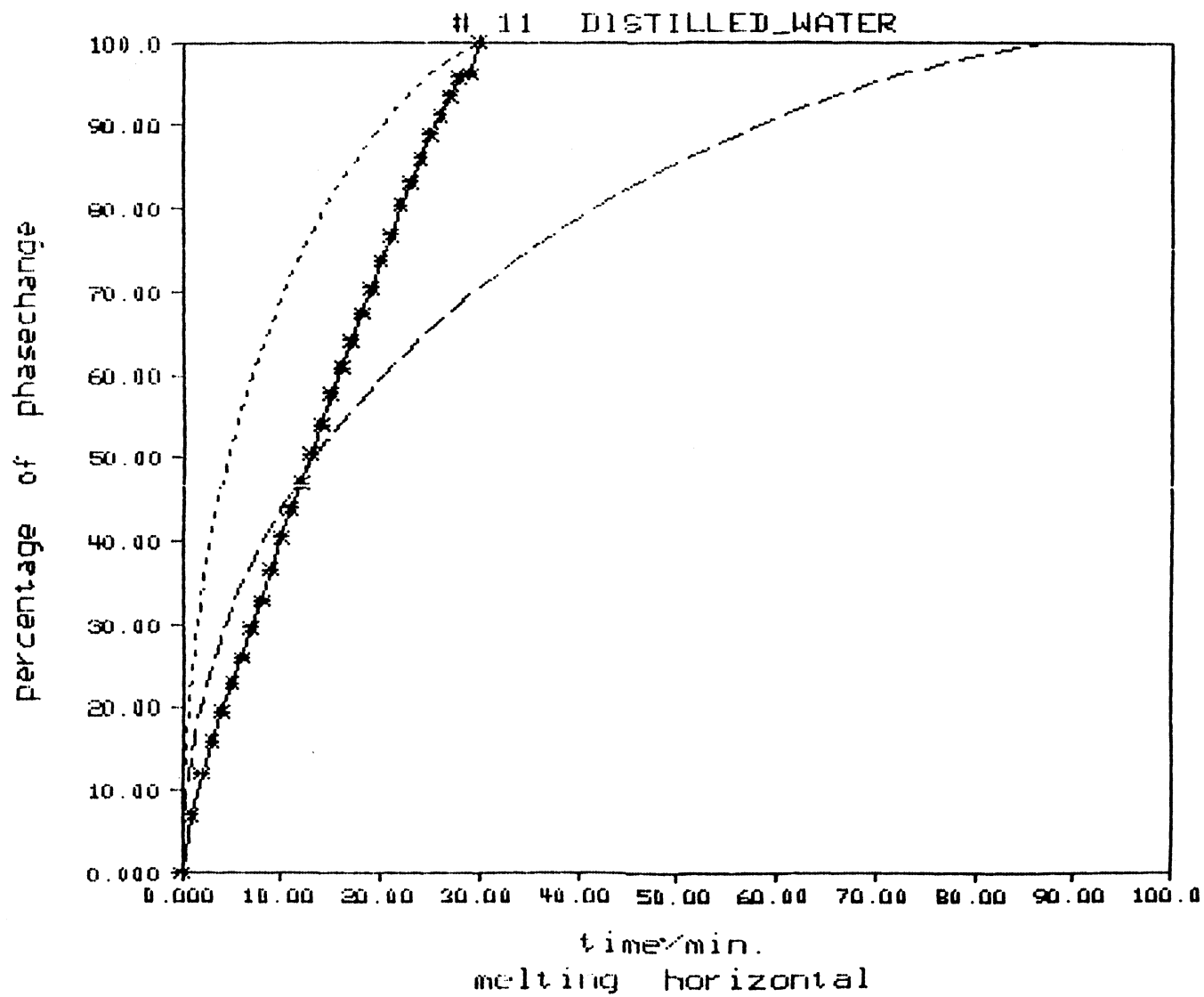
Experiment # 12

metal   : ALUMINUM
porosity   : phi = 0.424
discribtion : BEADS, diameter: 3.2mm
vol./area   : va = 0.0005 mm
density   : rhom= 2702.0 kg/m**2 .
specific heat: cm =   380.0 J/kg*K

FREEZING in a VERTICAL cylinder

temperature of bath .... : Tb = -15.0 C
ambient temperature .... : Tsur= 23.0 C
average wall temperature .... : Tw,a= -5.4 C
initial temperature of liquid phase: Ti =   0.3 C
average temperature of solid phase : Tsm = -2.7 C

total time for freezing: tt =   7.2 min

CONDUCTIVITY for solid phase at Tsm = -2.7 C

****
*   ksm= 43.71 W/m*K   *
****

compare with these conductivities at Tsm= -2.7 C

metal   : km   = 220.00 W/m*K
ice   : kice =   2.18 W/m*K
series   : kser =   5.08 W/m*K
parallel   : kpar = 127.58 W/m*K
empirical   : kemp = 31.07 W/m*K
geometrical : kgeo =   9.24 W/m*K
Veinberg   : kvein= 21.59 W/m*K

energy density   : Q'''= 0.152e+09 J/m**3
performance factor: pf =   21.6   W/m*K
storage factor   : s   = 0.328e+10 J*W/m**4*K

12   ALUMINUM_BEADS

freezing vertical

134
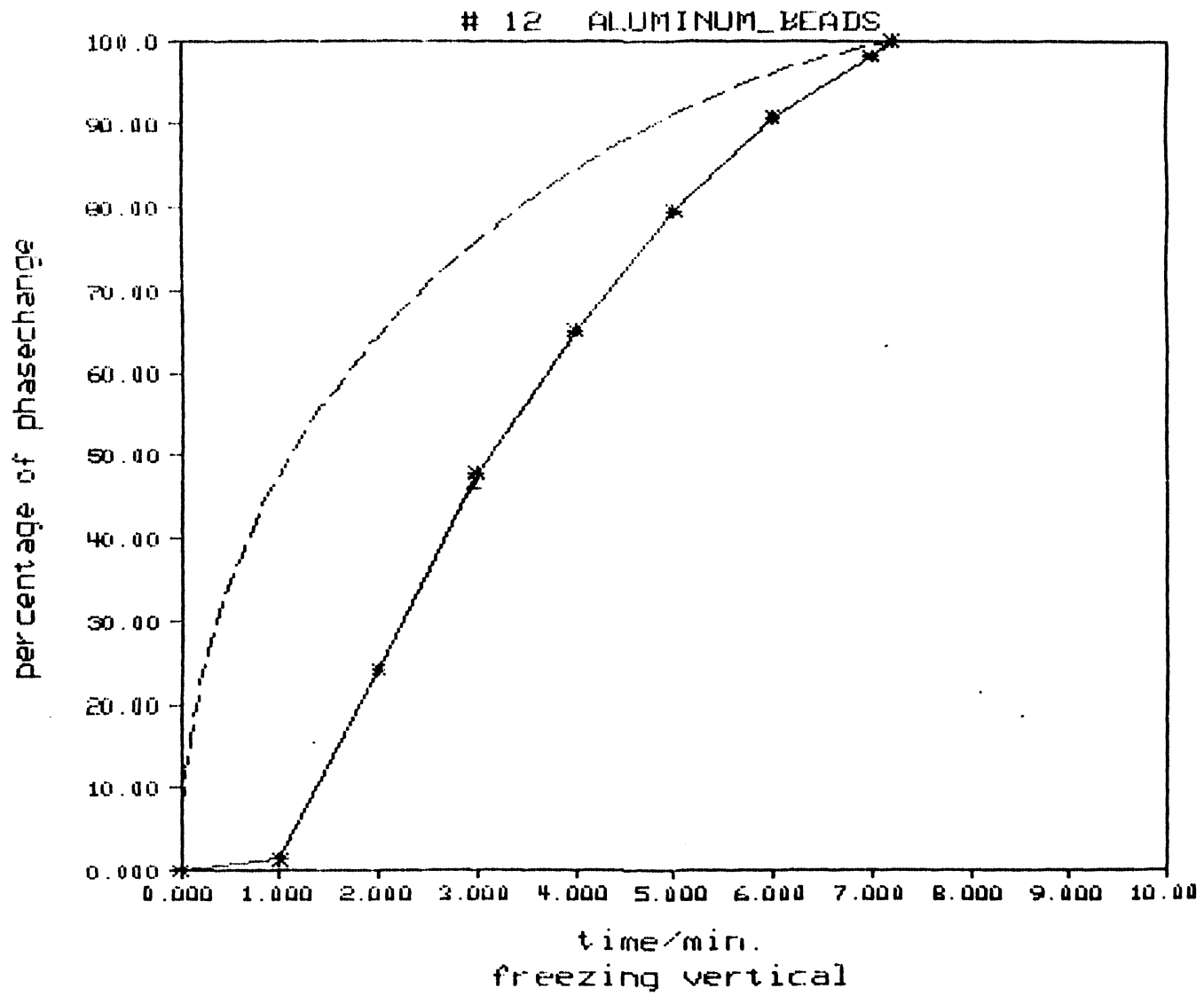
Experiment # 13

metal   : ALUMINUM
porosity   : phi = 0.424
discribtion : BEADS, diameter: 3.2mm
vol./area   : va = 0.5333 mm
density   : rhom=   2702.0 kg/m**2
specific heat: cm =   380.0 J/kg*K

MELTING in a VERTICAL cylinder

temperature of bath .... : Tb   =   20.0 C
ambient temperature .... : Tsur=   23.0 C
average wall temperature .... : Tw,a=   12.3 C
initial temperature of solid phase : Ti   =   -0.4 C
average temperature of liquid phase: Tlm =   6.2 C

total time for melting: tt =   7.5 min

CONDUCTIVITY for liquid phase at Tlm =   6.2 C

    keff=   18.42 W/m*K

****
*   klm=   18.42 W/m*K   *
****

compare with these conductivities at Tlm=   6.2 C

metal   : km   = 220.00 W/m*K
water   : kh2o =   0.57 W/m*K
series   : kser =   1.34 W/m*K
parallel   : kpar = 126.90 W/m*K
empirical   : kemp = 17.57 W/m*K
geometrical: kgeo =   2.49 W/m*K
Veinberg   : kvein=   6.84 W/m*K

energy density   : Q'''= 0.161e+09 J/m**3
performance factor: pf =   9.71   W/m*K
storage factor   : s   = 0.157e+10 J*W/m**4*K

13 ALUMINUM_BEADS

melting vertical
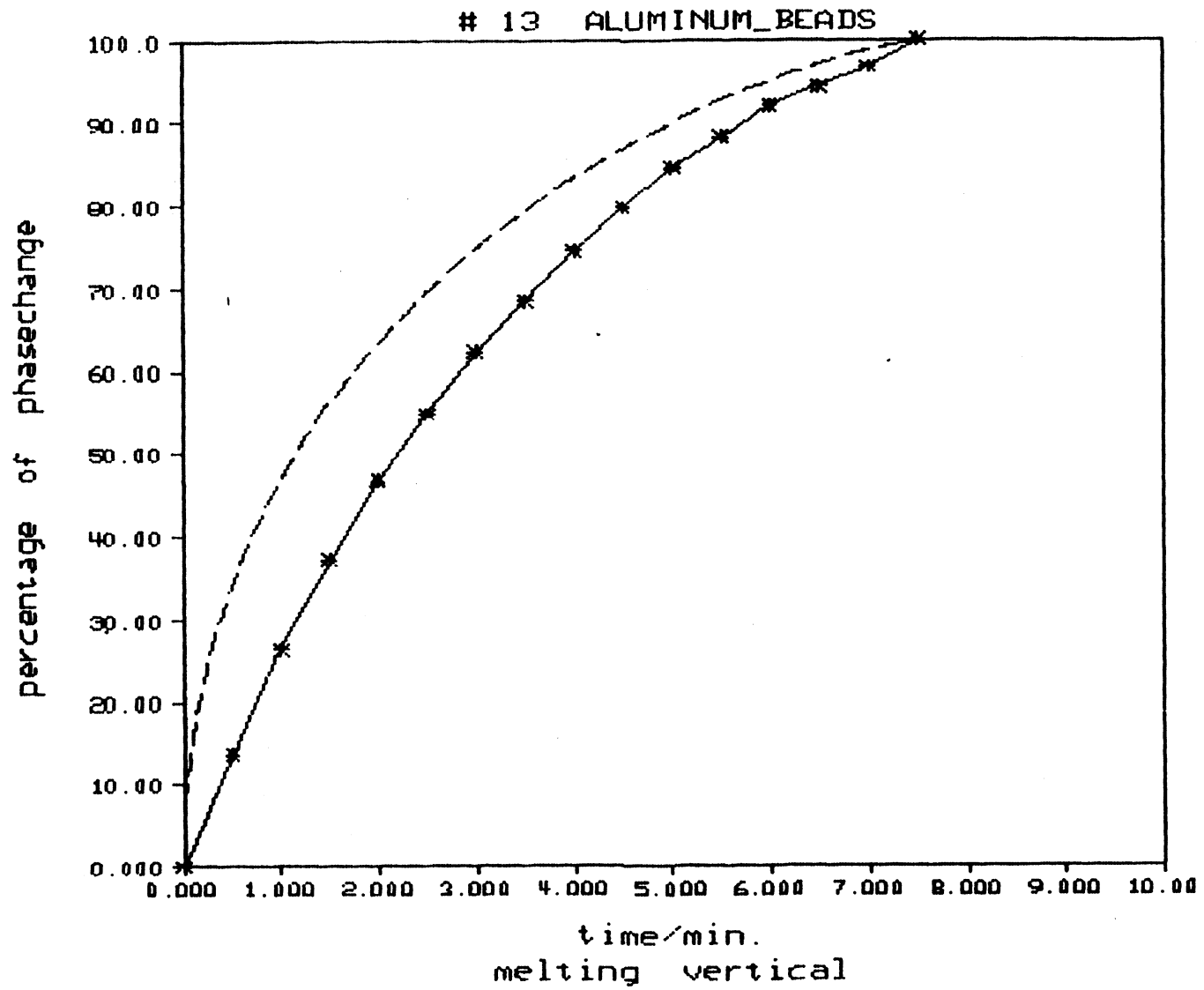
Experiment # 14

metal   : ALUMINUM
porosity   : phi = 0.424
discribtion   : BEADS, diameter: 3.2mm
vol./area   : va = 0.5333 mm
density   : rhom= 2702.0 kg/m**2
specific heat: cm =   880.0 J/kg*K

MELTING in a HORIZONTAL cylinder

temperature of bath .... : Tb   =   20.0 C
ambient temperature .... : Tsur=   23.0 C
average wall temperature .... : Tw,a=   14.1 C
initial temperature of solid phase : Ti   =   -0.3 C
average temperature of liquid phase: Tlm =   7.1 C

total time for melting: tt =   7.5 min

CONDUCTIVITY for liquid phase at Tlm =   7.1 C
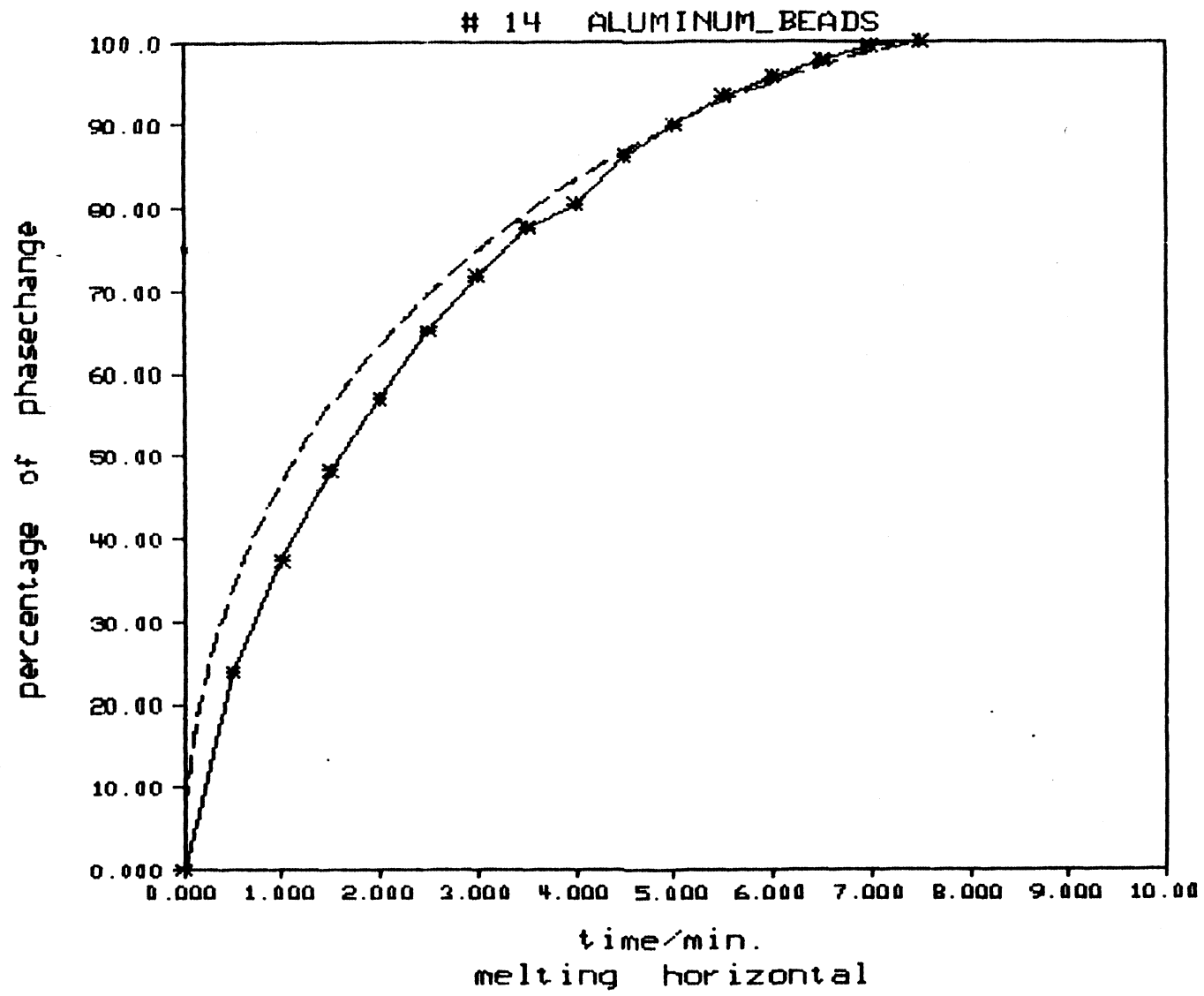

    keff= 16.07 W/m*K

****
*   klm= 16.07 W/m*K   *
****

compare with these conductivities at Tlm=   7.1 C

metal   : km   = 220.00 W/m*K
water   : kh2o =   0.57 W/m*K
series   : kser =   1.34 W/m*K
parallel   : kpar = 126.90 W/m*K
empirical   : kemp = 17.60 W/m*K
geometrical: kgeo =   2.50 W/m*K
Veinberg   : kvein=   6.86 W/m*K

energy density   : Q'''= 0.161e+09 J/m**3
performance factor: pf =   8.47   W/m*K
storage factor   : s   = 0.137e+10 J*W/m**4*K

14   ALUMINUM_BEADS

melting horizontal

138

Experiment # 15


```
metal          :  ALUMINUM
porosity       :  phi = 0.739
discribtion    :  SPIRALS #1, 0.5mm X 0.05m
vol./area      :  va  = 0.0231 mm
density        :  rhom= 2700.0 kg/m**2
specific heat:  cm  =    380.0 J/kg*K
```


FREEZING in a VERTICAL cylinder

```
temperature of bath ..............  :  Tb  = -25.0 C
ambient temperature ..............  :  Tsur=  22.0 C
average wall temperature .........  :  Tw,a= -17.1 C
initial temperature of liquid phase:  Ti  =   0.7 C
average temperature of solid phase :  Tsm =  -8.5 C
```

total time for freezing: tt =   36.0 min

CONDUCTIVITY for solid phase at Tsm =   -8.5 C


```
***************************
*   ksm=    2.76 W/m*K   *
***************************
```

compare with these conductivities at Tsm=   -8.5 C

```
metal        :  km   = 155.00 W/m*K
ice          :  kice =   2.21 W/m*K
series       :  kser =   2.23 W/m*K
parallel     :  kpar =   3.85 W/m*K
empirical    :  kemp =   2.31 W/m*K
geometrical:  kgeo =   2.24 W/m*K
Veinberg     :  kvein=   2.28 W/m*K
```

```
energy density     :  Q'''=  0.322e+09 J/m**3
performance factor:  pf  =   2.90      W/m*K
storage factor     :  s   =  0.934e+09 J*W/m**4*K
```

15   ALUMINUM_WOOL

freezing vertical
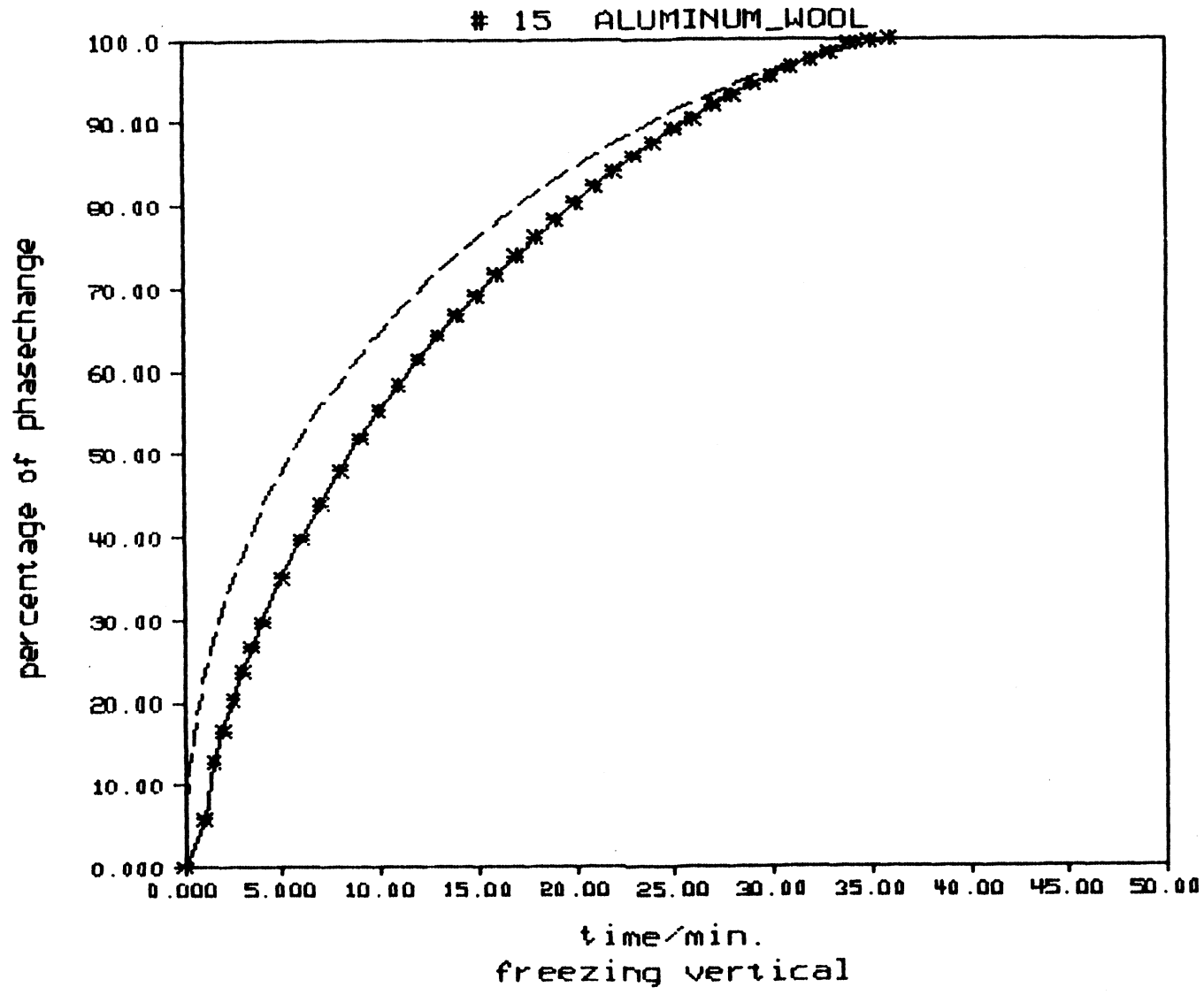
Experiment # 16

```
metal          : ALUMINUM
porosity       : phi = 0.789
discribtion    : SPIRALS #1, 0.5mm X 0.05m
vol./area      : vo  = 0.0231 mm
density        : rhom=  2700.0 kg/m**2
specific heat: cm  =    380.0 J/kg*K
```

MELTING in a VERTICAL cylinder

```
temperature of bath ............... : Tb   =   30.0 C
ambient temperature ............... : Tsur=   22.0 C
average wall temperature .......... : Tw,a=   26.1 C
initial temperature of solid phase : Ti   =   -0.7 C
average temperature of liquid phase: Tlm  =   13.0 C
```

total time for melting: tt =   32.0 min

CONDUCTIVITY for liquid phase at Tlm =   13.0 C
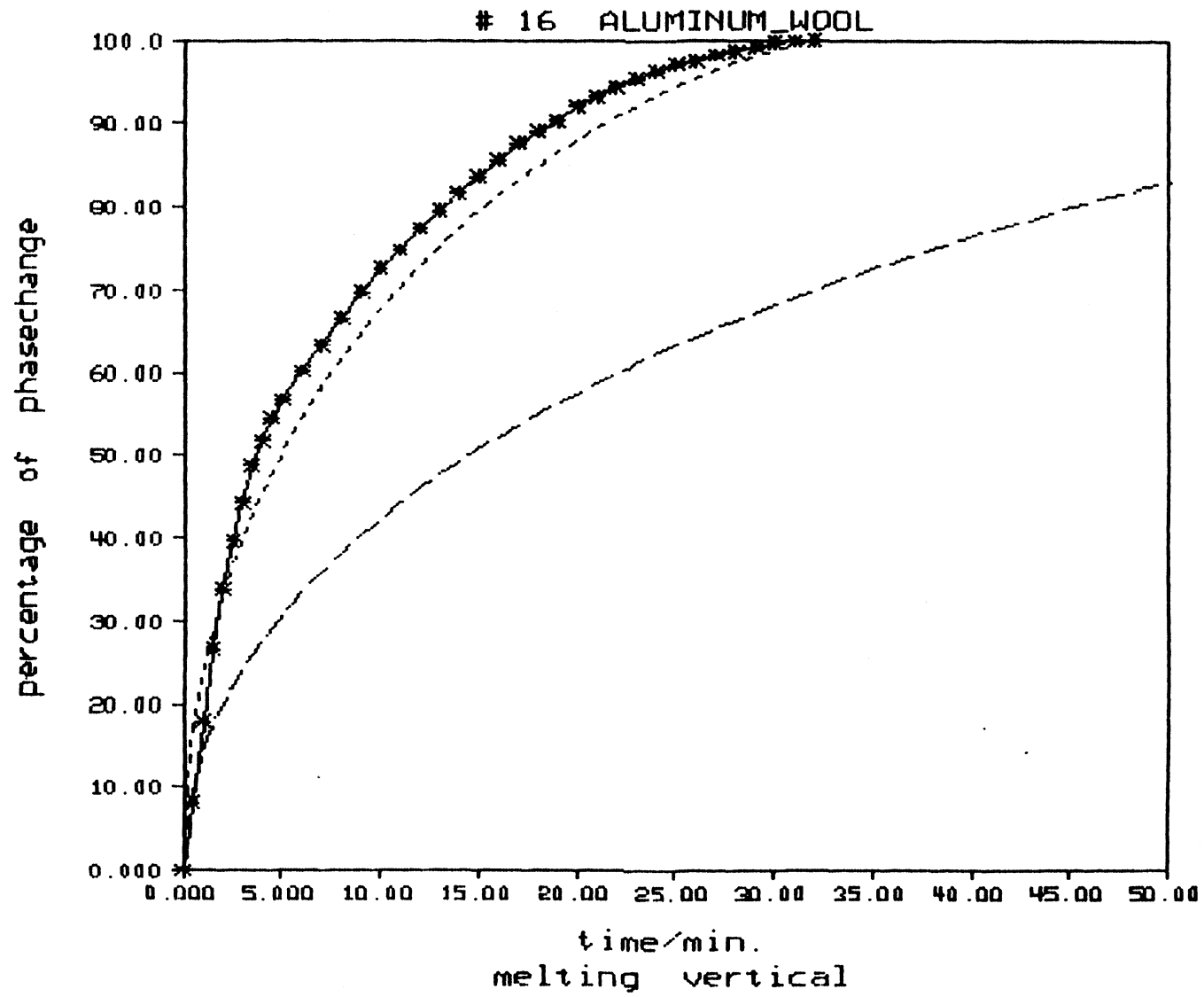
    keff=   2.04 W/m*K

```
*************************
*  klm=   0.69 W/m*K   *
*************************
```

compare with these conductivities at Tlm=   13.0 C

```
metal         : km   = 155.00 W/m*K
water         : kh2o =   0.58 W/m*K
series        : kser =   0.59 W/m*K
parallel      : kpar =   2.24 W/m*K
empirical     : kemp =   0.62 W/m*K
geometrical:  kgeo =   0.59 W/m*K
Veinberg      : kvein=   0.60 W/m*K
```

```
energy density    : Q'''=  0.345e+09 J/m**3
performance factor: pf  =   2.29      W/m*K
storage factor    : s   =  0.790e+09 J*W/m**4*K
```

16 ALUMINUM_WOOL

melting vertical

Experiment #   17

metal   : ALUMINUM
porosity   : phi = 0.939
discribtion   : SPIRALS #1, 0.5mm X 0.05m
vol./area   : va = 0.0231 mm
density   : rhom= 2700.0 kg/m**2
specific heat: cm =   380.0 J/kg*K

MELTING in a HORIZONTAL cylinder

temperature of bath .... : Tb = 30.0 C
ambient temperature .... : Tsur= 22.0 C
average wall temperature .... : Tw,a= 25.9 C
initial temperature of solid phase : Ti = -1.4 C
average temperature of liquid phase: Tlm = 13.0 C

total time for melting: tt = 22.0 min

CONDUCTIVITY for liquid phase at Tlm = 13.0 C

    keff=   2.78 W/m*K

****
* klm=   0.66 W/m*K   *
****

compare with these conductivities at Tlm= 13.0 C

metal   : km   = 155.00 W/m*K
water   : kh2o =   0.58 W/m*K
series   : kser =   0.59 W/m*K
parallel   : kpar =   2.24 W/m*K
empirical   : kemp =   0.62 W/m*K
geometrical: kgeo =   0.59 W/m*K
Veinberg   : kvein=   0.60 W/m*K

energy density   : Q'''= 0.345e+09 J/m**3
performance factor: pf =   3.35   W/m*K
storage factor   : s   = 0.116e+10 J*W/m**4*K

17 ALUMINUM_WOOL

melting horizontal

144
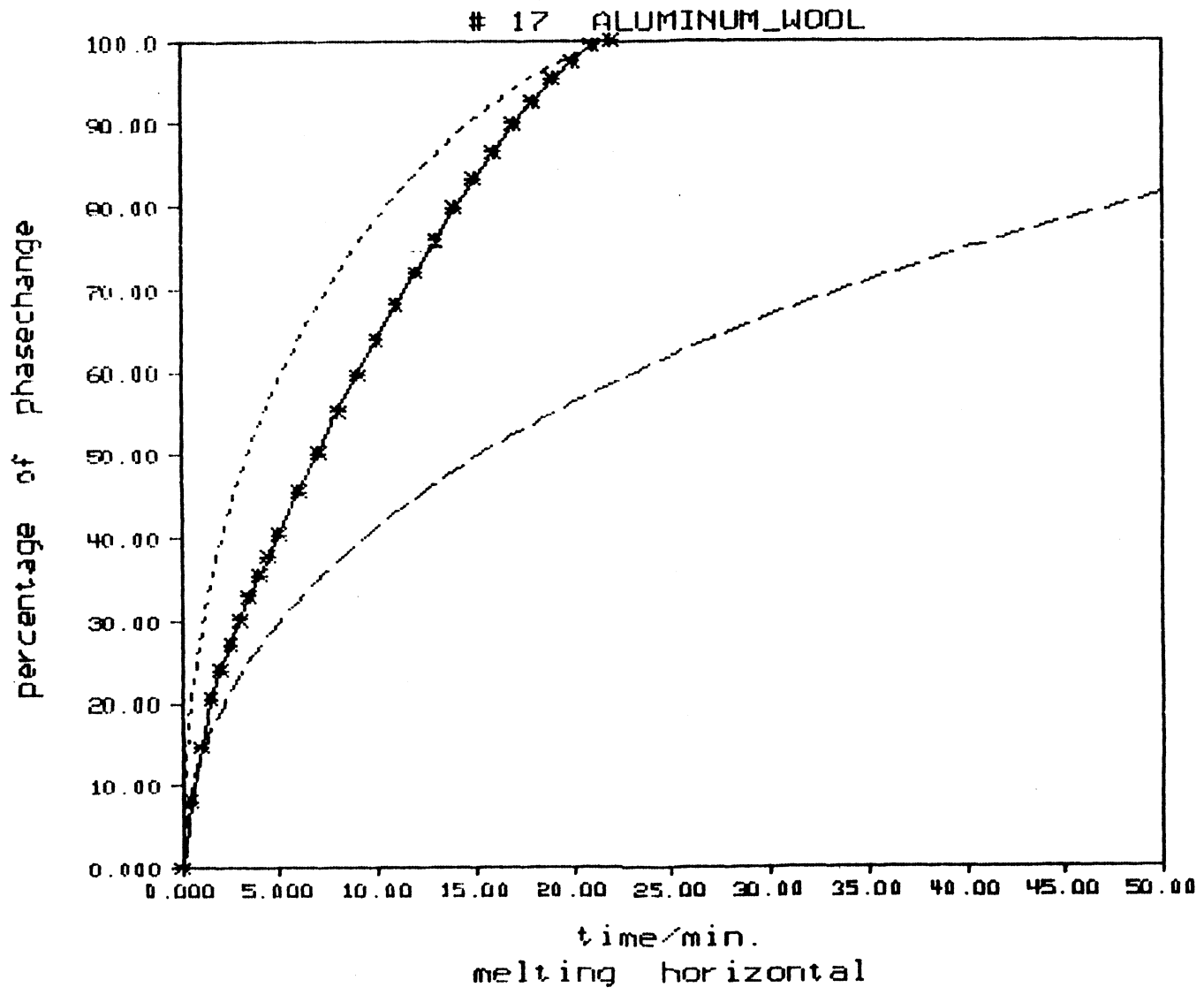
Experiment # 18

metal   : ALUMINUM
porosity   : phi = 0.903
description   : SPIRALS #2, 5.84mm X 0.15
vol./area   : va = 0.0743 mm
density   : rhom= 2700.0 kg/m**2
specific heat: cm =   380.0 J/kg*K

FREEZING in a VERTICAL cylinder

temperature of bath .... : Tb   = -13.0 C
ambient temperature .... : Tsur= 22.0 C
average wall temperature .... : Tw,a= -9.4 C
initial temperature of liquid phase: Ti   =   1.0 C
average temperature of solid phase : Tsm = -4.7 C

total time for freezing: tt = 35.0 min

CONDUCTIVITY for solid phase at Tsm = -4.7 C

****
*   ksm=   5.19 W/m*K   *
****

compare with these conductivities at Tsm= -4.7 C

metal   : km   = 155.00 W/m*K
ice   : kice =   2.19 W/m*K
series   : kser =   2.42 W/m*K
parallel   : kpar = 17.07 W/m*K
empirical   : kemp =   3.32 W/m*K
geometrical: kgeo =   2.58 W/m*K
Veinberg   : kvein=   2.74 W/m*K

energy density   : Q'''= 0.296e+09 J/m**3
performance factor: pf =   5.01   W/m*K
storage factor   : s   = 0.148e+10 J*W/m**4*K

18   ALUMINUM_CHIPS

time/min.
freezing vertical
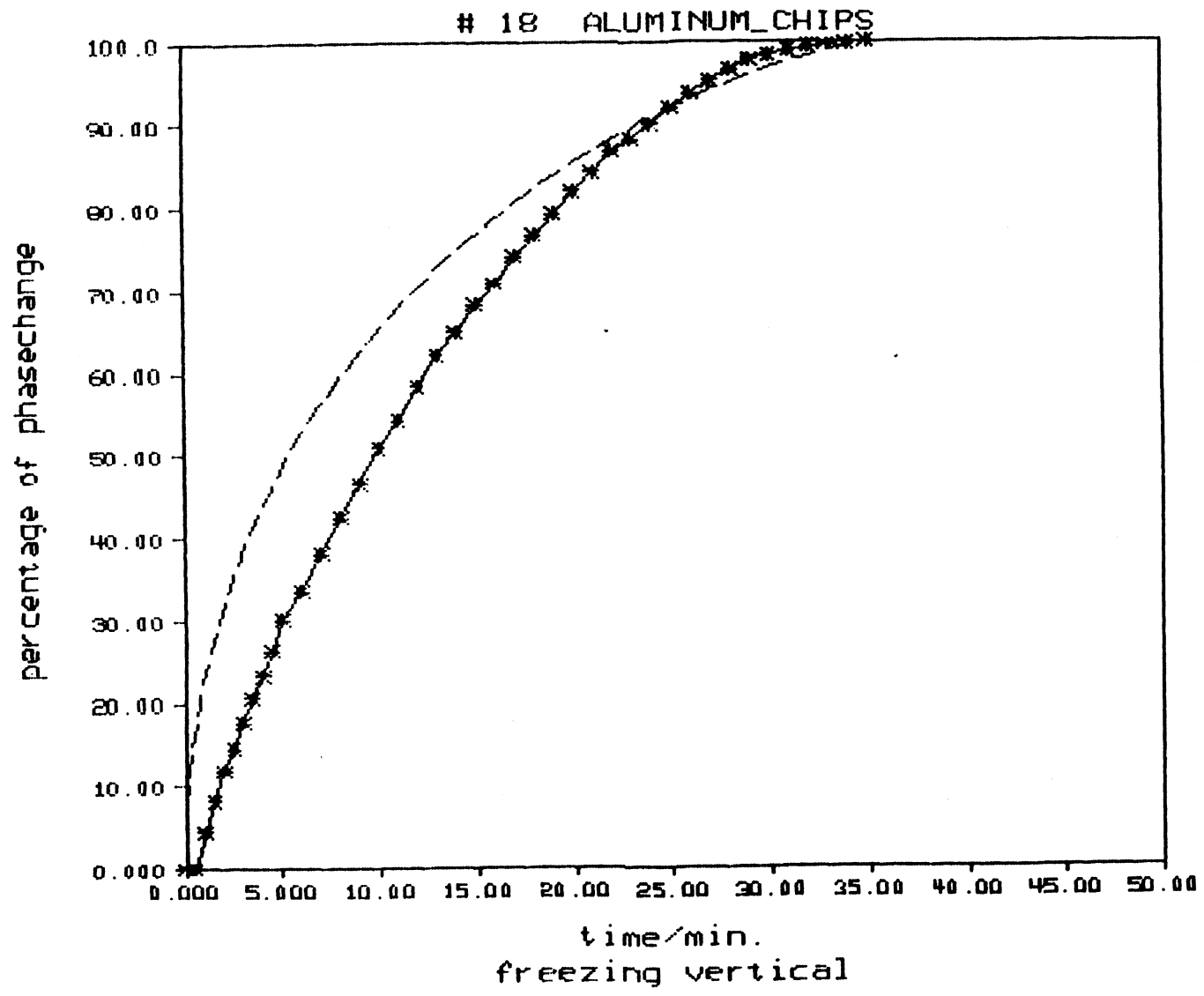
Experiment # 19

metal   : ALUMINUM
porosity   : phi = 0.903
description : SPIRALS #2, 5.84mm X 0.15
vol./area   : va = 0.0743 mm
density   : rhom=   2700.0 kg/m**2
specific heat: cm =   380.0 J/kg*K

MELTING in a VERTICAL cylinder

temperature of bath .... : Tb   =   30.0 C
ambient temperature .... : Tsur=   22.0 C
average wall temperature .... : Tw,a=   25.2 C
initial temperature of solid phase : Ti   = -0.6 C
average temperature of liquid phase: Tlm =   12.6 C

total time for melting: tt =   20.0 min

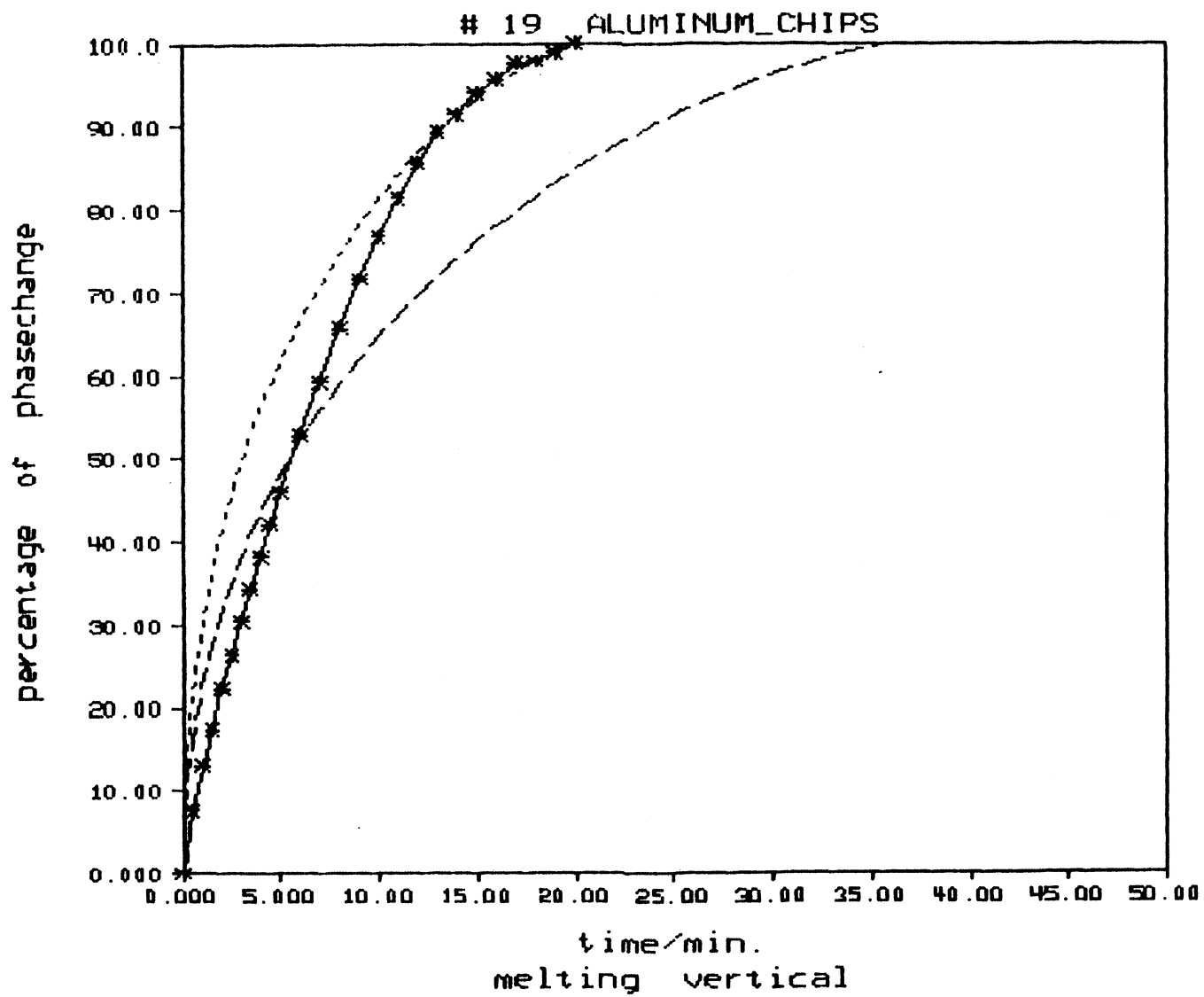CONDUCTIVITY for liquid phase at Tlm =   12.6 C

    keff=   0.37 W/m*K

****
*   klm=   1.08 W/m*K   *
****

compare with these conductivities at Tlm=   12.6 C

metal   : km   = 155.00 W/m*K
water   : kh2o =   0.58 W/m*K
series   : kser =   0.65 W/m*K
parallel   : kpar = 15.62 W/m*K
empirical   : kemp =   1.00 W/m*K
geometrical: kgeo =   0.69 W/m*K
Veinberg   : kvein=   0.79 W/m*K

energy density   : Q'''= 0.317e+09 J/m**3
performance factor: pf =   3.48   W/m*K
storage factor   : s   = 0.110e+10 J*W/m**4*K

19   ALUMINUM_CHIPS

percentage of phasechange

time/min.
melting   vertical

148

Experiment # 20


```
metal          : ALUMINUM
porosity       : phi = 0.703
description    : SPIRALS #2,  5.84mm X 0.15
vol./area      : va  = 0.0743 mm
density        : rhom=  2700.0 kg/m**2
specific heat: cm  =    380.0 J/kg*K
```


MELTING in a HORIZONTAL cylinder

```
temperature of bath ............... : Tb   =   30.0  C
ambient temperature ............... : Tsur=   22.0  C
average wall temperature ......... : Tw,a=   23.9  C
initial temperature of solid phase : Ti   =   -0.3  C
average temperature of liquid phase: Tlm  =   12.0  C
```

```
total time for melting:              tt   =   16.0 min
```

CONDUCTIVITY for liquid phase at Tlm =   12.0 C
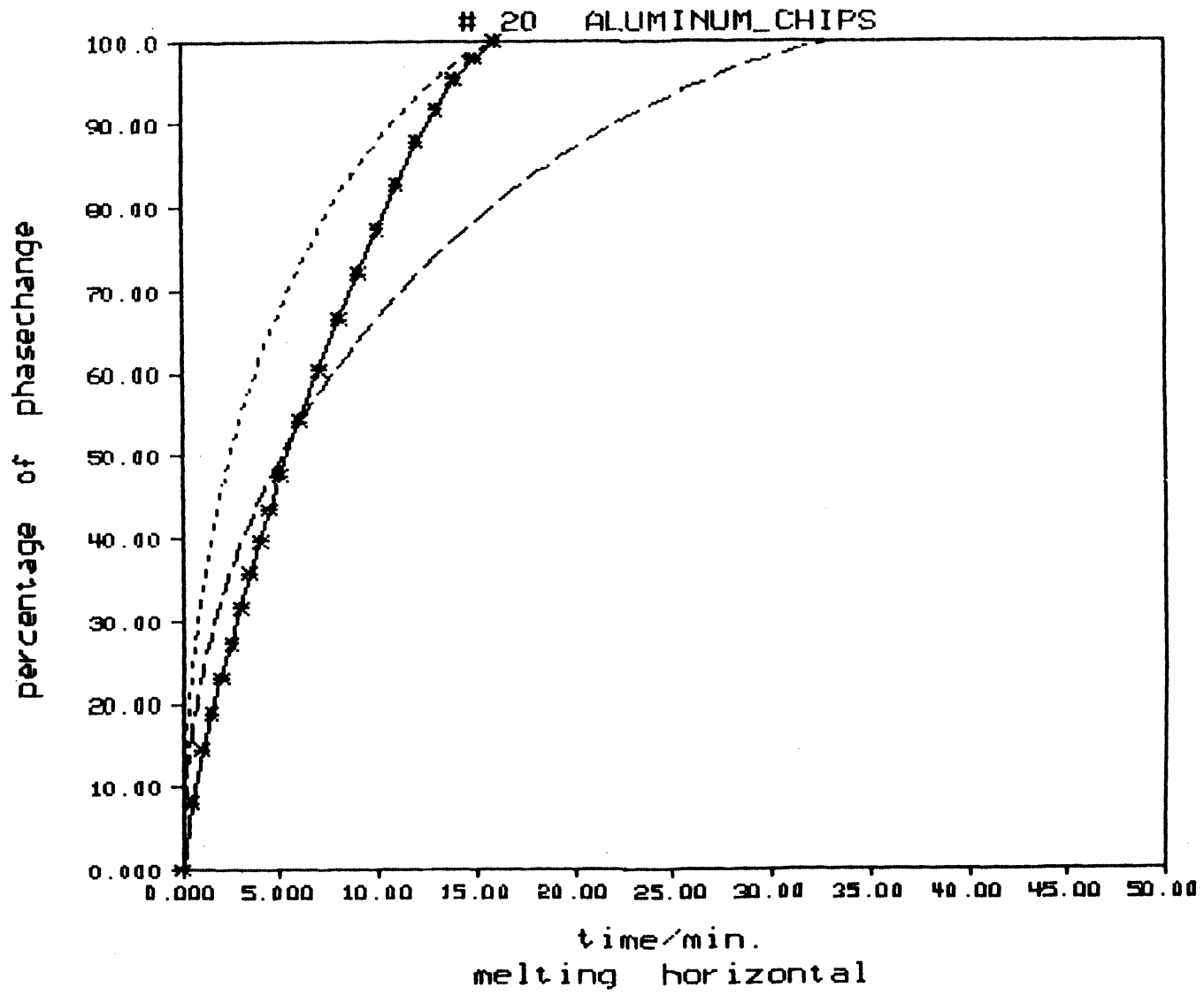
```
    keff=    4.44 W/m*K
```

```
*****************************
*   klm=    2.15 W/m*K    *
*****************************
```

compare with these conductivities at Tlm=   12.0 C

```
metal        : km   =  155.00 W/m*K
water        : kh2o =    0.58 W/m*K
series       : kser =    0.64 W/m*K
parallel     : kpar =   15.62 W/m*K
empirical    : kemp =    1.00 W/m*K
geometrical: kgeo =    0.69 W/m*K
Veinberg     : kvein=    0.79 W/m*K
```

```
energy density    : Q'''=  0.317e+09 J/m**3
performance factor: pf  =    4.59      W/m*K
storage factor    : s   =  0.145e+10 J*W/m**4*K
```

20   ALUMINUM_CHIPS

melting horizontal

Experiment # 21

```
metal          :  ALUMINUM
porosity       :  phi = 0.974
description    :  SPIRALS #3, 0.0508mm X 5.
vol./area      :  va  = 0.0252 mm
density        :  rhom=  2700.0 kg/m**2
specific heat:  cm  =    880.0 J/kg*K
```

FREEZING in a VERTICAL cylinder

```
temperature of bath .............. :  Tb   = -14.0 C
ambient temperature .............. :  Tsur=  22.0 C
average wall temperature ......... :  Tw,a=  -9.2 C
initial temperature of liquid phase:  Ti  =   0.8 C
average temperature of solid phase :  Tsm =  -4.6 C
```

total time for freezing: tt = 46.0 min

CONDUCTIVITY for solid phase at Tsm = -4.6 C

```
****************************
*   ksm=   4.03 W/m*K   *
****************************
```

compare with these conductivities at Tsm= -4.6 C

```
metal        :  km   = 155.00 W/m*K
ice          :  kice =   2.19 W/m*K
series       :  kser =   2.25 W/m*K
parallel     :  kpar =   6.14 W/m*K
empirical    :  kemp =   2.45 W/m*K
geometrical:  kgeo =   2.27 W/m*K
Veinberg     :  kvein=   2.36 W/m*K
```

```
energy density    :  Q'''=  0.317e+09 J/m**3
performance factor:  pf  =   4.17      W/m*K
storage factor    :  s   =  0.132e+10 J*W/m**4*K
```

21 ALUMINUM_CURLS

freezing vertical
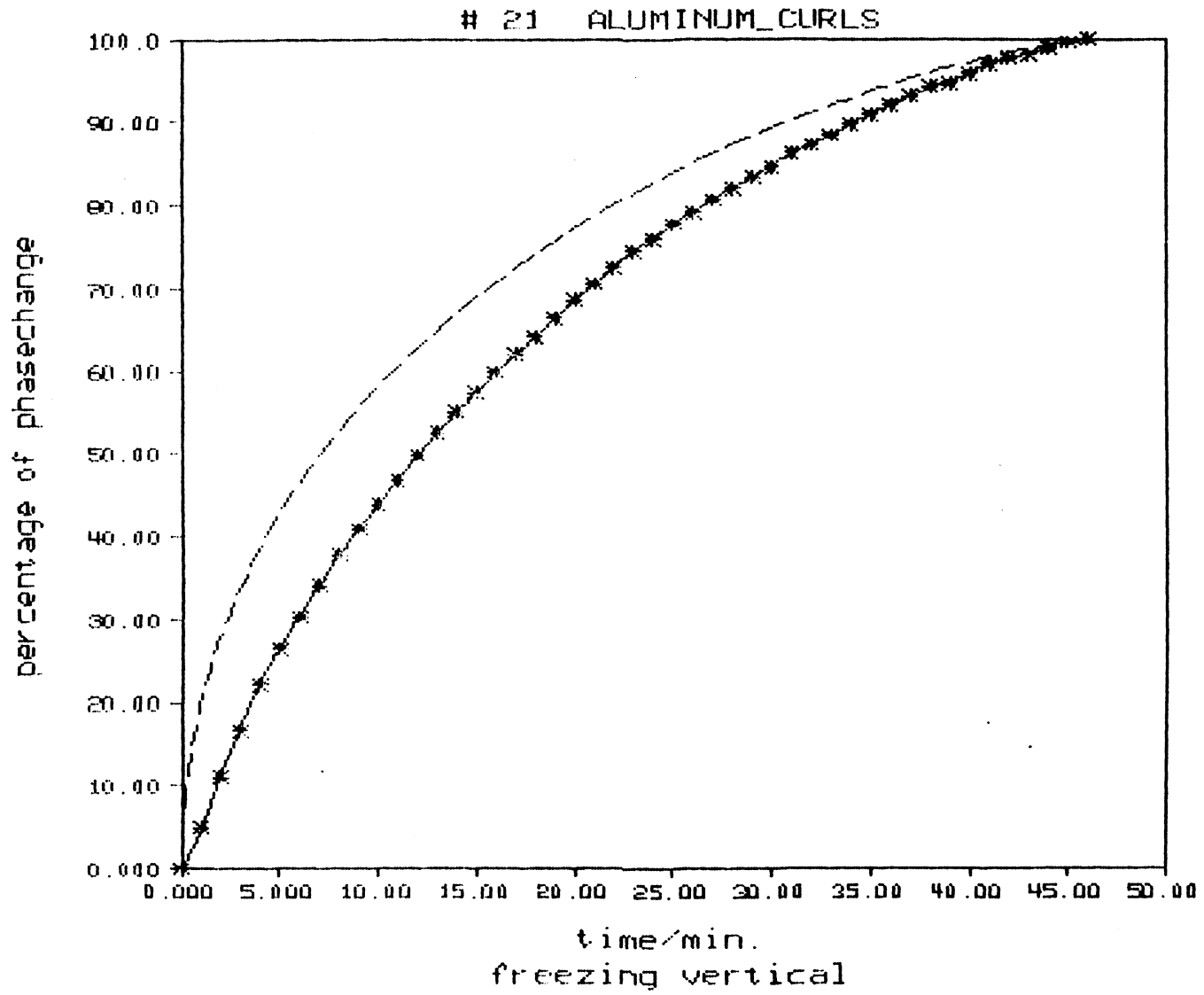
Experiment # 22


```
metal         : ALUMINUM
porosity      : phi = 0.774
description   : SPIRALS #3, 0.0508mm X 5.
vol./area     : va  = 0.0252 mm
density       : rhom=  2700.0 kg/m**2
specific heat: cm  =    880.0 J/kg*K
```


MELTING in a VERTICAL cylinder

```
temperature of bath .............. : Tb   =  30.0 C
ambient temperature .............. : Tsur=  22.0 C
average wall temperature ......... : Tw,a=  25.7 C
initial temperature of solid phase : Ti   =  -0.4 C
average temperature of liquid phase: Tlm  =  12.9 C
```

total time for melting: tt = 21.0 min

CONDUCTIVITY for liquid phase at Tlm = 12.9 C

    keff=   0.15 W/m*K


```
***********************
*   klm=   2.48 W/m*K   *
***********************
```

compare with these conductivities at Tlm= 12.9 C

```
metal        : km   = 155.00 W/m*K
water        : kh2o =   0.58 W/m*K
series       : kser =   0.60 W/m*K
parallel     : kpar =   4.58 W/m*K
empirical    : kemp =   0.67 W/m*K
geometrical: kgeo =   0.60 W/m*K
Veinberg     : kvein=   0.63 W/m*K
```

```
energy density    : Q'''=  0.340e+09 J/m**3
performance factor: pf  =   3.49      W/m*K
storage factor    : s   =  0.119e+10 J*W/m**4*K
```

22   ALUMINUM_CURLS

melting vertical

154
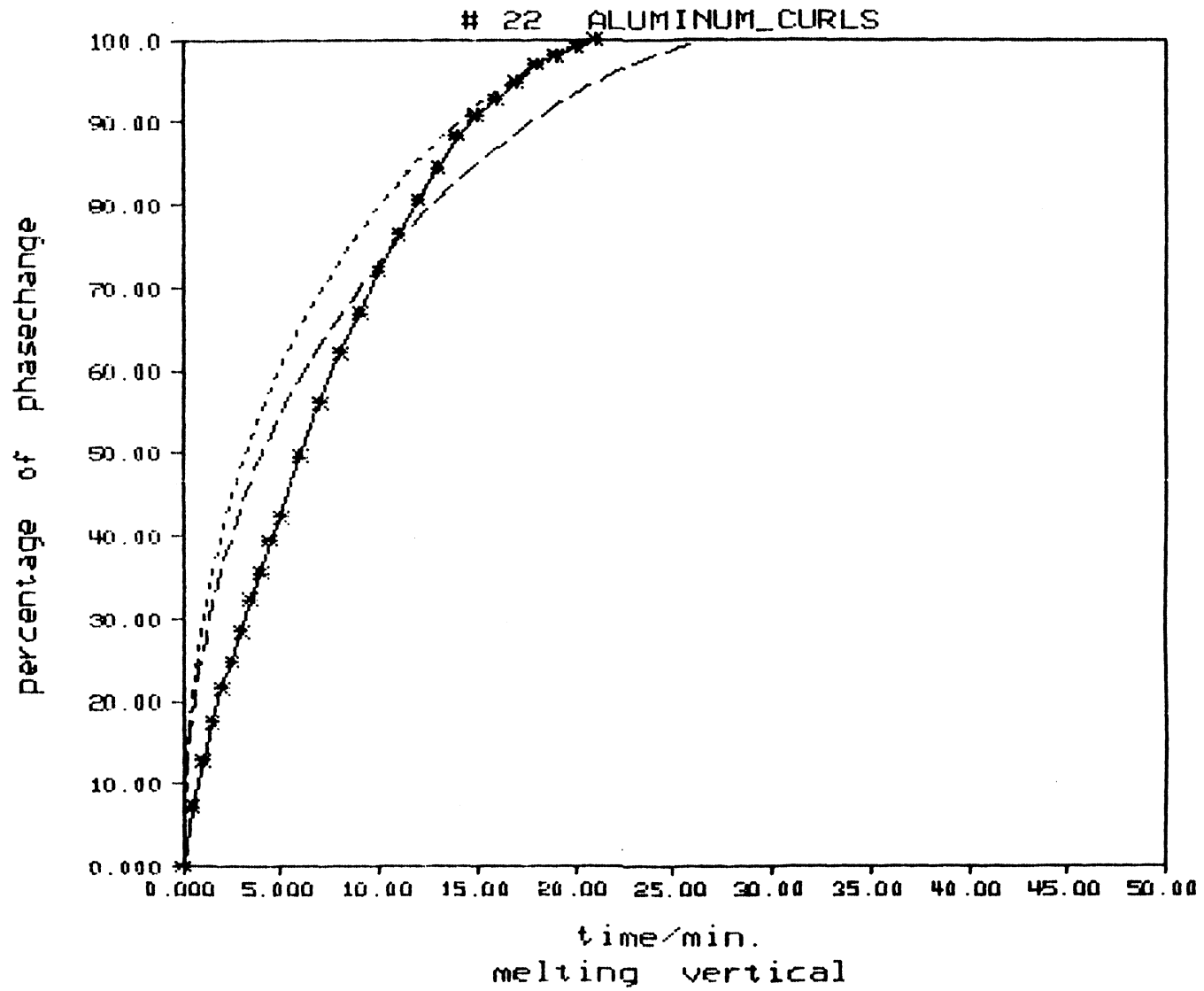
Experiment # 23

metal   : ALUMINUM
porosity   : phi = 0.974
description : SPIRALS #3, 0.0508mm X 5.
vol./area   : va = 0.0252 mm
density   : rhom= 2700.0 kg/m**2
specific heat: cm =   380.0 J/kg*K

MELTING in a HORIZONTAL cylinder

temperature of bath .... : Tb   = 30.0 C
ambient temperature .... : Tsur= 22.0 C
average wall temperature .... : Tw,a= 24.2 C
initial temperature of solid phase : Ti   = -0.5 C
average temperature of liquid phase: Tlm = 12.1 C

total time for melting: tt = 19.0 min

CONDUCTIVITY for liquid phase at Tlm = 12.1 C

    keff=   3.70 W/m*K

****
*   klm=   2.73 W/m*K   *
****

compare with these conductivities at Tlm= 12.1 C

metal   : km   = 155.00 W/m*K
water   : kh2o =   0.58 W/m*K
series   : kser =   0.60 W/m*K
parallel   : kpar =   4.57 W/m*K
empirical   : kemp =   0.67 W/m*K
geometrical : kgeo =   0.60 W/m*K
Veinberg   : kvein=   0.63 W/m*K

energy density   : Q'''= 0.340e+09 J/m**3
performance factor : pf =   4.10   W/m*K
storage factor   : s   = 0.139e+10 J*W/m**4*K

23   ALUMINUM_CURLS

melting horizontal

156
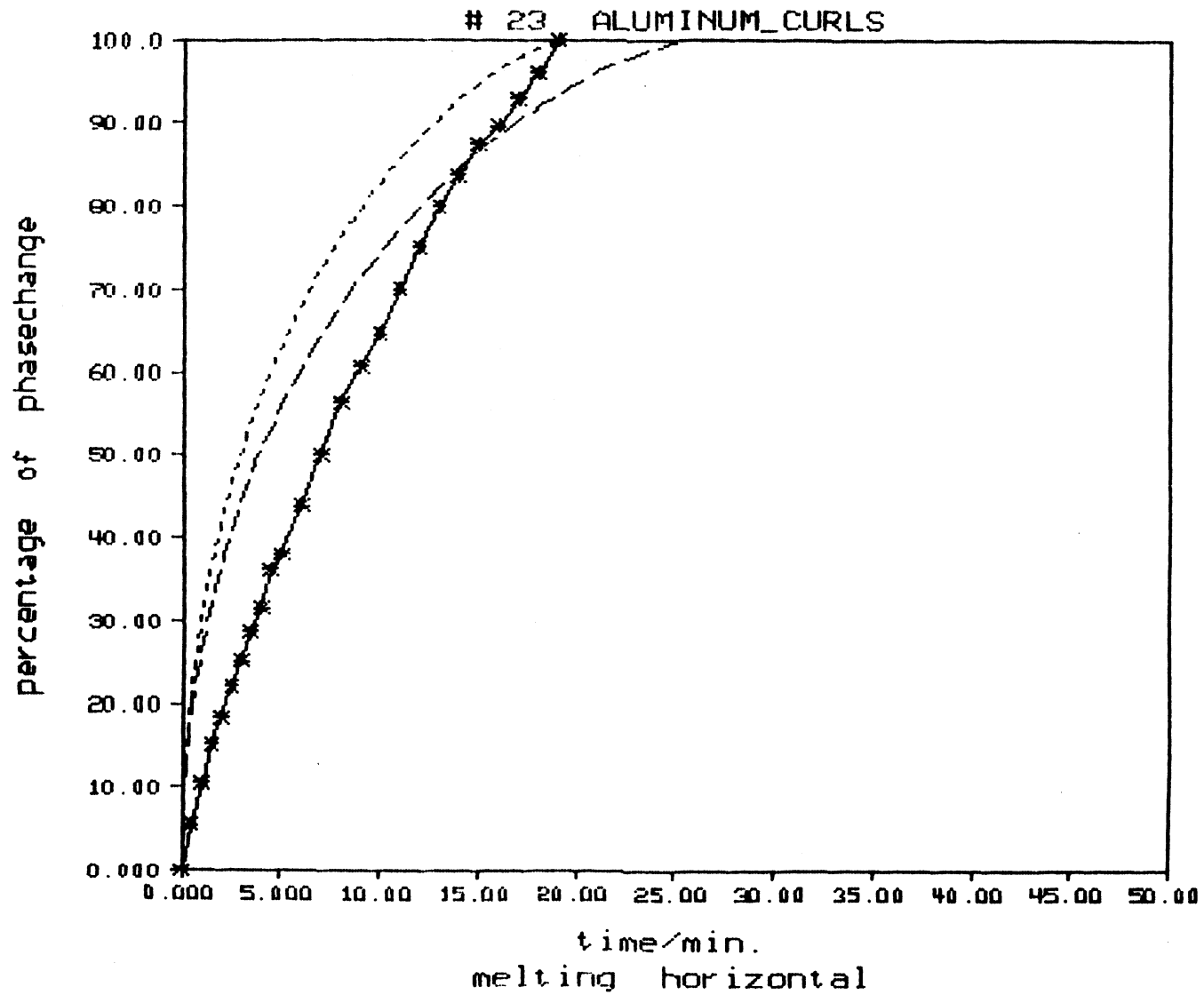
Experiment # 24

metal   : ALUMINUM
porosity   : phi = 0.532
description   : BEADS, diameter: 12mm
vol./area   : va = 2.0000 mm
density   : rhom= 2702.0 kg/m**2   .
specific heat: cm =   880.0 J/kg*K

FREEZING in a VERTICAL cylinder

temperature of bath .... : Tb = -14.0 C
ambient temperature .... : Tsur= 24.0 C
average wall temperature .... : Tw,a= -6.0 C
initial temperature of liquid phase: Ti =   2.5 C
average temperature of solid phase : Tsm = -3.0 C

total time for freezing: tt =   9.5 min


CONDUCTIVITY for solid phase at Tsm = -3.0 C

****
*   ksm= 29.09 W/m*K   *
****

compare with these conductivities at Tsm= -3.0 C

metal   : km   = 220.00 W/m*K
ice   : kice =   2.18 W/m*K
series   : kser =   4.07 W/m*K
parallel   : kpar = 104.18 W/m*K
empirical   : kemp = 18.93 W/m*K
geometrical: kgeo =   6.56 W/m*K
Veinberg   : kvein= 12.55 W/m*K

energy density   : Q'''= 0.184e+09 J/m**3
performance factor: pf =   18.0   W/m*K
storage factor   : s   = 0.330e+10 J*W/m**4*K

24   ALUMINUM_BEADS

freezing vertical
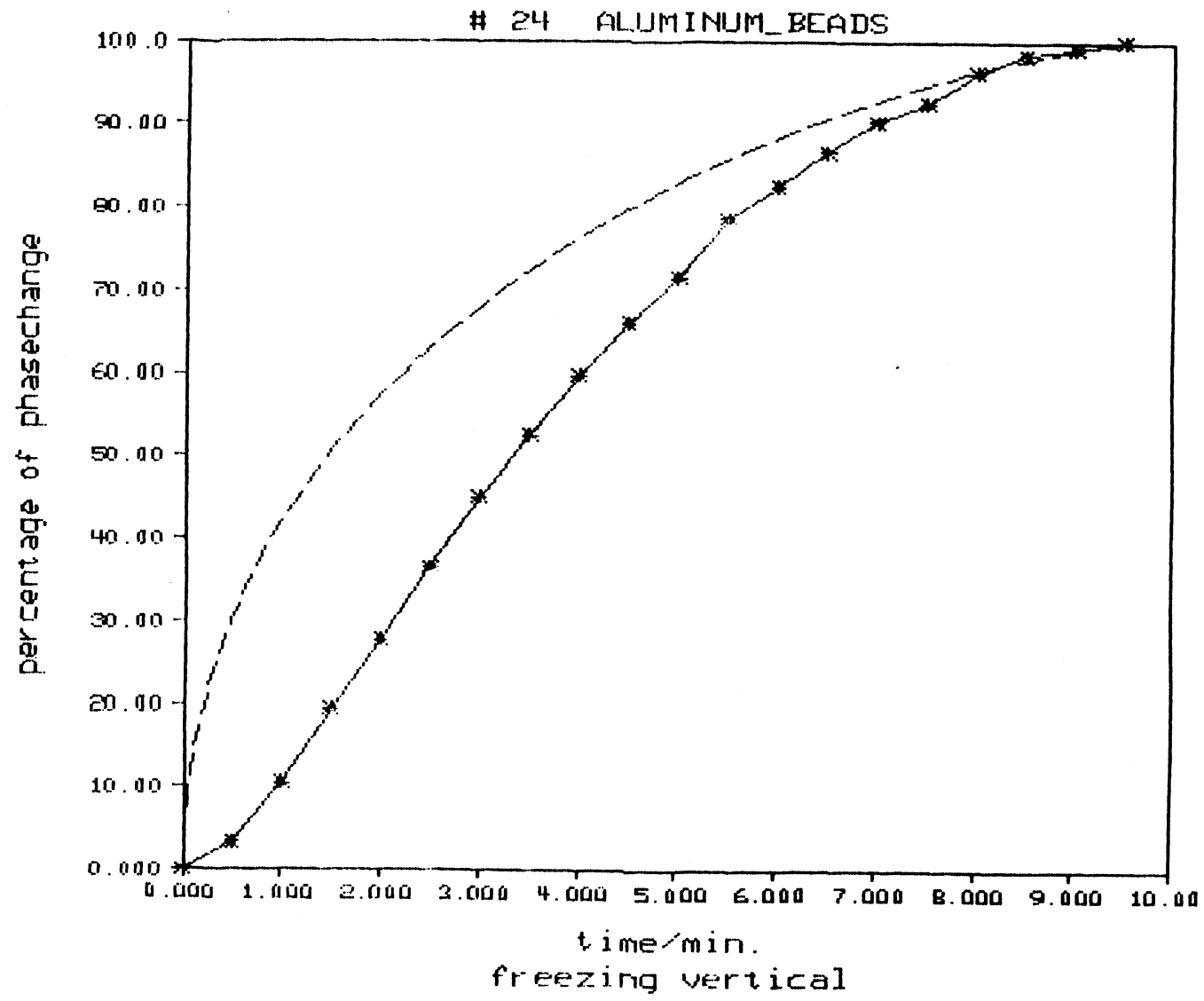
Experiment # 25

```
metal          :  ALUMINUM
porosity       :  phi = 0.532
description    :  BEADS, diameter: 12mm
vol./area      :  va  = 2.0000 mm
density        :  rhom=   2702.0 kg/m**2
specific heat:  cm  =    880.0 J/kg*K
```

MELTING in a VERTICAL cylinder

```
temperature of bath ............. :  Tb  =   30.0 C
ambient temperature ............. :  Tsur=   24.0 C
average wall temperature ........ :  Tw,a=   21.9 C
initial temperature of solid phase :  Ti  =   -0.5 C
average temperature of liquid phase:  Tlm =   10.9 C
```

total time for melting: tt =   6.0 min
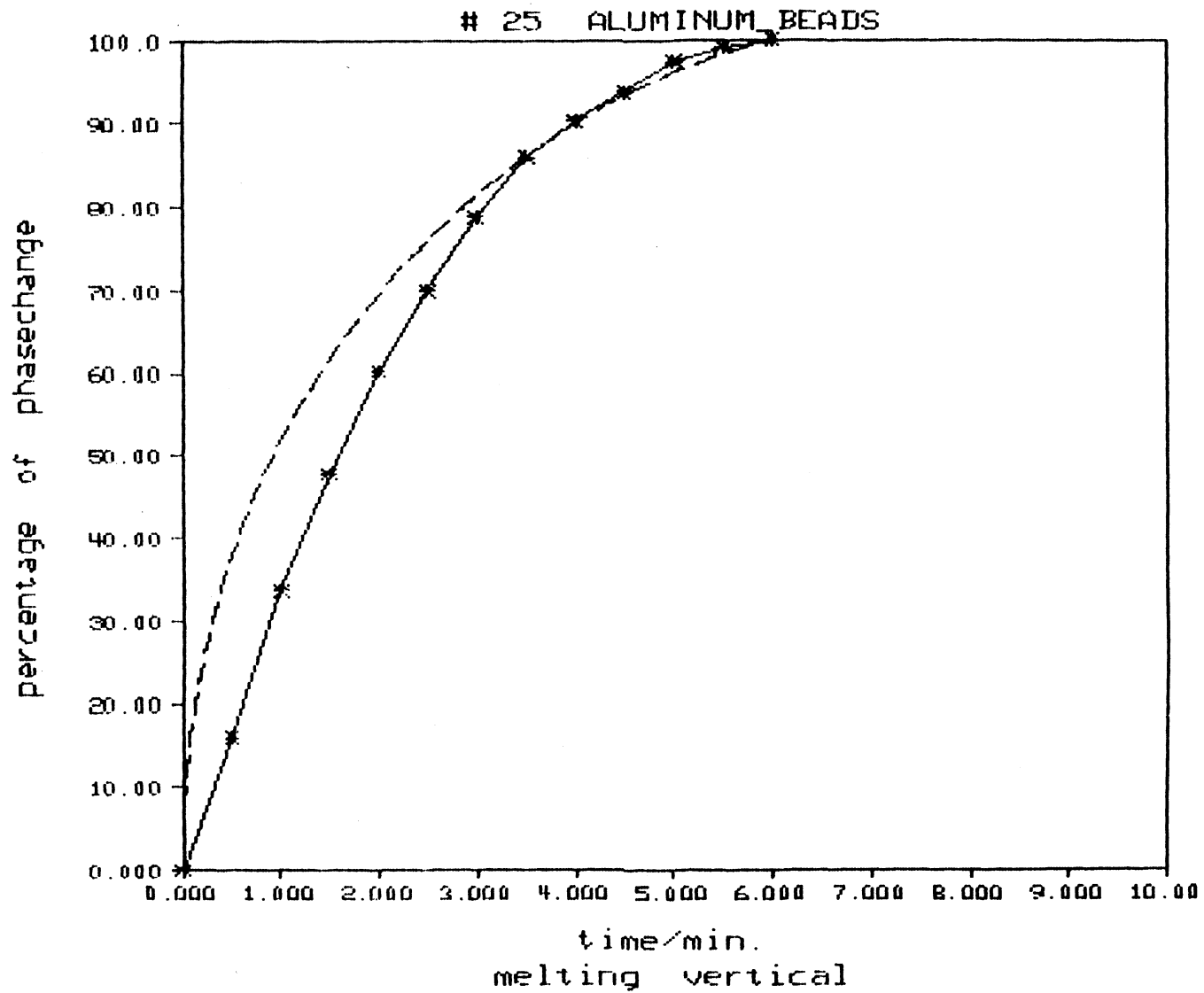
CONDUCTIVITY for liquid phase at Tlm =   10.9 C

keff= 12.75 W/m*K

```
*****************************
*  klm=  12.75 W/m*K   *
*****************************
```

compare with these conductivities at Tlm=   10.9 C

```
metal          :  km   = 220.00 W/m*K
water          :  kh2o =   0.58 W/m*K
series         :  kser =   1.09 W/m*K
parallel       :  kpar = 103.33 W/m*K
empirical      :  kemp =   7.35 W/m*K
geometrical:  kgeo =   1.78 W/m*K
Veinberg       :  kvein=   3.69 W/m*K
```

```
energy density     :  Q'''=  0.196e+09 J/m**3
performance factor:  pf  =    8.31     W/m*K
storage factor     :  s   =  0.163e+10 J*W/m**4*K
```

25   ALUMINUM BEADS

melting vertical

160

Experiment # 26

metal   : ALUMINUM
porosity   : phi = 0.532
description   : BEADS, diameter: 12mm
vol./area   : va   = 2.0000 mm
density   : rhom=   2702.0 kg/m**2
specific heat: cm   =   880.0 J/kg*K

MELTING in a HORIZONTAL cylinder

temperature of bath .... : Tb   =   30.0 C
ambient temperature .... : Tsur=   24.0 C
average wall temperature .... : Tw,a=   20.3 C
initial temperature of solid phase : Ti   =   -0.2 C
average temperature of liquid phase: Tlm =   10.1 C

total time for melting: tt   =   6.0 min

CONDUCTIVITY for liquid phase at Tlm =   10.1 C

    keff=   13.97 W/m*K

****
*   klm=   13.97 W/m*K   *
****

compare with these conductivities at Tlm=   10.1 C

metal   : km   = 220.00 W/m*K
water   : kh2o =   0.58 W/m*K
series   : kser =   1.08 W/m*K
parallel   : kpar = 103.33 W/m*K
empirical   : kemp =   9.34 W/m*K
geometrical: kgeo =   1.77 W/m*K
Veinberg   : kvein=   3.68 W/m*K

energy density   : Q'''=   0.196e+09 J/m**3
performance factor: pf =   8.95   W/m*K
storage factor   : s   =   0.176e+10 J*W/m**4*K

26   ALUMINUM BEADS

melting horizontal
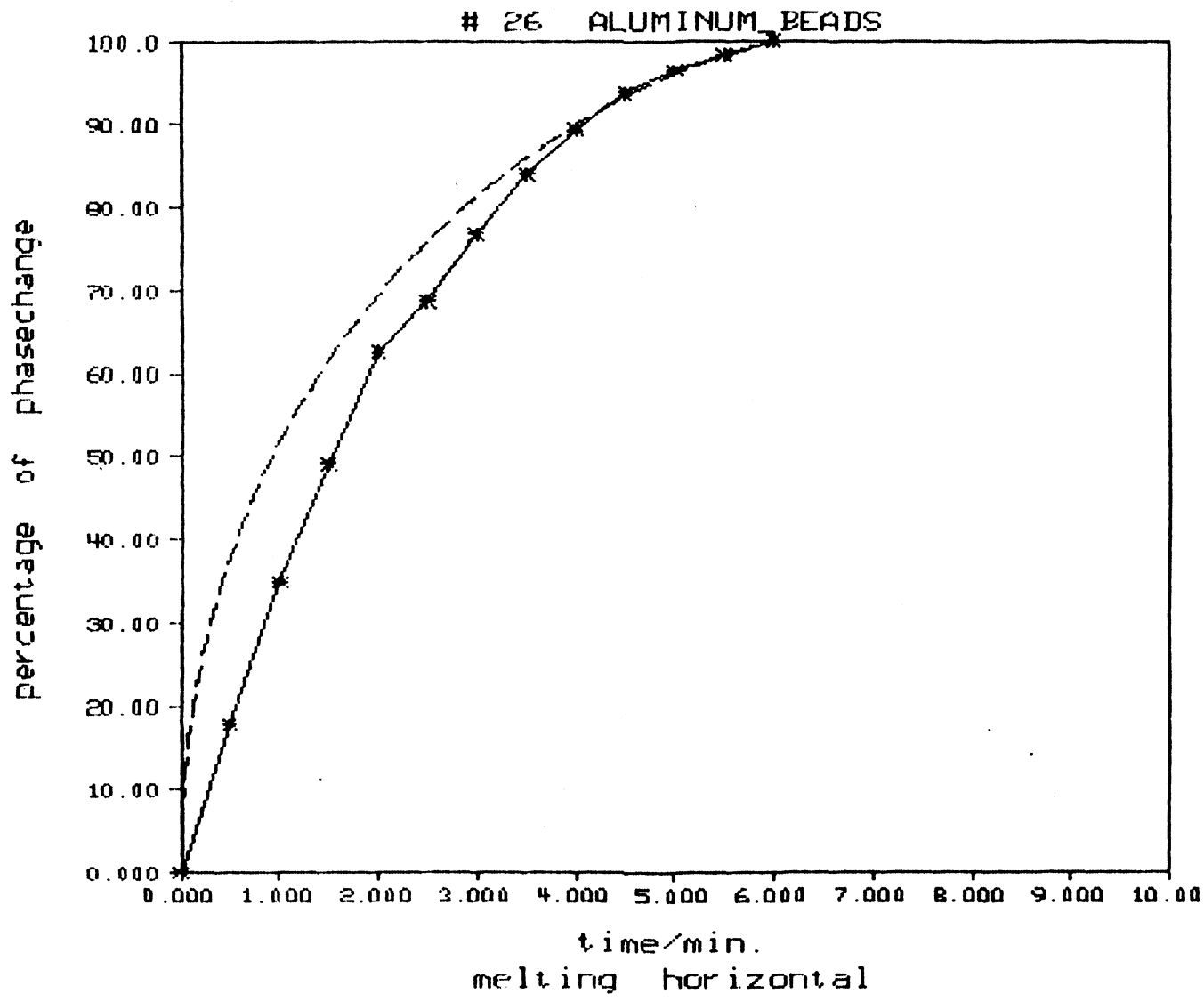
Experiment # 27

metal   : COPPER
porosity   : phi = 0.740
description   : SPIRALS; 0.5mm X 4mm
vol./area   : va = 0.5000 mm
density   : rhom=   8933.0 kg/m**2
specific heat: cm =   377.2 J/kg*K

FREEZING in a VERTICAL cylinder

temperature of bath .... : Tb   = -15.0 C
ambient temperature .... : Tsur= 22.0 C
average wall temperature .... : Tw,a= -9.5 C
initial temperature of liquid phase: Ti = -0.1 C
average temperature of solid phase : Tsm = -4.8 C

total time for freezing: tt = 29.0 min

CONDUCTIVITY for solid phase at Tsm = -4.8 C

****
*   ksm=   6.16 W/m*K   *
****

compare with these conductivities at Tsm= -4.8 C

metal   : km = 409.76 W/m*K
ice   : kice =   2.19 W/m*K
series   : kser =   2.33 W/m*K
parallel   : kpar = 26.80 W/m*K
empirical   : kemp =   3.00 W/m*K
geometrical: kgeo =   2.41 W/m*K
Veinberg   : kvein=   2.63 W/m*K

energy density   : Q'''= 0.307e+09 J/m**3
performance factor: pf =   6.19   W/m*K
storage factor   : s   = 0.190e+10 J*W/m**4*K

27 COPPER

freezing vertical
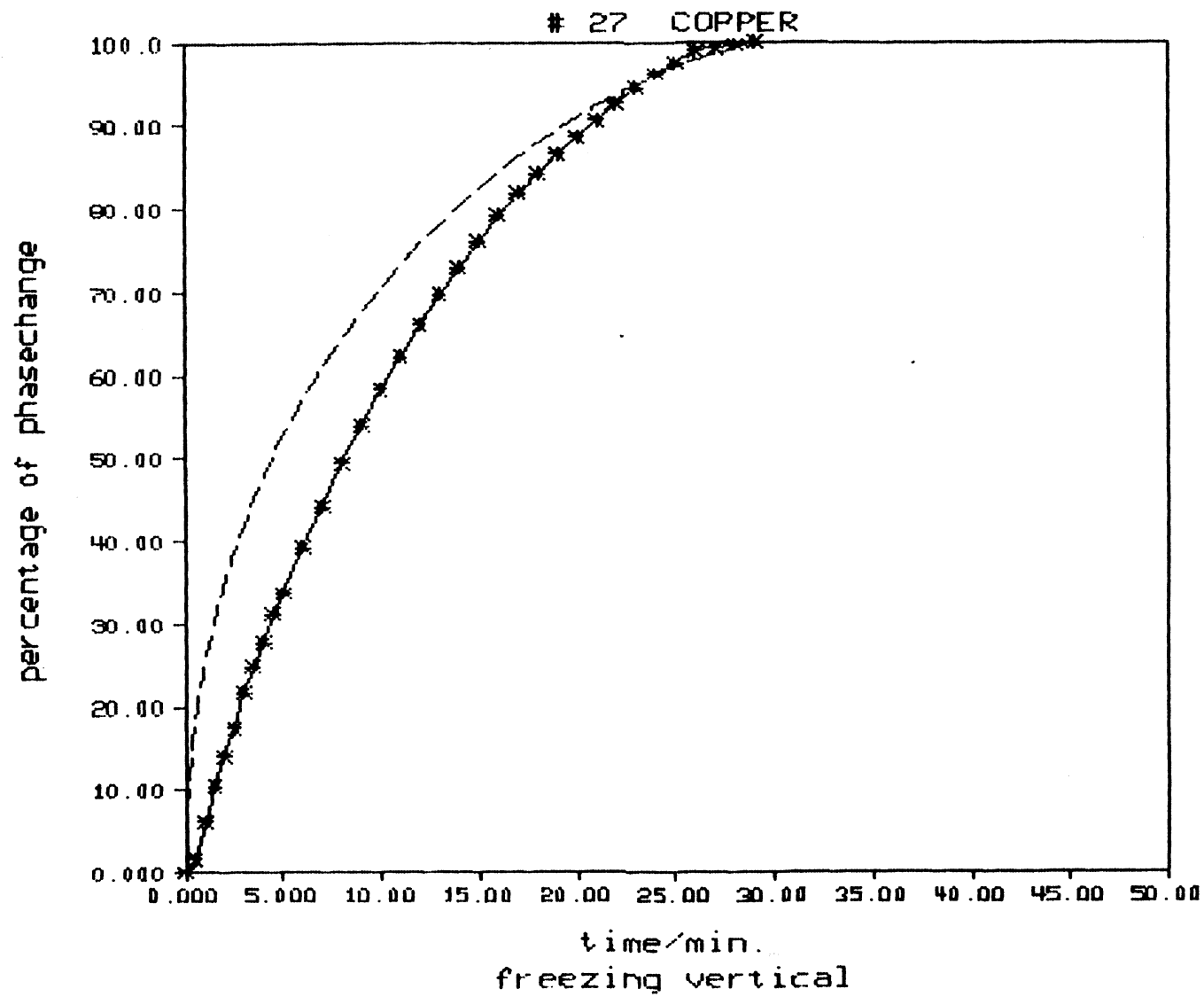
Experiment # 28


```
metal          : COPPER
porosity       : phi = 0.940
description    : SPIRALS; 0.5mm X 4mm
vol./area      : va  = 0.5000 mm
density        : rhom=   8933.0 kg/m**2
specific heat: cm  =    377.2 J/kg*K
```

MELTING in a VERTICAL cylinder

```
temperature of bath .............. : Tb   =   30.0 C
ambient temperature .............. : Tsur=   22.0 C
average wall temperature ......... : Tw,a=   25.7 C
initial temperature of solid phase : Ti   =   -0.5 C
average temperature of liquid phase: Tlm =    12.8 C
```

total time for melting: tt =   22.0 min

CONDUCTIVITY for liquid phase at Tlm =   12.8 C

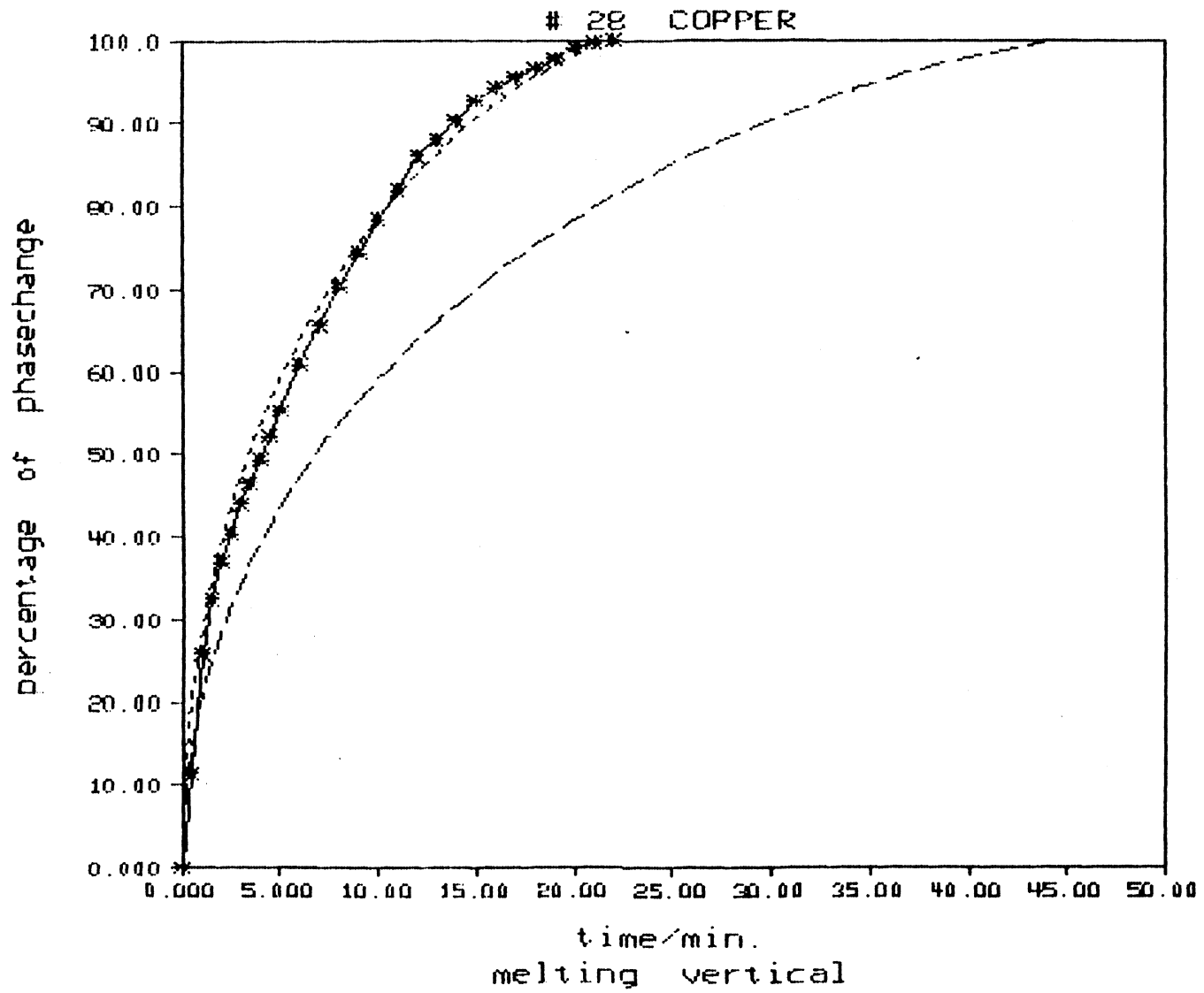   keff=   3.01 W/m*K


```
**************************
*   klm=    1.49 W/m*K   *
**************************
```

compare with these conductivities at Tlm=   12.8 C

```
metal         : km   = 409.76 W/m*K
water         : kh2o =   0.58 W/m*K
series        : kser =   0.62 W/m*K
parallel      : kpar =  25.29 W/m*K
empirical  : kemp =   0.87 W/m*K
geometrical: kgeo =   0.64 W/m*K
Veinberg    : kvein=   0.70 W/m*K
```

```
energy density    : Q'''=  0.329e+09 J/m**3
performance factor: pf  =   3.23      W/m*K
storage factor    : s   =  0.106e+10 J*W/m**4*K
```

28 COPPER

percentage of phasechange

time/min.
melting vertical

166

Experiment # 29

metal   : COPPER
porosity   : phi = 0.940
description   : SPIRALS; 0.5mm X 4mm
vol./area   : va = 0.5000 mm
density   : rhom=   8933.0 kg/m**2
specific heat: cm =   377.2 J/kg*K

MELTING in a HORIZONTAL cylinder

temperature of bath .... : Tb   =   30.0 C
ambient temperature .... : Tsur=   22.0 C
average wall temperature .... : Tw,a=   25.3 C
initial temperature of solid phase : Ti   =   -0.5 C
average temperature of liquid phase: Tlm =   12.6 C

total time for melting: tt =   17.0 min

CONDUCTIVITY for liquid phase at Tlm =   12.6 C

    keff=   3.75 W/m*K

****
*   klm=   1.61 W/m*K   *
****

compare with these conductivities at Tlm=   12.6 C

metal   : km   = 409.76 W/m*K
water   : kh2o =   0.58 W/m*K
series   : kser =   0.62 W/m*K
parallel   : kpar = 25.29 W/m*K
empirical   : kemp =   0.87 W/m*K
geometrical: kgeo =   0.64 W/m*K
Veinberg   : kvein=   0.70 W/m*K

energy density   : Q'''=   0.329e+09 J/m**3
performance factor: pf =   4.25   W/m*K
storage factor   : s   =   0.140e+10 J*W/m**4*K

29 COPPER

melting horizontal

168
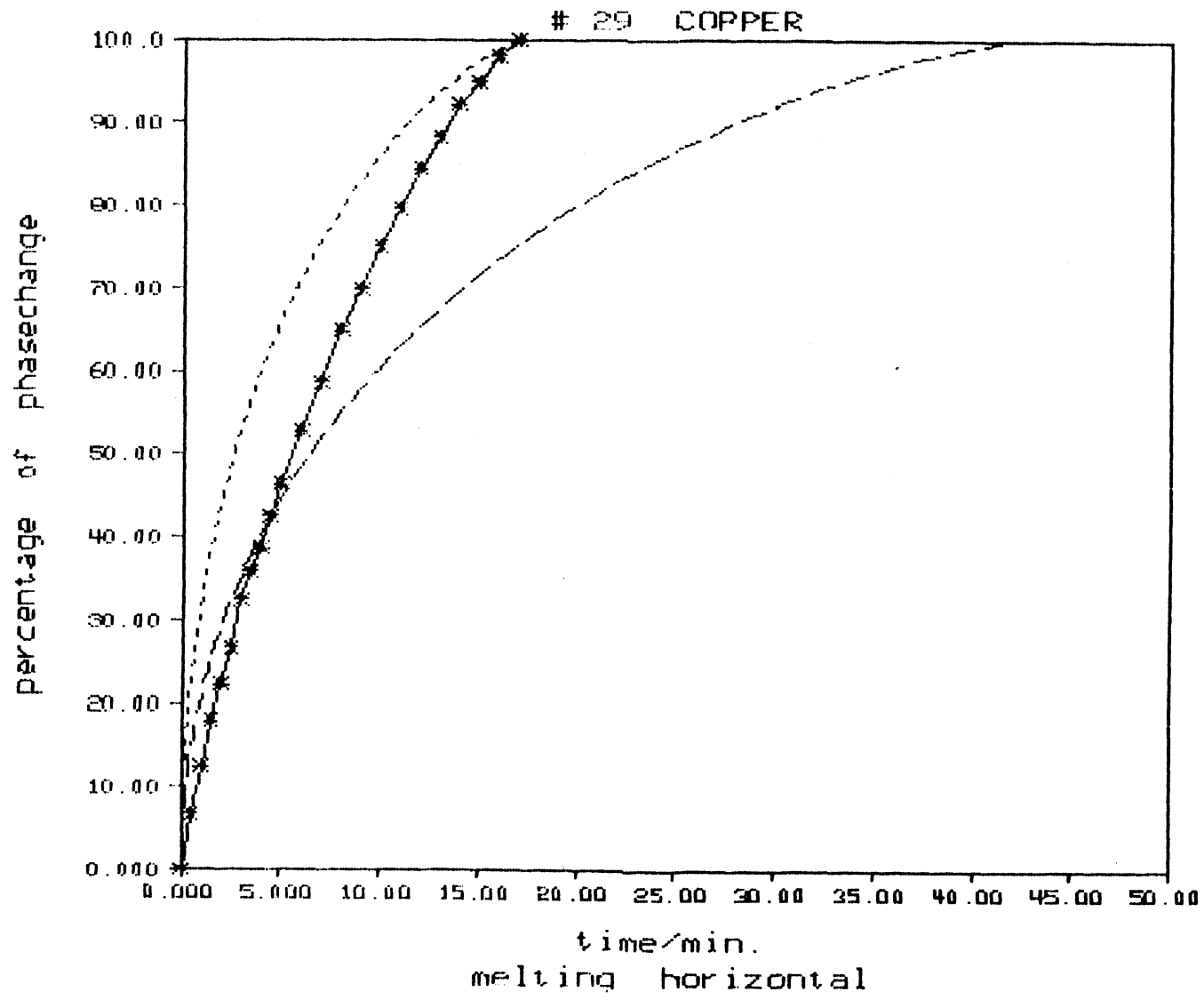
Experiment # 30

metal   : CARTRIDGE BRASS
porosity   : phi = 0.956
description   : 70% Cu, 30% Zn; SPIRALS
vol./area   : va = 0.0484 mm
density   : rhom=   8530.0 kg/m**2
specific heat: cm =   374.6 J/kg*K

FREEZING in a VERTICAL cylinder

temperature of bath .... : Tb = -15.0 C
ambient temperature .... : Tsur= 22.0 C
average wall temperature .... : Tw,a= -10.6 C
initial temperature of liquid phase: Ti =   1.4 C
average temperature of solid phase : Tsm = -5.3 C

total time for freezing: tt = 41.0 min

CONDUCTIVITY for solid phase at Tsm = -5.3 C

****
*   ksm=   3.93 W/m*K   *
****

compare with these conductivities at Tsm= -5.3 C

metal   : km   = 105.95 W/m*K
ice   : kice =   2.19 W/m*K
series   : kser =   2.29 W/m*K
parallel   : kpar =   6.80 W/m*K
empirical   : kemp =   2.60 W/m*K
geometrical: kgeo =   2.34 W/m*K
Veinberg   : kvein=   2.49 W/m*K

energy density   : Q'''= 0.312e+09 J/m**3
performance factor: pf =   4.00   W/m*K
storage factor   : s   = 0.125e+10 J*W/m**4*K

30   BRASS

percentage of phasechange

time/min.
freezing vertical
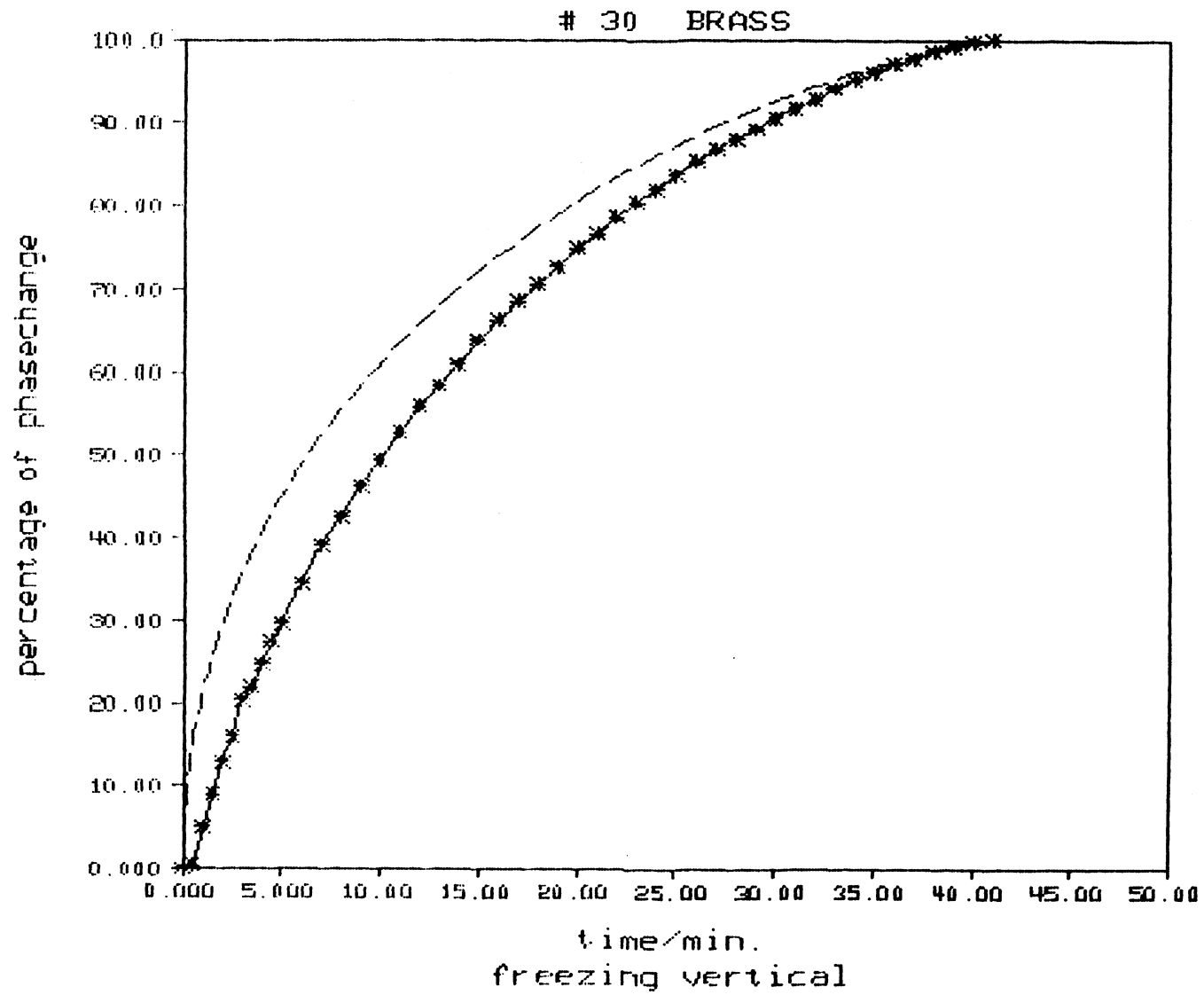
Experiment # 31

```
metal         : CARTRIDGE BRASS
porosity      : phi = 0.956
description   : 70% Cu, 30% Zn; SPIRALS
vol./area     : va  = 0.0484 mm
density       : rhom=   8530.0 kg/m**2
specific heat: cm  =    374.6 J/kg*K
```

MELTING in a VERTICAL cylinder

```
temperature of bath .............. : Tb   =   30.0 C
ambient temperature .............. : Tsur=   22.0 C
average wall temperature ......... : Tw,a=   26.6 C
initial temperature of solid phase : Ti   =   -0.7 C
average temperature of liquid phase: Tlm =   13.3 C
```

total time for melting: tt   =   28.0 min

CONDUCTIVITY for liquid phase at Tlm =   13.3 C

keff=   2.29 W/m*K

```
***************************
*   klm=   1.19 W/m*K   *
***************************
```

compare with these conductivities at Tlm=   13.3 C

```
metal       : km   = 105.95 W/m*K
water       : kh2o =   0.58 W/m*K
series      : kser =   0.61 W/m*K
parallel    : kpar =   5.26 W/m*K
empirical   : kemp =   0.74 W/m*K
geometrical: kgeo =   0.62 W/m*K
Veinberg    : kvein=   0.67 W/m*K
```

```
energy density     : Q'''=   0.334e+09 J/m**3
performance factor: pf  =   2.49      W/m*K
storage factor     : s   =   0.833e+09 J*W/m**4*K
```

31   BRASS

percentage of phasechange

time/min.
melting vertical

172
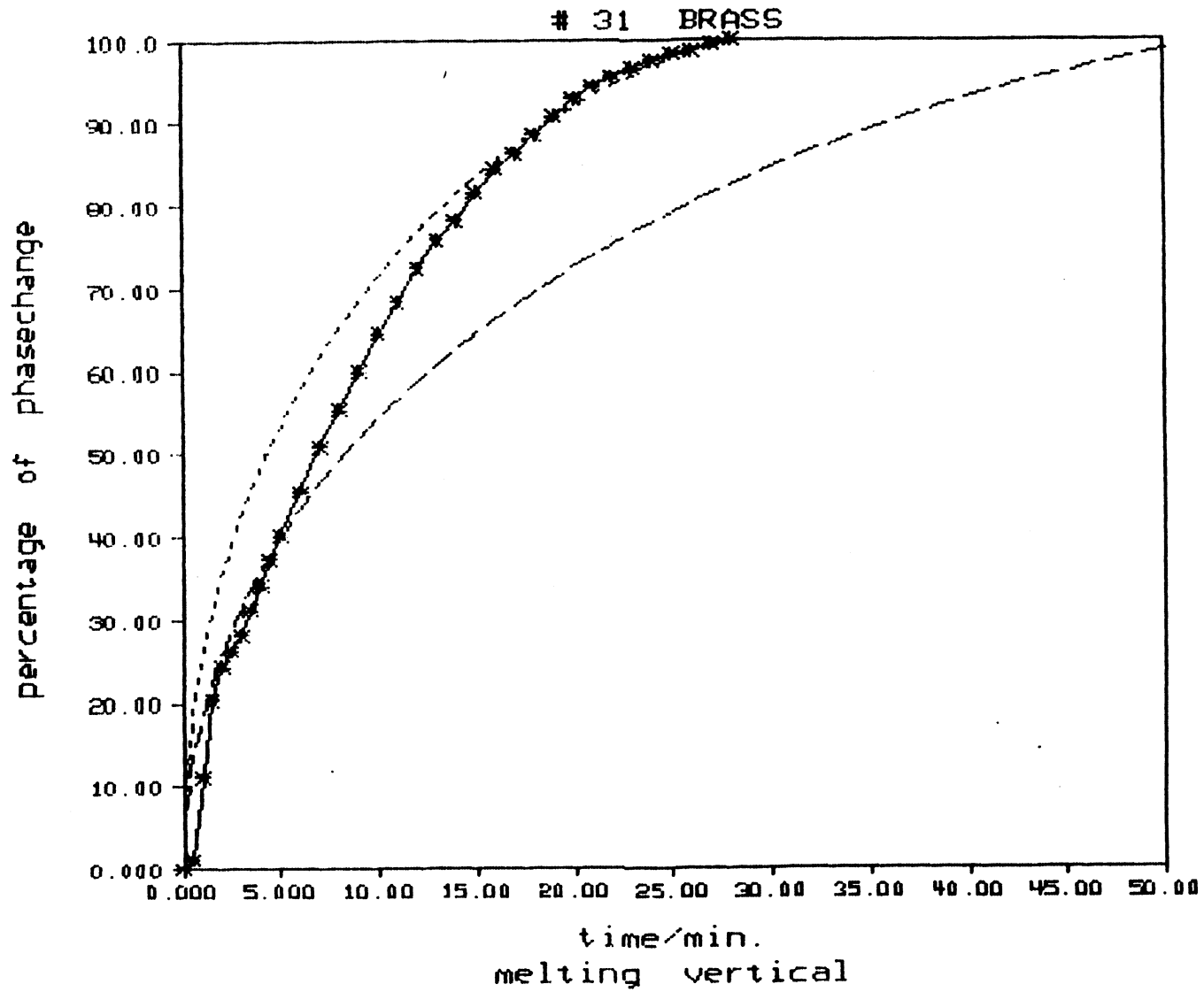
Experiment # 32

```
metal          : CARTRIDGE BRASS
porosity       : phi = 0.956
description    : 70% Cu, 30% Zn; SPIRALS
vol./area      : va  = 0.0484 mm
density        : rhom=   8530.0 kg/m**2
specific heat: cm  =    374.6 J/kg*K
```

MELTING in a HORIZONTAL cylinder

```
temperature of bath ............... : Tb   =   30.0 C
ambient temperature ............... : Tsur=   22.0 C
average wall temperature ......... : Tw,a=   26.4 C
initial temperature of solid phase : Ti   =   -0.8 C
average temperature of liquid phase: Tlm =   13.2 C
```

total time for melting: tt =   22.0 min

CONDUCTIVITY for liquid phase at Tlm =   13.2 C

     keff=   2.93 W/m*K

****
*   klm=   1.28 W/m*K   *
****

compare with these conductivities at Tlm=   13.2 C

```
metal       : km   = 105.95 W/m*K
water       : kh2o =   0.58 W/m*K
series      : kser =   0.61 W/m*K
parallel    : kpar =   5.26 W/m*K
empirical   : kemp =   0.74 W/m*K
geometrical: kgeo =   0.62 W/m*K
Veinberg    : kvein=   0.67 W/m*K
```

```
energy density     : Q'''=   0.334e+09 J/m**3
performance factor: pf  =   3.20      W/m*K
storage factor     : s   =   0.107e+10 J*W/m**4*K
```

32   BRASS

melting horizontal

174
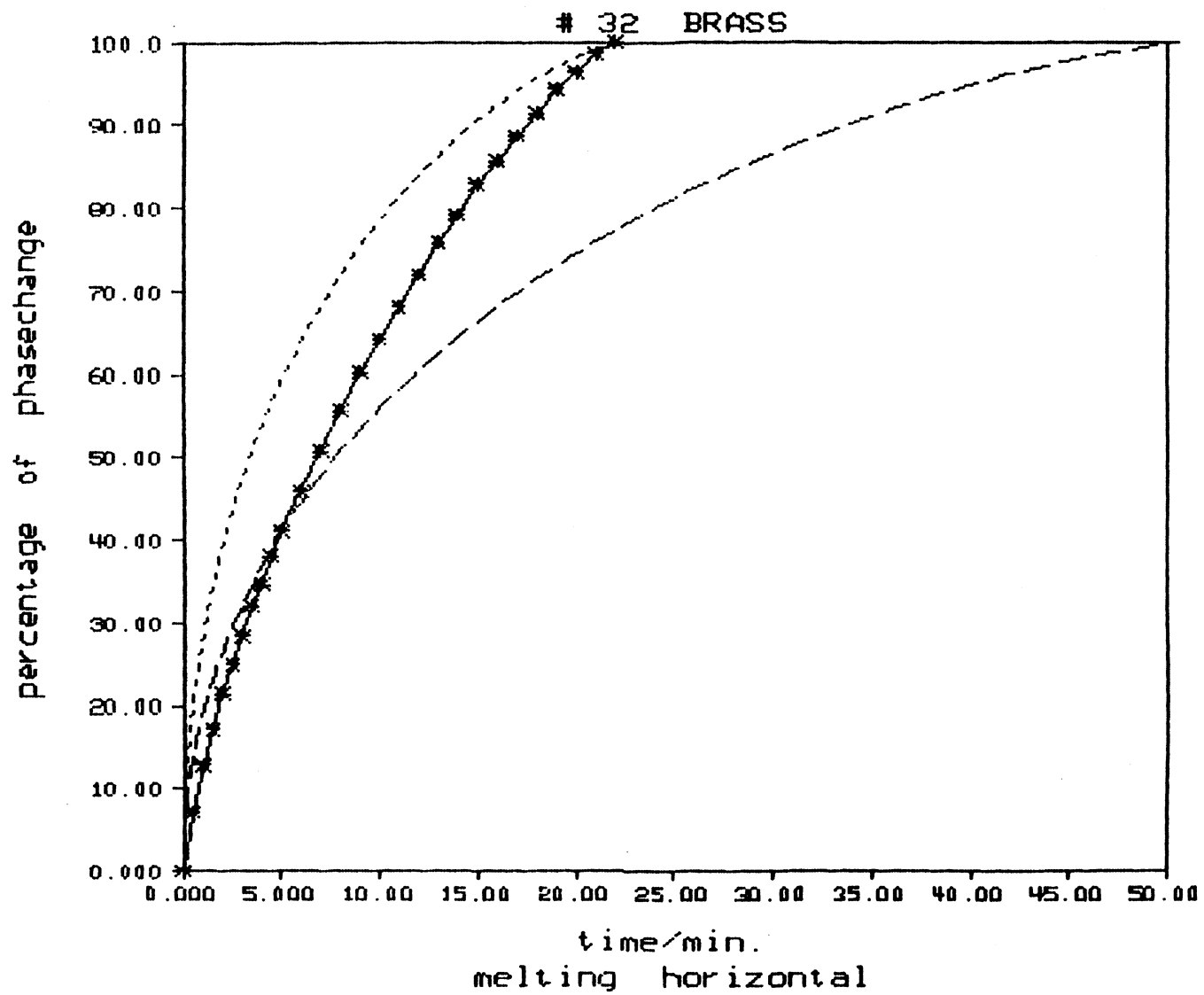
Experiment # 33

metal   : STAINLESS STEEL
porosity   : phi = 0.959
description   : AISI 304; SPIRALS; 0.1mm
vol./area   : va = 0.0484 mm
density   : rhom=   7900.0 kg/m**2
specific heat: cm =   456.8 J/kg*K

FREEZING in a VERTICAL cylinder

temperature of bath .... : Tb   = -15.0 C
ambient temperature .... : Tsur= 24.0 C
average wall temperature .... : Tw,a= -11.9 C
initial temperature of liquid phase: Ti   =   0.3 C
average temperature of solid phase : Tsm = -6.0 C

total time for freezing: tt = 56.0 min


CONDUCTIVITY for solid phase at Tsm =   -6.0 C

****
* ksm=   2.54 W/m*K   *
****

compare with these conductivities at Tsm=   -6.0 C

metal   : km   = 14.28 W/m*K
ice   : kice =   2.20 W/m*K
series   : kser =   2.28 W/m*K
parallel   : kpar =   2.69 W/m*K
empirical   : kemp =   2.37 W/m*K
geometrical: kgeo =   2.30 W/m*K
Veinberg   : kvein=   2.38 W/m*K

energy density   : Q'''=   0.313e+09 J/m**3
performance factor: pf =   2.60   W/m*K
storage factor   : s   =   0.814e+09 J*W/m**4*K

33   STEEL

percentage of phasechange

time/min.
freezing vertical
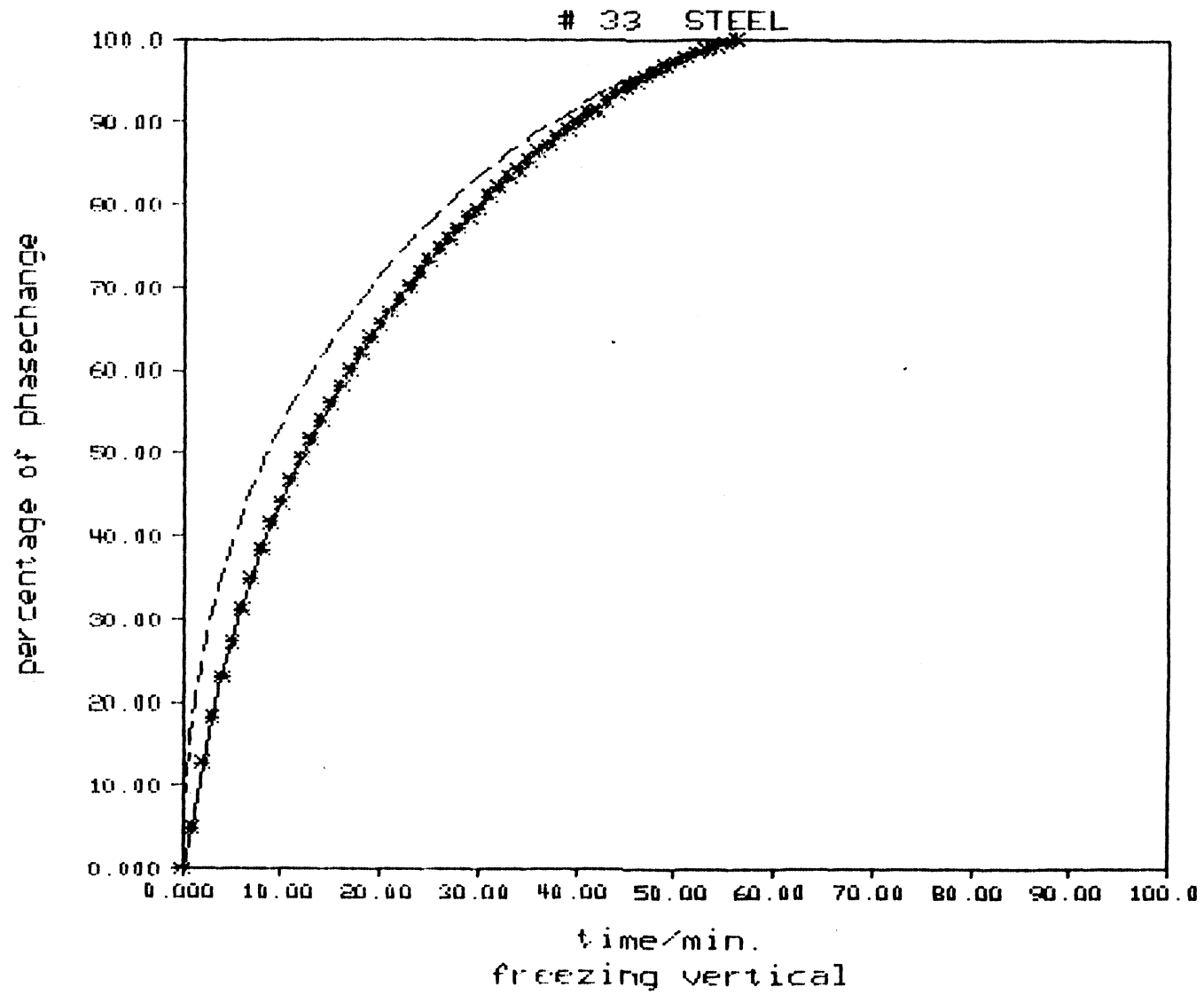
Experiment # 34

```
metal          : STAINLESS STEEL
porosity       : phi = 0.959
description    : AISI 304; SPIRALS; 0.1mm
vol./area      : va  = 0.0484 mm
density        : rhom=   7900.0 kg/m**2
specific heat: cm  =    456.8 J/kg*K
```

MELTING in a VERTICAL cylinder

```
temperature of bath .............. : Tb   =   30.0 C
ambient temperature .............. : Tsur=   24.0 C
average wall temperature ......... : Tw,a=   28.7 C
initial temperature of solid phase : Ti   =   -0.9 C
average temperature of liquid phase: Tlm =   14.3 C
```

```
total time for melting:            tt  =   30.0 min
```

CONDUCTIVITY for liquid phase at Tlm =   14.3 C

```
    keff=   1.77 W/m*K
```

```
*************************
*   klm=   0.92 W/m*K   *
*************************
```

compare with these conductivities at Tlm=   14.3 C

```
metal       : km   =   14.28 W/m*K
water       : kh2o =    0.59 W/m*K
series      : kser =    0.61 W/m*K
parallel    : kpar =    1.15 W/m*K
empirical   : kemp =    0.67 W/m*K
geometrical : kgeo =    0.62 W/m*K
Veinberg    : kvein=    0.65 W/m*K
```

```
energy density    : Q'''=   0.335e+09 J/m**3
performance factor: pf  =   2.16      W/m*K
storage factor    : s   =   0.725e+09 J*W/m**4*K
```

34 STEEL

melting vertical
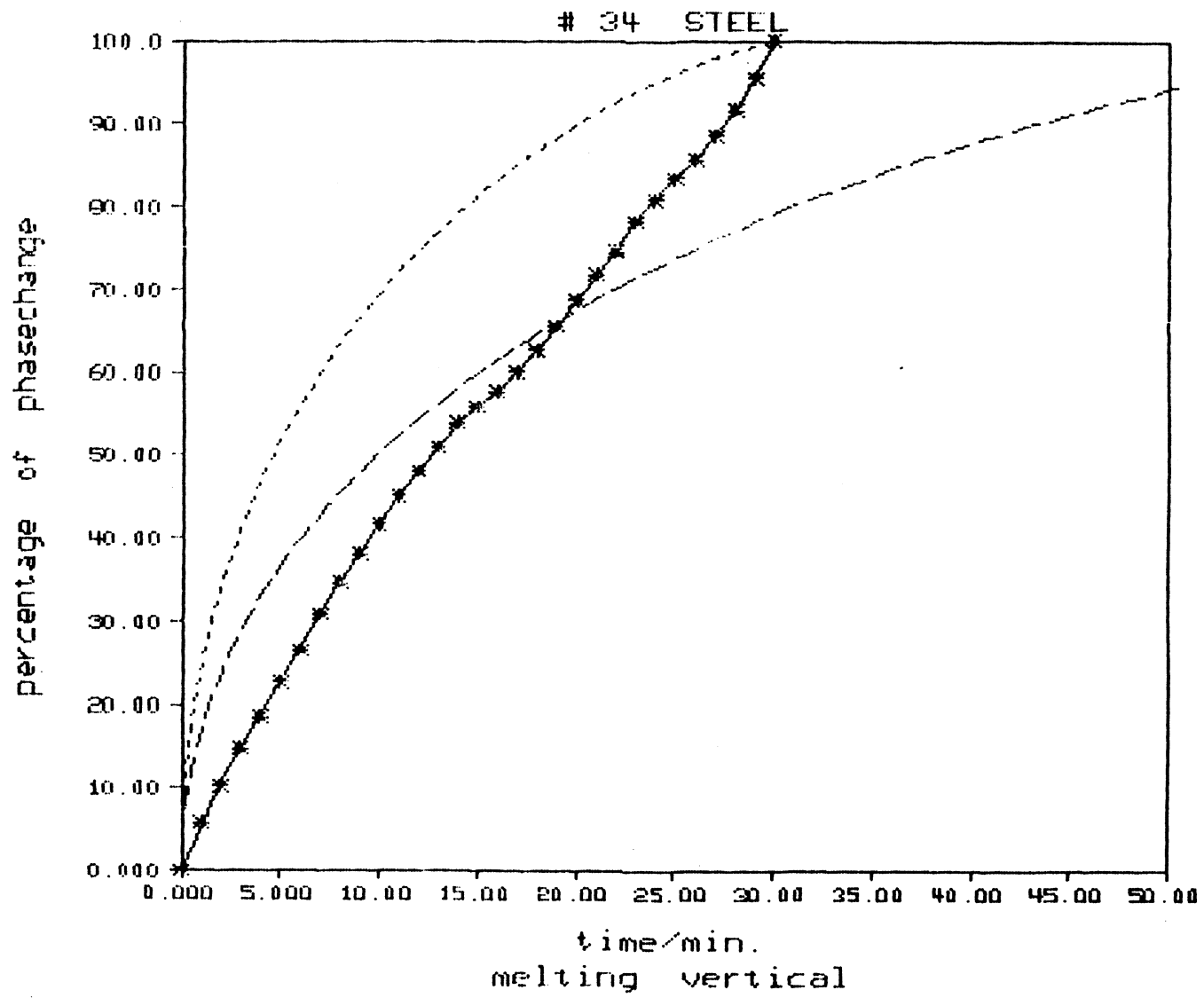
Experiment # 35

```
metal          : STAINLESS STEEL
porosity       : phi = 0.959
description    : AISI 304; SPIRALS; 0.1mm
vol./area      : va  = 0.0484 mm
density        : rhom=  7900.0 kg/m**2
specific heat: cm  =   456.8 J/kg*K
```

MELTING in a HORIZONTAL cylinder

```
temperature of bath ............... : Tb   =  30.0 C
ambient temperature ............... : Tsur=  24.0 C
average wall temperature .......... : Tw,a=  26.4 C
initial temperature of solid phase : Ti   =  -0.3 C
average temperature of liquid phase: Tlm  =  13.2 C
```

total time for melting: tt = 23.0 min

CONDUCTIVITY for liquid phase at Tlm =   13.2 C

keff=   2.30 W/m*K

```
*****************************
*   klm=   1.08 W/m*K   *
*****************************
```

compare with these conductivities at Tlm=   13.2 C

```
metal      : km   =  14.28 W/m*K
water      : kh2o =   0.58 W/m*K
series     : kser =   0.61 W/m*K
parallel   : kpar =   1.15 W/m*K
empirical  : kemp =   0.67 W/m*K
geometrical: kgeo =   0.62 W/m*K
Veinberg   : kvein=   0.65 W/m*K
```

```
energy density    : Q'''=  0.335e+09 J/m**3
performance factor: pf  =   3.07      W/m*K
storage factor    : s   =  0.103e+10 J*W/m**4*K
```

35 STEEL

melting horizontal

180
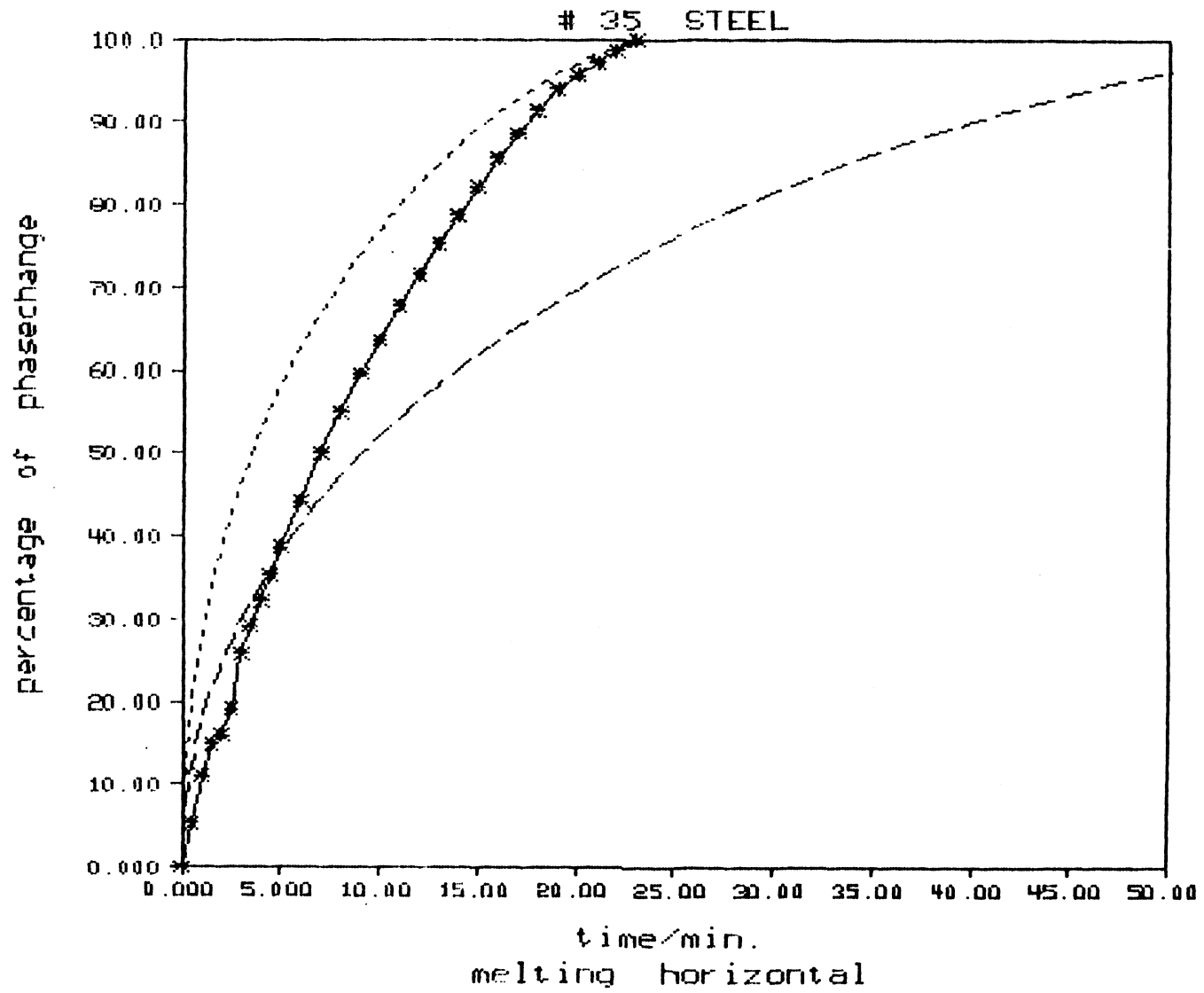
Appendix B. Derivations

Appendix B includes the derivations of Eq. 5.2.2.2, 5.2.2.3, and 5.2.2.4.

As long as the fusion fronts are not in contact the frozen fraction is

$$\overline{F} \equiv \frac{V(t)}{V_{all}}$$

The total volume for phase change V_{all} (see Fig. Appendix B) in a triangular unit of the tube bank is the area of the triangle V_{Δ} times the depth 1 without the volume of the tubes V_{tube}. The areas related to V_{Δ} and V_{all} are shown in Fig. App.B.

$$V_{\Delta} = \frac{1}{2} \; L \; L \; \sin 60^{\circ} \; 1 = \frac{1}{4} \; 3^{1/2} \; L^2 \; 1$$

$$V_{tube} = \frac{1}{2} \; R^2 \pi 1$$

$$V_{all} = V_{\Delta} - V_{tube}$$

The actual frozen volume is

$$V(t) = \frac{1}{2} \; r^2 \pi 1 - \frac{1}{2} \; R^2 \pi 1$$

Substituting $V(t)$ and V_{all} into the definition for the frozen fraction

$$\overline{F} = \frac{V(t)}{V_{all}} = \frac{r^2 - R^2}{\frac{3^{1/2}}{2\pi} \; L^2 - R^2}$$

and solving for r

$$r = R \left(\left[\frac{3^{1/2}}{2\pi} \left(\frac{L}{R}\right)^2 - 1 \right] \overline{F} + 1 \right)^{1/2} \qquad (5.2.2.3)$$

The fusion fronts meet at $r = \frac{L}{2}$ thus

$$\overline{F}_{meet} = \frac{\frac{1}{4} L^2 - R^2}{\frac{3^{1/2}}{2\pi} L^2 - R^2} \qquad (5.2.2.2)$$

After the fusion fronts make contact with one another, the calculation is continued for inward freezing. The frozen fraction is now

$$\overline{F}' = \frac{V'}{V'_{all}} = 1 - \left(\frac{r_v}{R_v}\right)^2 \qquad (*)$$

The total volume V_{all} inside the virtual cylinder of radius R_v is

$$V'_{all} = R_v^2 \pi l$$

and the actual frozen volume is

$$V' = R_v^2 \pi l - r_v^2 \pi l$$

where r_v is the radius of the assumed cylindrical fusion front which contains the same volume as the actual unfrozen part in the heat exchanger.

$$r_v^2 \pi l = V_{all} - V(t)$$

Substituting the last three equations into (*) and solving for r_v yields

$$r_v = R_v \left(1 - \frac{R_v^2 \pi 1 - (V_{all} - V(t))}{R_v^2 \pi 1}\right)^{1/2}$$

$$= R_v \left(\frac{V_{all}}{R_v^2 \pi 1} - \frac{V(t)}{V_{all}} \frac{V_{all}}{R_v^2 \pi 1}\right)^{1/2}$$

$$= R_v \left(\frac{V_{all}}{R_v^2 \pi 1} [1 - \overline{F}]\right)^{1/2}$$
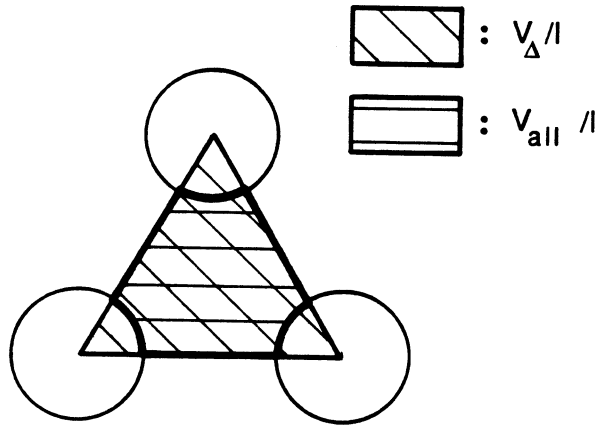
substituting V_{all} yields finally Eq. 5.2.2.4.

Figure B.1   Volumes in a triangular unit of staggered tubes.